1. RATES OF NUCLEAR REACTIONS IN WHITE-DWARF STARS

2. THE COOLING OF NEUTRON STARS

Thesis by

Richard Alan Wolf

In Partial Fulfillment of the Requirements

For the Degree of

Doctor of Philosophy

California Institute of Technology

Pasadena, California

1966

(Submitted November 11, 1965)

ACKNOWLEDGMENTS

I would like to thank my adviser, Dr. John Bahcall, for his consistent guidance and encouragement, and for many illuminating discussions. In addition, a large part of the work described herein on the cooling of neutron stars is due directly to him.

I would also like to thank Dr. R. F. Christy, Dr. John Faulkner, Dr. S. C. Frautschi, Dr. E. E. Salpeter, Dr. G. J. Stephenson, Jr., and Dr. W. G. Wagner for informative discussions. Correspondence with Dr. Hugh Van Horn has also been extremely helpful. I am grateful to Mrs. Frances Blackwell for her careful and efficient typing of the manuscript.

The financial support of the National Science Foundation, the Office of Naval Research, and the National Aeronautics and Space Administration is gratefully acknowledged.

ABSTRACT

1. Rates of Nuclear Reactions in White-Dwarf Stars

In stellar matter as cool and dense as the interior of a white dwarf, the Coulomb energies between neighboring nuclei are large compared to the kinetic energies of the nuclei. Each nucleus is constrained to vibrate about an equilibrium position, and the motion of the nuclei in the interior of a white dwarf is similar to the motion of the atoms in a solid or liquid. A method is proposed for calculating the rate at which a nuclear reaction proceeds between two identical nuclei oscillating about adjacent lattice sites. An effective potential $U(\underset{\sim}{r})$ derived by analyzing small lattice vibrations is used to represent the influence of the Coulomb fields of the lattice on the motion of the two reacting nuclei. The wave function describing the relative motion of the two reacting particles is obtained by solving a Schrödinger equation containing the effective potential $U(\underset{\sim}{r})$. From this wave function an expression for the reaction rate is derived. Applied to the p + p reaction, this method predicts a reaction rate about 100 times the original estimate made by Wildhack; applied to the $C^{12}+ C^{12}$ reactions, the present work implies a rate about ten orders of magnitude smaller than the rate calculated by the method previously suggested by Cameron.

ABSTRACT

2. The Cooling of Neutron Stars

The emission of neutrinos from neutron stars is studied, and those characteristics of neutron-star matter that affect cooling are investigated. The validity of the particle model (which we adopt) is discussed. The effects of strong interactions on the composition of neutron-star matter are described. The question of superfluidity in the neutron-proton gas is discussed, and the limit of stability of the nucleon-gas to formation of "nuclei" is estimated. Calculations of the rates of the cooling reactions $n + n \rightarrow n + p + e^- + \bar{\nu}_e$ and $n + \pi^- \rightarrow n + e^- + \bar{\nu}_e$ are presented; the rates of the closely related muon-producing reactions and the four inverse processes are also given. The calculated cooling rates indicate that a neutron star containing quasi-free pions would cool within a few days to a temperature so low that photon emission from the star's surface would be unobservable. Uncertainty about the properties of neutron-star matter prevents precise predictions about cooling rates, but it is possible to establish a lower limit on the cooling rate of a neutron star. This lower limit on the cooling rate implies that the discrete X-ray sources located in the direction of the galactic center are probably not neutron stars.

TABLE OF CONTENTS

Rates of Nuclear Reactions in White-Dwarf Stars

The Cooling of Neutron Stars

1. NUCLEAR REACTIONS IN WHITE-DWARF STARS*

I. INTRODUCTION

The motions of nuclei in the interiors of cool, dense stars resemble the motions of atoms in solids or liquids. The mean free path between collisions suffered by a given nucleus is much smaller than the average distance between nuclei and may be comparable to the particle's quantum-mechanical wavelength. Each nucleus is, therefore, forced to oscillate about a fixed position in a lattice structure.[1],[2],[3]

Reactions between charged particles in stars are inhibited by the small probability of penetrating the Coulomb barrier between nuclei. However, the probability of penetrating the barrier increases rapidly with the energies of the colliding particles. In most stars, the effective energies are due primarily to thermal motions. In stars as cold as white dwarfs, the thermal energies alone are too small to allow charged particles to react at significant rates. However, the Coulomb potential of the lattice combined with the ground-state vibrational energy of the reacting nuclei can, at high densities, enable nuclei at adjacent lattice sites to react rapidly even at zero temperature.

It is important that one be able to calculate the rates of reactions occurring at high densities and low temperatures, reactions to

*A very similar report on this work was published in Phys. Rev., 137, B1634 (1965).

which Cameron[4] has applied the name "pycnonuclear". Cameron has suggested that such reactions might be the source of energy for nova explosions. A knowledge of the rates of pycnonuclear reactions would also be useful in mathematical studies of white dwarfs. From the rates of reactions at high densities, one can infer certain limitations on the possible compositions of the interiors and envelopes of white dwarf stars[5], compositions which would otherwise be completely unknown. Any future attempts to evolve stellar models into the white-dwarf state from higher temperature configurations will also require detailed knowledge of the rates of pycnonuclear reactions.

In the present work we attempt to calculate the rate at which nuclear reactions proceed between particles vibrating about adjacent lattice sites. We consider only reactions among nuclei in a lattice of identical particles. For reactions between particles with $Z > 2$, the solid-state approach applies to the temperatures and densities in Region I of Figure 1. Figure 1 also shows typical central temperatures and densities for various types of stars.

The problem of reactions between identical particles in a lattice was first considered about twenty-five years ago by Wildhack[1], who made a rough estimate of the rate of the p + p reaction. Van Horn[6] has recently carried out calculations on the rate of reactions between nuclei in a lattice of identical particles; his methods are similar to the ones used in the present work.

A related problem has recently been considered by Kopyshev[7]; he calculated the rate of the p + p reaction for the case where a small

number of protons act as interstitials in a lattice of nuclei having Z approximately equal to ten. He neglects the motion of the heavy nuclei of the lattice, and considers just the motion of pairs of protons in the fixed Coulomb field of the lattice ions.

In a lattice of identical nuclei, the motions of any pair of nuclei are strongly coupled to the motions of other nuclei nearby. In order to compute the mean lifetime for a reaction between two adjacent nuclei without solving the complete many-body problem exactly, we make the fundamental assumption that the effect of the rest of the lattice on the relative motion of the two reacting particles can be adequately represented by a static potential $U(\underset{\sim}{r})$. The reaction rate depends strongly on $U(\underset{\sim}{r})$ through the barrier penetration factor. In Section II, we analyze the small vibrations of the lattice to find $U(\underset{\sim}{r})$. Then in Section III, we solve the Schrödinger equation for the wave function characterizing the relative motion of the two reacting particles. Having found this wave function, we derive an expression for the reaction rate. Section IV contains a discussion of the limitations of the solid-state treatment. In Section V, we present numerical results for the rates of the p+p and $C^{12}+C^{12}$ reactions. Applied to the p+p reaction, the present method predicts rates about 100 times the rates originally calculated by Wildhack[1]. Applied to the $C^{12}+C^{12}$ reaction, our method predicts rates about ten orders of magnitude slower than those obtained using the procedure of Cameron[4]. Salpeter[8] has developed a way of calculating reaction rates at temperatures higher than those covered by the solid-state method; our results are consistent with those of Salpeter.

II. THE EFFECTIVE POTENTIAL

A. Formulation of the Problem

We consider a piece of stellar matter containing N nuclei, each of mass M and charge Z. The number density of nuclei is taken to be b^{-3}; we assume that there is also a number density Zb^{-3} of electrons to assure overall charge neutrality.

The electrons are highly degenerate at the temperatures and densities to which the solid-state model applies. The energy of the Coulomb interaction between an electron and a nucleus is comparable to the average electron kinetic energy only at distances small compared to the electron's wavelength. Consequently, the fields of individual nuclei cannot significantly affect the electron wave functions. The electrons can react only to lattice vibrations with very long wavelengths. By solving the Thomas-Fermi equation for the electron distribution, one can show that the electron motion affects a negligible part of the vibrational spectrum as long as

$$b \ll a_o Z^{-1/3} \quad , \tag{II.1}$$

where a_o is the Bohr radius. Since inequality (II.1) always holds under the conditions to which the solid-state model applies, we assume a uniform distribution of electrons.

The electrostatic potential energy felt by the nuclei is thus the sum of two terms, one representing the interaction between the nuclei and the uniform distribution of electrons, and the other representing the Coulomb interactions among the nuclei themselves.

The lowest energy state of a collection of positively charged identical particles in a negatively charged medium is a body-centered cubic lattice[9], providing the particle density is sufficiently low*. We shall assume that the nuclei perform small oscillations about equilibrium positions in such a lattice, and consider the rate at which a nuclear reaction proceeds between two nuclei (labelled 1 and 2) oscillating about adjacent lattice sites. We let the relative displacement $\underset{\sim}{r}_1 - \underset{\sim}{r}_2$ of particles 1 and 2 be $\underset{\sim}{r}$, and assume that the equilibrium positions of the two nuclei are separated by a distance b_{nn} along the z axis.

We assume that the nearest-neighbor distance b_{nn} is much larger than the nuclear radii. The rate at which a nuclear reaction proceeds between particles 1 and 2 is the product of $\rho(\underset{\sim}{r} \approx 0)$, the probability density for particles 1 and 2 being very close together, and a factor that depends primarily on the properties of the nuclear reaction itself.

Because of the strong coupling of the motions of the many nuclei in the lattice, the motions of all the nuclei have to be considered in the calculation of $\rho(\underset{\sim}{r})$. The density matrix for a group of N nuclei at a temperature $(k\beta)^{-1}$ can be written in terms of Feynman's path integrals as follows:

$$\rho(\underset{\sim}{r}_1' \cdots \underset{\sim}{r}_N'; \underset{\sim}{r}_1 \cdots \underset{\sim}{r}_N) = \iint \mathcal{D}\underset{\sim}{x}_1 \cdots \underset{\sim}{x}_N \exp\left\{-\int_0^\beta du\left[\sum_i \frac{M}{2\hbar^2}\left(\frac{d\underset{\sim}{x}_i}{du}\right)^2 + V(\underset{\sim}{x}_1 \cdots \underset{\sim}{x}_N)\right]\right\} \tag{II.2}$$

The integral includes all paths such that $\underset{\sim}{x}_i(0)$ and $\underset{\sim}{x}_i(\beta)$ are equal respectively to $\underset{\sim}{r}_i$ and $\underset{\sim}{r}_i'$. To obtain $\rho(\underset{\sim}{r})$ from $\rho(\underset{\sim}{r}_1' \cdots \underset{\sim}{r}_N'; \underset{\sim}{r}_1 \cdots \underset{\sim}{r}_N)$,

*The density limitation for the solid-state treatment is discussed in Section IV.

we set $\underset{\sim}{r}_i'$ equal to $\underset{\sim}{r}_i$, integrate over all the $\underset{\sim}{r}_i$ except $\underset{\sim}{r}_1$ and $\underset{\sim}{r}_2$, and then integrate over the center of mass $\frac{1}{2}(\underset{\sim}{r}_1+\underset{\sim}{r}_2)$ for particles 1 and 2. Although exact calculation of the density matrix would clearly be difficult, Eq. (II.2) is relatively transparent in two simple cases, for $\underset{\sim}{r}_1-\underset{\sim}{r}_2$ and $\underset{\sim}{r}_1'-\underset{\sim}{r}_2'$ approximately equal to zero, and for small displacements from equilibrium.

In the first case, all important paths would involve only $\underset{\sim}{x}_1-\underset{\sim}{x}_2$ approximately equal to zero. Thus, $\underset{\sim}{x}_1-\underset{\sim}{x}_2$ could be set equal to zero in all terms in $V(\underset{\sim}{x}_1\ldots\underset{\sim}{x}_n)$, except for the term $Z^2e^2/|\underset{\sim}{x}_1-\underset{\sim}{x}_2|$, which represents the direct interaction between particles 1 and 2. Integrating over all the coordinates except $\underset{\sim}{x}_1-\underset{\sim}{x}_2$ to obtain $\rho(\underset{\sim}{r})$, we then find that, for small r,

$$\rho(\underset{\sim}{r}) \approx A\iint \mathcal{D}_{(\underset{\sim}{x}_1-\underset{\sim}{x}_2)} \exp\left\{-\int_0^\beta du\left[\frac{\mu}{2\hbar^2}\left(\frac{d(\underset{\sim}{x}_1-\underset{\sim}{x}_2)}{du}\right)^2+\frac{Z^2e^2}{|\underset{\sim}{x}_1-\underset{\sim}{x}_2|}\right]\right\} \quad , \quad (II.3)$$

where A is a constant that is difficult to calculate, and μ is equal to $\frac{1}{2}M$. We now assume that there exists some effective potential $U(\underset{\sim}{x}_1-\underset{\sim}{x}_2)$ such that

$$\rho(\underset{\sim}{r}) \approx A\iint \mathcal{D}_{(\underset{\sim}{x}_1-\underset{\sim}{x}_2)} \exp\left\{-\int_0^\beta du\left[\frac{\mu}{2\hbar^2}\left(\frac{d(\underset{\sim}{x}_1-\underset{\sim}{x}_2)}{du}\right)^2+\frac{Z^2e^2}{|\underset{\sim}{x}_1-\underset{\sim}{x}_2|}+U(\underset{\sim}{x}_1-\underset{\sim}{x}_2)\right]\right\} \quad (II.4)$$

for all $\underset{\sim}{r}$. In the next subsection, we calculate $U(\underset{\sim}{x}_1-\underset{\sim}{x}_2)$ in the small-displacement region, where $\underset{\sim}{x}_1-\underset{\sim}{x}_2$ is near $(0,0,b_{nn})$.

B. Small Vibrations

For small displacements of the nuclei from their equilibrium positions, the potential energy can be written to good accuracy in the form

$$V = V_0 + V_2 \quad , \quad (II.5)$$

where V_0 is independent of the nuclear displacements, and V_2 is a homogeneous polynomial of second order in the displacements. Using the usual normal mode procedure*, we can find linear combinations Q_s of the displacements of the nuclei such that the total Hamiltonian of the system of nuclei can be written in the form

$$H = \tfrac{1}{2}\Sigma_s \left(P_s^2 M_s^{-1} + M_s \omega_s^2 Q_s^2\right) \quad , \tag{II.6a}$$

where, classically,

$$P_s = M_s \dot{Q}_s \quad , \tag{II.6b}$$

and M_s and ω_s^2 are constants independent of the nuclear displacements.

For the case of small displacements, the density matrix can thus be written as the product of the density matrices for all the normal modes. The diagonal elements of the density matrix for a single harmonic oscillator can be written

$$\rho(Q_s;Q_s) = B \exp\left[-\tfrac{1}{2}Q_s^2/\langle Q_s^2\rangle\right] \quad , \tag{II.7a}$$

where

$$\langle Q_s^2\rangle = \tfrac{1}{2}(\hbar/M_s\omega_s) \coth \tfrac{1}{2}\beta\hbar\omega_s \quad , \tag{II.7b}$$

and β is an irrelevant normalization constant. Since the normal coordinates Q_s are linear combinations of the displacements of the various particles from their equilibrium positions, the diagonal elements of the density matrix can be written in the form

---

*For a discussion of the normal-mode approach as applied to solid lattices, see, for example, J. M. Ziman, Electrons and Phonons, (Oxford University Press, London, 1960) Chapter 1.

$$\rho(\underset{\sim}{r}_1 \cdots \underset{\sim}{r}_N ; \underset{\sim}{r}_1 \cdots \underset{\sim}{r}_N) = C \exp\Big[- \sum_{i=1}^{3} \sum_{j=1}^{3} \sum_{k=1}^{N} \sum_{m=1}^{N} C_{ijkm} (r_k - a_k)_i (r_m - a_m)_j \Big] , \tag{II.8}$$

where $\underset{\sim}{a}_k$ is the equilibrium position of nucleus k.

Successive integrations of $\rho(\underset{\sim}{r}_1 \cdots \underset{\sim}{r}_n ; \underset{\sim}{r}_1 \cdots \underset{\sim}{r}_n)$ over the displacements do not alter the general functional form. Each integration yields a pure exponential with a homogeneous polynomial of second order as the exponent. Assuming the lattice invariant under the operations $(x \to -x,\ y \to y)$, $(x \to x,\ y \to -y)$, and $(x \to y,\ y \to -x)$, we obtain an expression of the form

$$\rho(\underset{\sim}{r}) = D \exp\Big[-\tfrac{1}{2} \frac{(x^2 + y^2)}{\langle x^2 \rangle} - \frac{z^2}{2\langle z^2 \rangle} \Big] \tag{II.9a}$$

where

$$\underset{\sim}{r} = (x, y, z) \quad . \tag{II.9b}$$

Comparing Eqs. (II.7) and (II.9) we find that the probability density for the relative motion of particles 1 and 2 is, for small displacements from equilibrium, the same as the probability density for a three-dimensional harmonic oscillator. Thus, if we are to represent the effects of the lattice on the relative motion of 1 and 2 by a potential $U(\underset{\sim}{r})$, we must require that, for $\underset{\sim}{r} \approx (0, 0, b_{nn})$,

$$\frac{z^2 e^2}{r} + U(\underset{\sim}{r}) \approx \frac{z^2 e^2}{b_{nn}} + U(0, 0, b_{nn}) + \tfrac{1}{2} \mu \Omega_x^2 (x^2 + y^2) + \tfrac{1}{2} \mu \Omega_z^2 (z - b_{nn})^2 \tag{II.10a}$$

where

$$\langle x^2 \rangle = \langle y^2 \rangle = \tfrac{1}{2} (\hbar / \mu \Omega_x) \coth (\tfrac{1}{2} \beta \hbar \Omega_x) \tag{II.10b}$$

and

$$\langle (z-b_{nn})^2 \rangle = \tfrac{1}{2}(\hbar/\mu\,\Omega_z)\coth(\tfrac{1}{2}\beta\hbar\,\Omega_z) \quad . \qquad \text{(II.10c)}$$

We shall consider the calculation of $\langle x^2 \rangle$ and $\langle (z-b_{nn})^2 \rangle$ in Sec. IID.

C. Choice of the Effective Potential

We have shown that an effective potential accurately describes the effects of the lattice Coulomb fields in two cases: r near zero and $\underset{\sim}{r}$ near $(0,0,b_{nn})$. We assume that an effective potential can adequately represent the effects of the lattice Coulomb fields on $\rho(\underset{\sim}{r})$ for all $\underset{\sim}{r}$. In accordance with Eq. (II.3) and (II.4), we choose the zero of energy such that

$$U(0,0,0) = 0. \qquad \text{(II.11)}$$

Since nuclei 1 and 2 are assumed identical, the potential $U(\underset{\sim}{r})$ satisfies the relation

$$U(\underset{\sim}{r}) = U(\underset{\sim}{r}_1 - \underset{\sim}{r}_2) = U(\underset{\sim}{r}_2 - \underset{\sim}{r}_1) = U(-\underset{\sim}{r}) \quad ,$$

which implies that

$$\nabla U(0,0,0) = 0 \quad . \qquad \text{(II.12)}$$

Considering Eqs. (II.10), (II.11) and (II.12), we assume that

$$U(\underset{\sim}{r}) = k_2\, r^2 + k_3\, r^3 + k'(x^2+y^2) \quad , \qquad \text{(II.13a)}$$

where

$$k_2 = 2\,Z^2e^2\,b_{nn}^{-3} - \tfrac{1}{2}\mu\,\Omega_z^{\,2} \quad , \qquad \text{(II.13b)}$$

$$k_3 = -Z^2e^2 b_{nn}^{-4} + 1/3\,\mu\,\Omega_z^{\,2} b_{nn}^{-1} \quad , \qquad \text{(II.13c)}$$

and

$$k' = \tfrac{1}{2}\mu\,\Omega_x^{\,2} \quad . \qquad \text{(II.13d)}$$

The reaction rate depends on $U(\underset{\sim}{r})$ primarily through a WKB barrier penetration integral. This integral depends strongly on the behavior of $U(\underset{\sim}{r})$ near the equilibrium position $(0,0,b_{nn})$, but it does not depend strongly on the behavior of $U(\underset{\sim}{r})$ for smaller $\underset{\sim}{r}$. Since the value of $U(\underset{\sim}{r})$ for $\underset{\sim}{r}$ near $(0,0,b_{nn})$ is determined directly by Eq. (II.10), the value of the barrier penetration integral is relatively insensitive to the arbitrariness in the choice of a form for $U(\underset{\sim}{r})$. Several other smooth forms chosen for $U(\underset{\sim}{r})$, forms still consistent with Eqs. (II.10) to (II.12), have been found to give values of the barrier penetration integral that are within a few percent of the values obtained using Eq. (II.13).

D. Calculation of the Oscillator Frequencies

The effective potential $U(\underset{\sim}{r})$ can now be determined if we can calculate the quantities $\langle x^2 \rangle$ and $\langle (z-b_{nn})^2 \rangle$. The oscillator frequencies Ω_x and Ω_z could then be determined using Eqs. (II.10b) and (II.10c), and the parameters k_2, k_3, and k' could be calculated from Eqs. (II.13b) - (II.13d).

The phonon approach of solid-state physics provides an easy way of calculating $\langle x^2 \rangle$ and $\langle (z-b_{nn})^2 \rangle$. For the case of a periodic lattice, the normal mode vibrations can be described as lattice waves with given wave numbers and polarizations. The characteristic frequencies and polarization vectors for a body-centered cubic lattice were calculated numerically for several thousand wave numbers in the first Brillouin zone*, and the expectation values $\langle x^2 \rangle$ and $\langle (z-b_{nn})^2 \rangle$ were computed

*The normal-mode eigenvalues and eigenvectors for the lattice of like charges have been calculated by other authors for the purpose of calculating the ground-state energy of the lattice. See, for example, reference 9.

using a suitable average over the first Brillouin zone. For zero temperature, we obtain, using Eqs. (II.10b) and (II.10c).

$$\Omega_x = 1.28\ \omega_o \quad , \tag{II.14a}$$

and

$$\Omega_z = 1.88\ \omega_o \quad , \tag{II.14b}$$

where

$$\omega_o = Ze\ (Mb^3)^{-\frac{1}{2}} \quad . \tag{II.14c}$$

These numerical values are expected to be accurate to within 1% for the physical model adopted here.

The oscillators frequencies Ω_x and Ω_z are nearly independent of temperature: Their values at all temperatures are within about 20% of the zero-temperature values. Since we shall find that the solid state approach applies only to temperatures small compared to $\hbar\omega_o/k$, it is sufficient to use just the zero-temperature values.

E. Comparison with the Static Model

We have determined the lattice potential $U(\underset{\sim}{r})$ by examining small vibrations of the lattice. The strong coupling between the relative motion of two reacting particles and the motion of neighboring nuclei is thus taken into account approximately.

The frequencies Ω_x and Ω_z can be obtained more easily if one neglects the lattice motion and calculates $U(\underset{\sim}{r})$ using a purely electrostatic model. This procedure has the advantage of allowing direct numerical calculation of $U(\underset{\sim}{r})$ for any $\underset{\sim}{r}$, thereby eliminating the need for relying on an extrapolation formula like Eq. (II.13a). Van Horn

has shown that, in this static approximation,

$$\Omega_x = 1.85\ \omega_o \qquad \text{(II.15a)}$$

and

$$\Omega_z = 2.39\ \omega_o \qquad \text{(II.15b)}$$

for the bcc lattice structure.

Comparison of Eqs. (II.15) with Eqs. (II.14) indicates that coupling to the lattice motion decreases the oscillator frequencies somewhat. The second derivatives $\partial^2 V/\partial z^2\ (0,0,b_{nn})$ and $\partial^2 V/\partial x^2\ (0,0,b_{nn})$ are reduced by 38% and 52%, respectively, by the motion of the lattice. The lattice effectively polarizes under the influence of the motion of the two reacting particles. This polarization acts to reduce the Coulomb fields that oppose displacements of the reacting nuclei from their equilibrium positions. Lattice polarization increases the reaction rate noticeably. Figure 3 compares reaction rates computed using the static and dynamic values of Ω_x and Ω_z.

III. CALCULATION OF THE REACTION RATE

In this section, we derive an expression for the reaction rate. We begin by finding a formula for the reaction rate in terms of the wave function corresponding to the nonnuclear potential

$$V(\underset{\sim}{r}) = Z^2e^2r^{-1} + k_2r^2 + k_3r^3 + k'(x^2 + y^2) \quad . \qquad \text{(III.1)}$$

In Subsections III-B and III-C, we derive the wave function, and in Subsection III-D we obtain the reaction rate itself.

A. General Expression for the Reaction Rate

The total potential affecting the relative motion of two reacting particles is the sum of the nonnuclear potential $V(\underset{\sim}{r})$ of Eq. (III.1) and a nuclear potential. The nuclear potential is effectively zero except within a radius R, where

$$R \ll b_{nn} \quad , \qquad \text{(III.2)}$$

since we limit ourselves to densities well below nuclear densities.

We decompose the regular solution to the Schrödinger equation

$$\left\{\nabla^2 + 2\mu\hbar^{-2}\,[E - V(\underset{\sim}{r})]\right\}\Psi(\underset{\sim}{r}) = 0 \qquad \text{(III.3)}$$

in terms of spherical harmonics as follows:

$$\Psi(\underset{\sim}{r}) = \sum_{LM} a_{LM}\, f_L(E;r)\, Y_{LM}(\Omega) \quad . \qquad \text{(III.4)}$$

Let the regular solution to the Coulomb-wave Schrödinger equation

$$\left\{\nabla^2 + 2\mu\hbar^{-2}\,[E - Z^2e^2r^{-1}]\right\}\Psi^c(\underset{\sim}{r}) = 0. \qquad \text{(III.5)}$$

be written

$$\Psi^c(\underset{\sim}{r}) = \sum_{LM} a^c_{LM} f_L^c(E;r)\, Y_{LM}(\Omega) \quad . \qquad \text{(III.6)}$$

Since

$$V(r) \approx Z^2 e^2 r^{-1} \qquad \text{(III.7)}$$

for $r \ll b_{nn}$, the radial functions $f_L(E;r)$ and $f_L^c(E;r)$ must differ only by a constant factor when r is near the nuclear radius R, which is small compared to b_{nn}. Thus it is interesting to compare the reaction rate $\Gamma(E)$ for an external potential $V(\underset{\sim}{r})$ with the rate $\Gamma^c(E)$ of the same reaction at the same energy but with an external potential $Z^2e^2r^{-1}$.

We limit ourselves to reactions in which one incident orbital angular momentum value L dominates the reaction rate. We also choose a $\Psi^c(\underset{\sim}{r})$ which approaches a plane wave of unit intensity as $r \to \infty$, except for the usual slowly varying phase factor characteristic of Coulomb waves. We normalize $f_L^c(E;r)$ such that

$$f_L^c(E;r) \to (\kappa r)^{-1} \sin [\kappa r - \alpha(r)] \qquad \text{(III.8)}$$

as $r \to \infty$. Then one can show that the reaction rates for external potentials $V(\underset{\sim}{r})$ and Z^2e^2/r are related as follows:

$$\frac{\Gamma_L}{\Gamma_L^c} = \frac{\Sigma_M |a_{LM}|^2}{4\pi(2L+1)} \lim_{r \to 0} \left| \frac{f_L(E;r)}{f_L^c(E;r)} \right|^2 \quad . \qquad \text{(III.9)}$$

In the following subsections, we find expressions for a_{LM} and $f_L(E;r)$ for substitution in Eq. (III.9).

B. The Radial Equation

The remaining problem is to solve Eq. (III.3) for $\Psi(\underset{\sim}{r})$. We concluded in Sec. II that the harmonic oscillator approximation is valid near the point $(0,0,b_{nn})$. Thus near $(0,0,b_{nn})$ we can write

$$\sum_{LM} a_{LM} f_L(r) Y_{LM}(\Omega) = U_x(n_x;x)\, U_y(n_y;y)\, U_z(n_z;z) \ . \tag{III.10a}$$

The right side of Eq. (III.10a) represents a normalized three-dimensional harmonic oscillator wave function with frequencies Ω_x, Ω_x, and Ω_z and occupation numbers n_x, n_y, and n_z.

The harmonic oscillator wave functions describe the total wave function accurately except in regions far from the classically allowed domain. Since the wave function is extremely small in the remote regions where the harmonic oscillator approximation breaks down, the harmonic oscillator approximation provides an excellent approximation to the energy eigenvalues. Taking account of the fact that the potential is not zero at the equilibrium position, we find that

$$E \approx V(0,0,b_{nn}) + (n_z + \tfrac{1}{2})\,\hbar\Omega_z + (n_x + n_y + 1)\,\hbar\Omega_x \ . \tag{III.10b}$$

The harmonic oscillator wave functions are large only near $x = 0$, $y = 0$, $z = b_{nn}$, or, in other words, $r = b_{nn}$, $\theta = 0$. Thus the product $U_x(n_x;x)\, U_y(n_y;y)$ essentially expresses the angular dependence of the wave function while $U_z(n_z;z)$ describes the radial dependence. Hence we can write

$$f_L(n_z;r) \approx U_z(n_z;r) b_{nn}^{-1} \tag{III.11}$$

for r near b_{nn} and

$$a_{LM}(n_x n_y) \approx b_{nn}^{-1} \int_{-\infty}^{\infty} dx \int_{-\infty}^{\infty} dy\, U_x(n_x;x)\, U_y(n_y;y)\, Y_{LM}^{*}[\Omega(x,y)] \quad . \tag{III.12a}$$

In this approximation the coefficients a_{LM} depend on n_x and n_y, but not on n_z. We have shown that the radial wave function is independent of n_x and n_y for r near b_{nn}, and we shall show later that f_L is approximately independent of n_x and n_y for smaller r.

We should note that the integration in Eq. (III.12a) can be performed readily for the important special case where $n_x = n_y = L = M = 0$, and the result is

$$a_{oo}(0,0) \approx \hbar^{\frac{1}{2}} (\mu \Omega_x b_{nn}^{2})^{-\frac{1}{2}} \quad . \tag{III.12b}$$

According to Eq. (III.11), $f_L(n_z;r)$ must satisfy the same differential equation as $U_z(n_z;r)$ for r near b_{nn}. Thus we find that

$$\left[-\frac{d^2}{dr^2} + g_1(r) \right] f_L(n_z,r) \approx 0 \tag{III.13a}$$

for r near b_{nn}. The quantity $g_1(r)$ is defined by

$$g_1(r) = 2\mu\hbar^{-2} [V(0,0,r) - V(0,0,b_{nn}) - (n_z + \tfrac{1}{2})\hbar\Omega_z] \quad . \tag{III.13b}$$

We want to compare Eqs. (III.13) with the equation f_L satisfies for small r. At small r, we can neglect the anisotropy of the potential and separate the solution into radial and angular components in the usual way. Then, for $r \ll b_{nn}$, f_L satisfies the equation

$$\left[-\frac{d^2}{dr^2} + \frac{L(L+1)}{r^2} + g_2(r)\right] \left[r\, f_L(n_z;r)\right] = 0 \quad , \qquad \text{(III.14a)}$$

where

$$g_2(r) = g_1(r) - 2\,\mu\,\hbar^{-1}\,\Omega_x\,(n_x + n_y + 1) \quad . \qquad \text{(III.14b)}$$

It would, of course, be convenient if $f_L(n_z;r)$ satisfied the same differential equation for all r, $0 < r < b_{nn}$. We now show that the radial wave function approximately satisfies the differential equation

$$\left[-\frac{d^2}{dr^2} + \frac{L(L+1)}{r^2} + g_1(r)\right] \left[r\, f_L(n_z;r)\right] = 0 \qquad \text{(III.15)}$$

both for $r \approx b_{nn}$ and for $r \ll b_{nn}$ by noticing that Eqs. (III.13a) and (III.15) are approximately the same for r near b_{nn} and that Eqs. (III.14a) and (III.15) are essentially equivalent for small r. Comparing Eqs. (III.13a) and (III.15) we note the following facts: (1) the term $L(L+1)r^{-2}$ in Eq. (III.15) is negligibly small for r near b_{nn} providing the expectation value $\langle (z-b_{nn})^2 \rangle$ is small compared to b_{nn}^2; and (2) the quantity $rf_L(n_z;r)$ can be accurately approximated by $b_{nn}\, f_L(n_z;r)$ for r near b_{nn}. It follows that Eqs. (III.13a) and (III.15) are essentially the same for r near b_{nn}. Comparing Eqs. (III.14a) and (III,15) for $r \ll b_{nn}$, we notice that the quantity ϵ_{xy} defined by

$$\epsilon_{xy} = 2\,\mu\,\Omega_x\hbar^{-1}\,(n_x + n_y + 1) \quad , \qquad \text{(III.16)}$$

is small compared to $2\,\mu\,Z^2e^2\hbar^{-2}r^{-1}$. Thus Eqs. (III.14a) and (III.15) differ little for $r \ll b_n$. We have now established that Eq. (III.15) holds accurately in the limits of large and small r. We assume that it holds approximately for intermediate r.

By making various approximations we have shown that the radial wave function satisfies Eq. (III.15) for all r. In Subsection III-C we use a modified WKB approximation to solve Eq. (III.15) for $f_L(n_z;r)$. The effects of the approximations made in deriving Eq. (III.15) can be estimated by examining the WKB barrier-penetration integral. One finds that the most serious approximation involved in Eq. (III.15), the neglect of ϵ_{xy} for small and intermediate r, should cause an error of less than 2% in the barrier penetration integral.

C. The Radial Wave Function

Our method of solving Eq. (III.15) approximately for $f_L(n_z;r)$ is algebraically complicated but straightforward. It introduces errors small compared to those due to the approximations involved in Eq. (III.15) itself. Thus we only outline the procedure briefly.

We use the modified WKB approximation[10] in which the centrifugal potential is represented by $(L+\frac{1}{2})^2 r^{-2}$ instead of $L(L+1)r^{-2}$. We determine the normalization by matching the WKB approximation to the harmonic oscillator wave function for r near b_{nn}. The WKB integral cannot be evaluated analytically, but it can be expressed to a good approximation as the sum of two integrals which can be calculated exactly. The first integral is the one that appears in the WKB approximation to a Coulomb wave function. Thus the radial wave function $f_L(n_z;r)$ can be written as the product of a Coulomb wave function and a correction factor. The Coulomb wave function appearing in $f_L(n_z;r)$ is $f_L^c(E';r)$, where

$$E' = Z^2 e^2 r_c^{-1} (1+\xi^{-1}) \quad . \qquad \text{(III.17)}$$

The relation

$$\xi = 2 \mu Z^2 e^2 \hbar^{-2} (l+\tfrac{1}{2})^{-2} r_c \qquad \text{(III.18)}$$

defines the parameter ξ, which is usually much larger than one. Thus E' is approximately the energy of a pure Coulomb wave with classical turning point r_c. The classical turning point radius can be expressed in the approximate form

$$r_c \approx b_{nn} - [\hbar(2n_z + 1)]^{\frac{1}{2}} (\mu \Omega_z)^{-\frac{1}{2}} \quad , \qquad \text{(III.19)}$$

providing the vibrations are small.

To find the reaction rate using Eq. (III.9), we must calculate the ratio Q given by

$$Q = \lim_{r \to 0} \frac{f_L(n_z;r)}{f_L^{\,c}(E;r)} \quad , \qquad \text{(III.20)}$$

where E is defined in Eq. (III.10b). The quotient Q is the ratio of the Coulomb wave functions for energies E' and E multiplied by a correction factor.

We must define four parameters occurring in the two Coulomb wave functions. The expressions

$$K = \hbar^{-1} (2\mu E)^{\frac{1}{2}} \qquad \text{(III.21)}$$

and

$$K' = \hbar^{-1} (2\mu E')^{\frac{1}{2}} \qquad \text{(III.22)}$$

express the wave numbers in terms of the energies, while the equations

$$\eta = Z^2 e^2 \mu \hbar^{-2} \kappa^{-1} \quad , \tag{III.23}$$

and

$$\eta' = Z^2 e^2 \mu \hbar^{-2} (\kappa')^{-1} \quad , \tag{III.24}$$

give the Coulomb field parameters in terms of the wave numbers.

We must also define some parameters occurring in the correction factor that multiplies the ratio of the Coulomb wave functions. Let

$$\zeta = 2 \mu k_2 \hbar^{-2} (L+\tfrac{1}{2})^{-2} r_c^{\,4} \quad , \tag{III.25}$$

and

$$\sigma = 2 \mu k_3 \hbar^{-2} (L+\tfrac{1}{2})^{-2} r_c^{\,5} \quad . \tag{III.26}$$

Then define A, B, C, and D by the relations

$$A = (1/16)\,(3\xi^3 + 4\xi^2 - 4\xi)\,(1+\xi)^{-7/2} \quad , \tag{III.27}$$

$$B = (1/128)\,(29\xi^4 + 72\xi^3 + 24\xi^2 - 32\xi - 48)\,(1+\xi)^{-9/2} \quad , \tag{III.28}$$

$$C = (1/24)\,(9\xi^2 + 32\xi + 8)\,(1+\xi)^{-3} \quad , \tag{III.29}$$

$$D = (1/192)\,(87\xi^3 + 356\xi^2 + 356\xi + 192)\,(1+\xi)^{-4} \quad , \tag{III.30}$$

Finally, let

$$I = (L+\tfrac{1}{2})\,[(\cos^{-1}\alpha)\,(\zeta A + \sigma B) + \zeta C + \sigma D] \quad , \tag{III.31a}$$

where

$$\alpha = -\xi(\xi+2)^{-1} \quad . \tag{III.31b}$$

Then one can show that

$$Q = F \exp[\tfrac{1}{2} I - \pi(\eta' - \eta)] \quad , \tag{III.32a}$$

where

$$F = \left[\frac{2\mu\Omega_z (\kappa')^{2L}}{\pi\hbar\kappa^{2L-1}} \prod_{s=1}^{L} \left(\frac{1+\eta'^2 s^{-2}}{1+\eta^2 s^{-2}}\right)\right]^{\frac{1}{2}} \quad , \tag{III.32b}$$

The quantity Q gives the ratio of the wave function $f_L(n_z;r)$ to the Coulomb wave function for the energy E. We now use Eqs. (III.32) in Eq. (III.9) to find the reaction rate.

D. The Reaction Rate

We first consider the reaction rate from an initial state (n_x,n_y,n_z). Substituting Eqs. (III.32) in Eq. (III.9) yields

$$\Gamma_L(n_x,n_y,n_z) = G\Gamma_L^c(E) \quad , \tag{III.33a}$$

where

$$G = [4\pi(2L+1)]^{-1} F^2 \Sigma_M \left|a_{LM}(n_x,n_y)\right|^2 \exp [I-2\pi(\eta'- \eta)] \quad , \tag{III.33b}$$

and $\Gamma_L^c(E)$ is the reaction rate for a pure Coulomb wave with energy E.

To find the average lifetime of a nucleus in a stellar interior, we must perform a thermal average over oscillator states. We shall find in Section IV that the theory applies only to temperatures low enough that

$$\hbar\,\Omega_x(kT)^{-1} \gg 1. \tag{III.34}$$

Thus we assume n_x and n_y are both zero. The sum over n_z must be carried out, however, due to the strong dependence of η' on n_z. Consistent with our previous assumption of a bcc lattice, we assume each nucleus has eight nearest neighbors and obtain the expression

$$\tau_L^{-1} = 8 \sum_{n_z=0}^{\infty} \Gamma_L(0,0,n_z) \exp \left[- n_z \hbar\, \Omega_z(kT)^{-1}\right] \quad , \tag{III.35}$$

for the inverse lifetime.

In the important special case of an s-wave interaction, the reaction rate corresponding to a Coulomb wave with unit number density at infinity is often written[11]

$$\Gamma_o^c = S(E)\, vE^{-1} e^{-2\pi\eta} \quad , \qquad \text{(III.36)}$$

where the cross-section factor S(E) can usually be determined from the results of laboratory experiments; it contains all of the purely nuclear aspects of the reaction rate. The quantity v in Eq. (III.36) is the velocity corresponding to energy E and wave number K. Using Eqs. (II.14), (III.12b), (III.32b), (III.33), and (III.36) in Eq. (III.35), one finds that the inverse lifetime for an s-wave reaction is given by

$$\tau_o^{-1} = J \sum_{n_z} S(E) \exp\left[-2\pi\eta' + I - n_z \hbar\Omega_z (kT)^{-1}\right] \qquad \text{(III.37a)}$$

where

$$J = 1.00\, (\rho/M)^{2/3} \hbar^{-1} \quad . \qquad \text{(III.37b)}$$

The quantities η' and I were defined in Eqs. (III.24) and (III.31), respectively. The energy E can be written in the convenient form

$$E = 1.48\, Z^2 e^2\, (\rho/M)^{1/3} + 1.88\, (n_z + \tfrac{1}{2})\, \hbar Z e \rho^{\frac{1}{2}} M^{-1} \qquad \text{(III.38)}$$

Equations (III.35) and (III.37) give the inverse lifetime of a nucleus in a solid lattice of density ρ. In Section IV we describe the range of temperatures and densities to which these formulae apply.

IV. LIMITATIONS

A. Assumption of One L-Value

We have assumed that one initial value of orbital angular momentum dominates the reaction rate. Reactions between light nuclei are predominantly s-wave, but several different orbital angular momenta may be important in reactions between heavier nuclei. Incorrectly assuming that one L-value dominates the rate, one may overlook the effects of interference and may make errors in the geometrical factors a_{IM}, but such errors are unlikely to amount to as much as a factor of ten. The barrier penetration factors for reactions between heavy particles range from about e^{-50} to e^{-150} for the conditions to which the solid-state model applies. Due to our incomplete knowledge of $U(\underset{\sim}{r})$ and our approximate method of solving the Schrödinger equation, we are likely to make errors of several percent in the barrier penetration exponents. These errors are likely to be larger than any caused by incorrect assumptions about the dominant L-values.

B. Resonant Reactions

The treatment outlined above does not apply directly to reactions with strong resonances at energies smaller than about two or three times $Z^2e^2b^{-1}$, which ranges from less than 1 keV for protons at 10^5 gm/cc to several hundred keV for carbon nuclei at 10^{10} gm/cc. The widths of the harmonic oscillator states are likely to be large compared to the widths of the nuclear resonances. To apply the solid-state treatment to a reaction like

$$3\,He^4 \rightarrow C^{12} + \gamma \quad ,$$

which involves low-lying resonances, one would have to estimate the widths of the oscillator states and replace the sum in Eq. (III.37a) by an integral.

C. High-Density Limit

At high densities, the amplitudes of the ground-state vibrations may become comparable to b_{nn}. When this happens, the nuclei no longer form a bcc lattice, as assumed in Sections II and III. Several investigators have estimated the "melting density" of a lattice consisting of electrons immersed in a uniform distribution of positive charge. These estimates can easily be converted to apply to the case of a lattice of nuclei in a uniform negative charge density. The most recent estimates are those by de Wette[12]. His work locates the melting density in the range

$$1.6 \times 10^4 \, Z^6 A^4 < \rho_m < 1.6 \times 10^5 \, Z^6 A^4 \quad , \qquad \text{(IV.1)}$$

where ρ_m is in gm/cc. Earlier work[13],[14] indicated a melting density of about $10^6 \, Z^6 A^4$ gm/cc.

Just above the melting point, the nuclei form a fluid rather than a periodic lattice, but the motion is still largely vibrational. In this liquid range, where the mean free path between collisions is small compared to b_{nn} but the vibrations are still too large to allow a strictly periodic lattice, it still seems reasonable to treat the relative motion of two particles using the potential of Eq. (II.13a) That potential depends on the assumption of a bcc lattice through the parameters b_{nn}, Ω_x and Ω_z. The nearest-neighbor distance varies only

a few percent from one lattice structure to another. The frequencies Ω_x and Ω_z have been calculated for the fcc lattice and for a "smeared out" lattice intended to resemble a liquid, and the results are within about 10% of the values obtained for the bcc lattice. Thus we conclude that the parameters b_{nn}, Ω_x, and Ω_z are nearly independent of the geometrical arrangement of the lattice, although they depend strongly on the density and on the charge and mass of the nuclei. It is, therefore, reasonable to expect that the values of b_{nn}, Ω_x, and Ω_z for the bcc lattice also suffice for the range of densities where the nuclei execute small vibrations in a nonperiodic lattice. The range of applicability of the formula could then be extended to a density given by the approximate relation

$$\rho_c \approx 10^6 Z^6 A^4 \text{ gm/cc} \quad . \tag{IV.2}$$

The above considerations are important mainly for reactions between protons. At densities greater than about 10^6 gm/cc, a zero-temperature proton star could be described more accurately as a degenerate gas than as a solid. Thus the solid-state approach fails to apply to protons at densities well below those expected in neutron stars.

We have also assumed that the nearest-neighbor distance is large compared to the nuclear radius. Thus the solid-state model applies only if

$$\rho \ll 10^{14} \text{ gm/cc} \quad . \tag{IV.3}$$

D. High-Temperature Limit

The temperature enters the expression for the reaction rate through the sums over n_z in Eqs. (III.35) and (III.37). Below a critical temperature T_c, given approximately by the relation

$$T_c \approx 1200\ ZA^{-1}\ \rho^{\frac{1}{2}} \quad , \tag{IV.4}$$

where T_c is in $^{\circ}K$ and ρ is in gm/cc, essentially all reactions take place from the ground state. Thus for $T \ll T_c$, the rate is independent of T. Near the temperature T_c, the first few excited states become important, and the rate begins to increase with temperature. At a temperature just slightly above T_c, most reactions take place from unbound states, and the solid-state approach fails. Just above the critical temperature, most of the nuclei in the lattice are still in their ground states because

$$\hbar\Omega_x(kT_c)^{-1} \approx 2.4 \quad , \tag{IV.5}$$

and

$$\hbar\Omega_z(kT_c)^{-1} \approx 3.5 \quad . \tag{IV.6}$$

However, the exceptionally energetic nuclei that are most likely to react have enough energy to break through the lattice. The mean free path between collisions of these unusually energetic nuclei is large compared to b_{nn}, and they can be treated approximately as gas particles. Salpeter[18] has developed a method for calculating reaction rates for $T \gg T_c$.

V. NUMERICAL RESULTS

A. Proton-Proton Reactions

Equations (III.37) have been used to calculate the mean lifetime of the protons in hydrogen stars at various temperatures and densities. The protons were assumed to undergo the reactions

$$H^1 + H^1 \longrightarrow H^2 + e^+ + \nu \qquad (V.1)$$

and

$$H^1 + e^- + H^1 \longrightarrow H^2 + \nu \quad . \qquad (V.2)$$

For densities greater than about 10^5 gm/cc, the extreme degeneracy of the electrons causes the capture reaction (V.2) to dominate the process of hydrogen burning.

Figure 2 shows the temperature dependence of the mean lifetime at a density of 10^5 gm/cc. Below a critical temperature of about 2×10^5 ^oK, the reaction rate is independent of temperature. Above about 10^6 ^oK, the formula of Salpeter[8] should be accurate.

B. Carbon-Carbon Reactions

The mean lifetime of C^{12} nuclei in stars of pure carbon have also been computed. Two carbon nuclei may react to form the following products: $Mg^{24} + \gamma$, $Na^{23} + H^1$, $Mg^{23} + n$, $Ne^{20} + He^4$, and $O^{16} + 2He^4$. Equations (III.37) were used to calculate the mean lifetime of the carbon nuclei, even though there is no reason to expect that the reactions are predominantly s-wave. Reeves[15] has expressed the rate of the carbon-carbon reactions in terms of the cross section parameter S(E). The small errors caused by estimating the

geometrical factors a_{IM} incorrectly and by neglecting interference effects should not be serious because of the strong density-dependence of the reaction rate.

Figure 3 shows the mean lifetime of a carbon nucleus at 10^7 ^oK. At low temperatures the reaction rate is significant for densities greater than about 10^{10} gm/cc. The rate of the $C^{12}+ C^{12}$ reactions depends much more strongly on density than the rate of the proton-proton reactions because the barrier penetration exponent is much larger for Z = 6 than for Z = 1.

C. Comparison with Earlier Work

Cameron[4] has suggested calculating the rates of pycnonuclear reactions by treating the system of nuclei as a gas with Coulomb interactions between the particles. The curve marked "GAS(CAMERON)" in Figure 3 was computed by a method similar to that proposed by Cameron, using the same value of the cross-section parameter S(E)[15] as in the solid-state calculation.

Figure 3 indicates that for the $C^{12}+ C^{12}$ reaction, the solid-state method predicts rates ten to fifteen orders of magnitude smaller than those computed by the gas model. The large discrepancy in the predictions of the two models is due to the different estimates of the classical turning point radius, r_c, which is an important factor in the barrier penetration exponent. According to the solid-state approach, r_c is slightly less than the nearest-neighbor distance. According to Cameron's model of electrostatic screening at low temperatures, r_c is slightly less than the charge-cloud radius, given by

$(3Z_1)^{1/3}(4\pi n_e)^{-1/3}$, where $Z_1 \geq Z_2$. For $Z_1 = Z_2$, this charge-cloud radius is only 0.57 of our nearest-neighbor distance. Due to the strong dependence of the barrier penetration factor on the classical turning point, this factor of 0.57 causes a large difference in the predicted rates. Cameron's method should be reasonably accurate, however, if $Z_1 \gg Z_2$.

Shortly after the importance of the p+p reaction in main-sequence stars was first pointed out, Wildhack[1] made an estimate of the rate of the p+p reaction in white-dwarf stars. As in the present work, he estimated the rate at which the reaction proceeds between protons oscillating about adjacent lattice sites. Wildhack was primarily interested in answering the simple question of whether the interior of a white dwarf could be made up primarily of protons; he was not interested in obtaining an accurate number for the reaction rate. Consequently, he made only a rough analysis of the lattice Coulomb fields and he neglected motions of neighboring protons. He also used the unmodified WKB approximation in a way that is known not to be valid. Consequently, his estimates of the rate of the p+p reaction are about two orders of magnitude smaller than the results obtained here, for densities less than 10^5 gm/cc. At higher densities, Wildhack's rate diverges further from ours because he neglected reaction (V.2).

2. THE COOLING OF NEUTRON STARS*

I. INTRODUCTION

The existence of neutron stars was long ago predicted theoretically by Landau[1], Baade and Zwicky[2], and others. Neutral matter at densities of 10^{14} or 10^{15} gm/cm^3 should, except at extremely high temperatures, consist primarily of neutrons. Stellar models[3]-[6] indicate that stable stars with masses less than about one solar mass could exist with central densities of 10^{14} to 10^{15} gm/cm^3. Such dense configurations might be seen in nature as remnants of supernova explosions. It has recently been suggested that neutron stars might be detected indirectly through the effects of their oscillations,[7],[8] but the most obvious and convincing way to establish the existence of a neutron star would be to detect photons radiated from the star's surface. The thermal photons should be in the X-ray region because of the high temperatures expected on the surfaces of neutron stars.

Measurements made on recent rocket flights above the earth's atmosphere have demonstrated the existence of several discrete sources of galactic X-rays[9]-[12], and various authors[13]-[15] have suggested that these observed sources might be the long awaited neutron stars. Other authors have proposed that the observed X-rays may be synchrotron radiation from energetic electrons in magnetic fields[16] or bremsstrahlung radiation from hot clouds of electrons and nuclei.[16],[17]

---

*A preliminary account of this work is given in the following communication: J. N. Bahcall and R. A. Wolf, Phys. Rev. Letters 14, 343 (1965). The details of the treatment are described in two papers that are to be published in the Physical Review, and observational consequences are discussed in a brief note to be published in the Astrophysical Journal.

The neutron star hypothesis is the most specific of the suggested X-ray producing mechanisms, and it is thus the easiest hypothesis to disprove by observations. The most obvious property of a neutron star, its small size, has led to observational proof[18] that the principal X-ray source in the Crab nebula is not a neutron star; the results of the recent occultation experiment indicate that the source in the Crab has a diameter of the order of one light year. Another important property of a neutron star is that it should radiate approximately as a black body. Recent detailed measurements[19],[20] performed on the X-ray source in Scorpius have shown that the spectrum of the source does not resemble that of a black body and that the flux of high-energy photons is much greater than one would expect from a neutron star with a reasonable surface temperature. These observations have not, of course, shown that neutron stars do not contribute any of the X-rays from the Crab or Scorpius, but they do show that most of the X-rays from the Crab come from a diffuse source, and that most of the short-wavelength radiation from Scorpius comes from something other than a neutron star.

In the present work, we attempt to estimate the rate of neutrino emission from neutron-star matter. Our original goal in performing detailed cooling calculations was to derive a unique, reasonably accurate expression for the rate at which a neutron star must cool. This goal has not been attained fortwo reasons. First, we have found that the rate of neutrino emission depends strongly on the density of the neutron-star matter; the cooling rates of stars with different masses may, therefore, differ by several orders of magnitude. Second, more careful consideration of the processes involved in neutrino emission

from neutron-star matter has increased, rather than decreased, the apparent theoretical uncertainty about the cooling rate of a given star. In particular, the cooling rate depends strongly on the assumptions made about the following difficult theoretical points: the existence of quasi-free pions in neutron-star matter, the existence of a superfluid-gap in the excitation spectra of the neutron and proton gases, and the stability of neutron-star matter to the formation of large-scale irregularities that resemble nuclei.

Although one cannot give a unique, reliable formula for the cooling rate of a neutron star, one can with reasonable confidence place a lower limit on the cooling rate, taking into account the obvious theoretical uncertainties as well as the variation of the cooling rates with stellar mass. This lower limit on the rate is still sufficiently high that it can be of some use in interpreting the X-ray observations. For example, the limiting cooling rate implies that the X-ray sources observed in the direction of the galactic center are very unlikely to be neutron stars.

We attempt to calculate the rates of the reactions

$$n + n \longrightarrow n + p + e^- + \bar{\nu}_e \quad , \tag{I.1}$$

$$n + n \longrightarrow n + p + \mu^- + \bar{\nu}_\mu \quad , \tag{I.2}$$

$$\pi^- + n \longrightarrow n + e^- + \bar{\nu}_e \quad , \tag{I.3}$$

and

$$\pi^- + n \longrightarrow n + \mu^- + \bar{\nu}_\mu \quad , \tag{I.4}$$

as well as the inverse processes

$$n + p + e^- \rightarrow n + n + \nu_e \quad , \tag{I.5}$$

$$n + p + \mu^- \rightarrow n + n + \nu_\mu \quad , \tag{I.6}$$

$$n + e^- \rightarrow n + \pi^- + \nu_e \quad , \tag{I.7}$$

and

$$n + \mu^- \rightarrow n + \pi^- + \nu_\mu \quad , \tag{I.8}$$

Reactions (I.1) and (I.5) were first discussed by Chiu and Salpeter[15] and the corresponding neutrino luminosities have previously been calculated[21], [22] under the implicit assumption that the neutrons and protons in a neutron star form a normal Fermi fluid. Our result for the rate of reactions (I.1) and (I.5) is, with the assumption of a normal Fermi fluid, about five times larger than any of the earlier results.

Reactions (I.3), (I.4), (I.7), and (I.8) would proceed extremely rapidly in any neutron star containing a significant number of quasi-free pions; the pionic reactions are so fast that a neutron star containing quasi-free pions would cool within a few days to a temperature so low that the star's surface radiation would be unobservable. The question of whether quasi-free pions can exist in neutron stars depends on the binding energies of protons, π^- mesons, and Σ^- particles in neutron-star matter. It is still unclear whether quasi-free pions can exist in neutron-star matter, because all of the relevant binding energies are difficult to calculate.

Reactions (I.1) to (I.8) are likely to contribute importantly to neutrino production in neutron-star matter between nuclear density and five or ten times nuclear density, for temperatures greater than about 2×10^8 $^\circ$K. The Appendix contains brief discussions of other relevant

reactions and their rates.

In this work, a neutron star is pictured as a collection of interacting particles, just as a nucleus is usually pictured as a collection of interacting neutrons and protons. We begin in Section II by discussing the limitations of this type of description. Then, adopting the particle-model once and for all, we discuss in Section III the calculation of the number densities of various species of particles in a neutron star. The Fermi-fluid model of neutron-star matter is discussed in Section IV. The formation of Cooper pairs is considered along with the question of the stability of large-scale irregularities in the nucleon gas. Section V is devoted to estimating the effective masses of neutrons and protons in neutron-star matter.

Section VI contains a discussion of the opacity of neutron-star matter to low-energy neutrinos. The calculated value of the mean free path of a neutrino in neutron-star matter is many orders of magnitude larger than the radius of a neutron star. Thus nearly all the neutrinos emitted from the interior of a neutron star escape from the star.

The last four sections are devoted primarily to the calculation of the contributions of reactions (I.1)-(I.8) to the cooling rate of a neutron star. Section VII includes, first, a general discussion of the calculation of the neutrino luminosity of a star, and, second, some simple heuristic arguments that indicate the proper orders of magnitude for the rates of neutrino production by the nucleon-nucleon and pion-nucleon reactions. Sections VIII and IX contain the details of the calculation of the rates of reactions (I.1)-(I.8). The connection

between the neutrino luminosity and the rate at which the star's surface cools is considered in Section X. The cooling rates are worked out in detail for several simple cases, and a lower limit is established for the cooling rate of a neutron star. The relation between cooling times and observability is discussed briefly.

II. THE PARTICLE MODEL

The baryon number and charge of a neutron star in gravitational equilibrium uniquely determine the star's ground-state and excitation spectrum, just as the atomic number A and charge Z determine the ground state and excitation spectrum of a nucleus. But to deduce the detailed properties of a neutron star theoretically from knowledge of the baryon number and charge, one must use a detailed model. Most theories of nuclear structure involve picturing a nucleus as a collection of interacting neutrons and protons; such particle-models have been reasonably successful in explaining the observed properties of nuclei. In the same spirit, we shall picture neutron stars as collections of interacting particles. All calculations performed so far on neutron stars have leaned heavily on the idea that these nucleus-like stars are collections of individual particles.

The particle-model is clearly the most reasonable one at low densities. Collisions between particles are then rare, and they can be treated adequately using phenomenological potentials. As the density increases, collisions become more frequent. Since collisions between nucleons involve virtual transitions to other baryon states, an increase in density brings a corresponding increase in the "amount of time" each nucleon "spends" in a virtual state involving strange particles. The particle-model also predicts that strange particles should appear in non-virtual, quasi-free states at high densities, because the neutron and proton Fermi energies become so high that formation of non-nucleonic hadrons becomes energetically favorable. Thus, if we pursue the particle

model to densities large compared to nuclear density, we find that the ground-state of neutron-star matter contains an abundance of strange particles in both virtual and non-virtual states.

The particle-model consequently loses its usefulness at high densities. The short-range part of the nucleon potential, the part that is due to the exchange of strange particles, is not at all well-known; the interactions among the strange particles themselves are not well understood; and the problem of treating a complex collection of relativistic strongly-interacting particles would be mathematically intractable even if the individual interactions were understood.

It is easy to place a high-density limit on the usefulness of the particle-model. The short-range part of the nucleon-nucleon potential, the part that is often represented by a hard core, has a range approximately equal to the Compton wavelength of the K-meson, which is about 0.4 F. The mean distance between nucleons is equal to 0.4 F at about 2×10^{16} gm/cm^3. Strange particles should be produced in profusion in a neutron star when the neutron Fermi energy is of the order of 400 Mev; which, according to the free-particle approximation, corresponds to a density of about 5×10^{15} gm/cm^3. It is clear that the individual-particle model is completely unworkable above about ten or twenty times nuclear density. (Nuclear density is about 3.7×10^{14} gm/cm^3).

The ultimate answer to the problem of describing matter at extremely high densities may lie in constructing a theory based on entities that, unlike particles, are conserved in strong interactions. But such a theory has not yet been constructed, and for the present work we shall use the particle model, hoping that its success in the treatment of

nuclei indicates its approximate validity for densities not too far from nuclear density. We restrict ourselves in the present work to densities less than about five times nuclear density.

III. CONCENTRATIONS OF PARTICLES

A. General Discussion

Having adopted the particle model, we now attempt to estimate the relative abundances of the different types of particles present in a neutron star. We follow the treatment of Ambartsumyan and Saakyan[23], but we generalize their work by formally including the effects of interactions between particles.

We begin by making some definitions. The conditions of chemical equilibrium among various species of particles are expressed most easily in terms of chemical potentials, and it is convenient to write the chemical potential μ_i for Fermion species i in the form $m_i c^2 + E_{Fi} + B_i$, where m_i is the rest mass for species i, E_{Fi} is the Fermi energy for that species, and B_i is what we shall call the binding energy for species i. The quantity B_i represents the change that the interparticle interactions cause in the chemical potential of species i. The chemical potential for a boson of species j is written in the form $m_j c^2 + B_j$, because, at zero temperature and in the absence of interactions between particles, all bosons settle into a single-particle state with zero kinetic energy.

Neutrino-opacity calculations summarized in Section VI show that neutrinos and antineutrinos escape readily from a neutron star. Thus the density of neutrinos and antineutrinos is essentially zero, and these particles make a negligible contribution to the free energy of a neutron star.

Minimizing the free energy F subject to the conditions of conservation of charge and baryon number produces the required equilibrium

relations among the various chemical potentials. It is thus convenient to make the definition

$$\Phi = F - \lambda \sum_i A_i - \sigma \sum_i Z_i \quad , \tag{III.1}$$

where A_i and Z_i are the baryon number and charge of a particle of species i, and λ and σ are Lagrange multipliers. Minimizing Φ with no external constraints is equivalent to minimizing F with charge and baryon number held constant.

B. Neutrons, Protons, and Electrons

For a system containing neutrons, protons, and electrons, minimizing Φ with respect to n_n, n_p, and n_e produces the relation

$$\mu_p + \mu_e - \mu_n = 0 \quad . \tag{III.2}$$

Writing Eq. (III.2) in terms of the binding energies B_i and neglecting the small quantity $(m_p + m_e - m_n)c^2 + B_e$, one then obtains the condition

$$E_{Fp} + E_{Fe} - E_{Fn} + B_p - B_n = 0 \quad . \tag{III.3}$$

The number densities of protons and electrons must be equal if the neutron-star matter is electrically neutral and contains no other species of particles. The neutrality condition and Eq. (III.3) are sufficient to determine the electron-proton number density as a function of the number density of neutrons. The composition of neutron-star matter has been determined in previous work[6],[23] on the basis of the free-particle approximation, the approximation in which the binding energies B_i are all set equal to zero. The free-particle approximation

produces the following numerical expressions:

$$n_n \approx 2 \times 10^{38}(\rho/\rho_{nucl})\ \mathrm{cm}^{-3}; \qquad \text{(III.4a)}$$

$$n_e \approx n_p \approx 2 \times 10^{36}(\rho/\rho_{nucl})^2\ \mathrm{cm}^{-3}; \qquad \text{(III.4b)}$$

$$E_{Fn} \approx E_{Fe} \approx 7 \times 10^{1}(\rho/\rho_{nucl})^{2/3}\ \mathrm{MeV}; \qquad \text{(III.4c)}$$

$$E_{Fp} \approx 3(\rho/\rho_{nucl})^{4/3}\ \mathrm{MeV}; \qquad \text{(III.4d)}$$

$$P_{Fn} \approx 4 \times 10^{2}(\rho/\rho_{nucl})^{1/3}\ \mathrm{MeV/c}; \qquad \text{(III.4e)}$$

$$P_{Fe} \approx P_{Fp} \approx 7 \times 10^{1}(\rho/\rho_{nucl})^{2/3}\ \mathrm{MeV/c}\ . \qquad \text{(III.4f)}$$

Here n_i, E_{Fi}, and P_{Fi} are, respectively, the number density, Fermi kinetic energy, and Fermi momentum for particles of type i, and ρ_{nucl} is the density of nuclear matter (3.7×10^{14} gm/cc). Equations (III.4) were derived in the low-temperature limit. At the neutron-star temperatures to be considered here, kT is less than about 0.2 MeV and is thus small compared to any of the relevant Fermi energies. We therefore consider only the low-temperature limit in estimating the number densities of particles.

C. Muons

As a second example, consider a system containing μ^- mesons and electrons. Minimizing Φ with respect to the number densities of muons and electrons, one finds that

$$\mu_\mu = \mu_e\ . \qquad \text{(III.5)}$$

The electrons and muons do not interact strongly with the neutron-star matter. Consequently B_μ and B_e are negligible, and

$$m_\mu c^2 + E_{F\mu} = m_e c^2 + E_{Fe} \quad . \qquad \text{(III.6)}$$

The threshold density for the production of muons is the density at which the electron Fermi energy reaches $(m_\mu - m_e)c^2$, or approximately 105 Mev. The free-particle approximation, Eq. (III.4c) implies that the threshold density for muon production is about 1.8 ρ_{nucl}.

D. Σ^- Particles

We next consider production of the Σ^- particle, which has a rest energy of 1198 Mev. Minimizing Φ with respect to n_n, n_e, and n_{Σ^-} yields the equation

$$\mu_{\Sigma^-} = \mu_n + \mu_e \quad . \qquad \text{(III.7)}$$

The threshold density for the production of Σ^- particles is the density at which

$$E_{Fe} + E_{Fn} = (m_{\Sigma^-} - m_n - m_e)c^2 + B_{\Sigma^-} - B_n \quad . \qquad \text{(III.8)}$$

In the free-particle approximation, Σ^- particles will be produced above about 2.5 ρ_{nucl}.

E. Pions

Finally, the production of the π^- meson is governed by the relation

$$\mu_\pi = \mu_e \quad , \qquad \text{(III.9)}$$

or

$$E_{Fe} = (m_\pi - m_e)c^2 + B_\pi \quad . \qquad \text{(III.10)}$$

The free-particle approximation implies that the threshold for formation of pions is higher than the threshold for the production of Σ^- particles. Above the Σ^- threshold, Σ^- particles tend to be formed

instead of electrons, and the electron Fermi energy then does not increase significantly with increasing density. Consequently, the free-particle approximation implies that pions should not be formed at densities less than 100 ρ_{nucl} [6],[23].

F. Effects of the Strong Interactions

Strong interactions have a number of effects on the composition of neutron-star matter. One of their important effects is to increase the number densities of protons and electrons. The quantity $B_p - B_n$ in Eq. (III.3) is apparently large and negative. (The effective neutron-proton force is attractive and is stronger than the neutron-neutron force. Since the number density of protons in a neutron star is much smaller than the number density of neutrons, protons are bound much more strongly in neutron-star matter than neutrons are.) Preliminary estimates of B_p and B_n indicate that the strong proton binding may increase the number densities of protons and electrons by as much as a factor of five at nuclear density. At higher densities, the enhancement in the numbers of charged particles may be sufficient to allow ordinary neutron decay, which normally proceeds extremely slowly in neutron-star matter, to occur very rapidly. (The rate of ordinary neutron decay in neutron-star matter is considered briefly in the Appendix.)

Strong interactions also enter importantly into the question of the existence of quasi-free pions in neutron-star matter. Pions are likely to occur at reasonable densities only if the threshold

for the π^- is lower than the threshold for the Σ^-. It will be shown in Section IX that the existence of quasi-free pions would tremendously increase the cooling rate of a neutron star. Thus it would be interesting to find out whether the strong interactions could shift the π^--threshold below the Σ^--threshold. Equations (III.3), (III.8), and (III.10) imply that the π^- - threshold will be lower than the Σ^- - threshold if $B_{\pi^-} \leq \frac{1}{2}[(m_{\Sigma^-} - m_p - 2m_\pi)c^2 - E_{Fp} + B_{\Sigma^-} - B_p]$ (III.11)

or

$$B_{\pi^-} < -10 \text{ Mev} + \tfrac{1}{2}[B_{\Sigma^-} - B_p - E_{Fp}] \quad . \qquad \text{(III.12)}$$

The binding energies B_{π^-} and B_{Σ^-} are difficult to estimate, and it is still not known whether inequality (III.12) is satisfied at reasonable densities. The question of the production of pions is further clouded by the questionable validity of the particle-model: We have not been able to justify our implicit assumption that Σ^--like and π^--like excitations can continue to exist at densities from one to five times nuclear density.

IV. THE STRUCTURE OF NEUTRON-STAR MATTER

To calculate the cooling rate of a neutron star, one must have some knowledge of the structure of the low-lying excited states of neutron-star matter. In this section we discuss several possible forms that neutron-star matter might take. For the purposes of the present discussion, we shall neglect the effects of pions and strange particles and consider low-density neutron-star matter in which the only strongly interacting particles are neutrons and protons.

A. Normal Fermi Fluid

The most obvious way to treat neutron-star matter is to employ the methods developed for the treatment of nuclear matter. (Nuclear matter by definition contains equal numbers of neutrons and protons. Neutron-star matter contains many more neutrons than protons, as was indicated in Section III-B.) In nuclear-matter calculations, the basic one-particle states are characterized by definite momentum. Collisions between particles cause local distortions in the wave function, but the exclusion principle prevents true scattering[24]. If the neutrons and protons form a normal Fermi fluid, the excitation spectrum is continuous: There is no gap between the ground-state and the first excited state. The effect of the interparticle interactions on the spectrum of low-lying excited states can be represented easily through the use of effective masses for the neutron and proton.

The present calculations of cooling rates are based primarily on the idea of a normal Fermi fluid. Section V contains estimates of the effective masses of the neutron and proton.

B. Formation of "Nuclei"

Ruderman[25] has suggested that a uniform Fermi fluid of neutrons and protons in a neutron star may be unstable to the formation of a lattice of "nuclei". Each "nucleus" would contain a higher density of both neutrons and protons than the surrounding medium, and all the protons might, in fact, be bound in the "nuclei". The properties of the "nuclei" (their charge, maximum density, etc.) have not yet been established.

The lowest state of neutral matter at densities less than about 10^8 gm/cm^3 involves only Fe^{56} nuclei and degenerate electrons. As the density increases above about 10^8 gm/cm^3, the ratio $\frac{A}{Z}$ of the stable nuclear species increases; then above about $10^{11.5}$ gm/cm^3, a degenerate gas of neutrons begins to form[26]. The neutron gas becomes dominant at higher densities, but remnants of the original nuclei apparently persist up to densities of the order of nuclear density, where they finally become unstable (as we now show).

The properties of these "nuclei" at densities near nuclear density are difficult to determine, but it is still possible to formulate a simple criterion for the stability of a uniform neutron-proton gas to formation of such large-scale irregularities. Let μ_n, μ_p, n_n, and n_p represent the chemical potentials and number densities of the neutrons and protons in neutron-star matter. Using the fact that $\frac{\partial \mu_n}{\partial n_n}$ and $\frac{\partial \mu_p}{\partial n_p}$ are positive one can show that the criterion for stability of the uniform neutron-proton gas is

$$\frac{\partial \mu_n}{\partial n_n}\frac{\partial \mu_p}{\partial n_p} - \frac{\partial \mu_n}{\partial n_p}\frac{\partial \mu_p}{\partial n_n} > 0 \quad . \qquad \text{(IV.1)}$$

Rough calculations of the quantities involved in Eq. (IV.1) indicate that the stability criterion is satisfied for densities greater than approximately nuclear density. Both $\frac{\partial \mu_n}{\partial n_n} \frac{\partial \mu_p}{\partial n_p}$ and $\frac{\partial \mu_n}{\partial n_p} \frac{\partial \mu_p}{\partial n_n}$ are positive, but $\frac{\partial \mu_n}{\partial n_p} \frac{\partial \mu_p}{\partial n_n}$, which is large at low densities, decreases much more rapidly with increasing density than $\frac{\partial \mu_n}{\partial n_n} \frac{\partial \mu_p}{\partial n_p}$ does.

C. Superfluidity

Ginzburg and Kirzhnits[27] have suggested that neutron-star matter may form a superfluid. The Bardeen-Cooper-Schrieffer (BCS) theory of superconductivity[28] implies that an attractive potential acting between particles in a Fermi gas causes an energy gap $2\epsilon_o$ between the ground-state and first excited state of the system.

The BCS theory is often applied to the treatment of heavy nuclei [29]-[31]. In particular, Brueckner, Soda, Anderson, and Morel[32] and Emery and Sessler[33] attempted to use the BCS theory to calculate the energy gap in nuclear matter, hoping thereby to explain the gap observed between the ground and first excited-states of heavy even-even nuclei. For the present work, we have converted the results of Emery and Sessler[33] to the case of neutron-star matter, despite the fact that Emery and Sessler were not successful in explaining the energy gap observed in heavy even-even nuclei. Their failure to obtain the observed gap may be attributable to surface effects, which are important in nuclei, but which were not included in the nuclear-matter calculations.

Our application of the results of Emery and Sessler indicates that, for a neutron effective mass of 1.0 m_n, the energy ϵ_o for a neutron in a

zero-temperature neutron star is between 1 Mev and 2.3 Mev for densities between 0.01 ρ_{nucl} and 0.3 ρ_{nucl} and is zero for densities greater than 0.5 ρ_{nucl}. For a proton effective mass of 0.6 m_n, the energy ϵ_o for a proton is between 0.1 Mev and 0.35 Mev for densities between 0.1 ρ_{nucl} and 1.8 ρ_{nucl} and is zero beyond about 2.8 ρ_{nucl}. It should be noted, however, that the energy gap is roughly proportional to the fourth power of the effective mass. We shall find in Section V that the uncertainty in the effective masses is about 15 to 20%, which implies a fairly large uncertainty in the energy gaps for neutrons and protons.

Aside from sensitivity to the effective masses, there are several other reasons for doubting the validity of our straightforward calculation of the proton and neutron energy gaps. First, the BCS theory has never been successful in predicting the observed values of the energy gaps in superconducting metals or in nuclei. The BCS theory itself is not necessarily responsible for this lack of success, however, because the electron-electron interaction in metals is not known with any accuracy at all, and complete energy-gap calculations for finite nuclei have, as far as I know, never been carried out. Nevertheless, the ability of the BCS theory to predict energy gaps has never been demonstrated.

We have based our estimates of the energy gaps on the work of Emery and Sessler, who applied only the most straightforward form of the BCS theory to nuclear matter. In particular, they neglected the complex problem of three-body collisions. Polarization of the neutron medium by the protons might make a significant contribution to the effective proton-proton force in neutron-star matter.

The question of angle-dependent pair-correlations will not be discussed here. Treatments based on such non-isotropic correlations have been unsuccessful in explaining the low-temperature properties of liquid He^3.* Angle-dependent correlations change the density of states above the Fermi level, but do not produce a true gap in the spectrum. Consequently, their effects on the cooling rates of neutron stars are much smaller than the effects of ordinary superfluidity caused by attractive S-wave potentials.

---

*For example, K. A. Brueckner, T. Soda, P. W. Anderson, and P. Morel, Phys. Rev. 118, 1442 (1960), and V. J. Emery and A. M. Sessler, Phys. Rev. 119, 43 (1960), predicted a phase transition in liquid He^3 at about 0.1°K. No transition has been observed above 0.01°K, but there may be a phase change at a lower temperature. See V. P. Peshkov, Soviet Physics JETP 19, 1023 (1964), and W. R. Abel, A. C. Anderson, W. C. Black, and J. C. Wheatley, Phys. Rev. Letters 14, 129 (1965).

V. THE EFFECTIVE MASSES

A. Definitions

According to the individual-particle model, the expression for the density of states available to a single nucleon is

$$\rho(E) = 2^{-1}\pi^{-2}\hbar^{-3}p^2\ dp/dE \quad , \tag{V.1}$$

where $\rho(E)$ is the number of states per unit energy interval per unit volume, and p and E are the momentum and energy of the nucleon. For a non-relativistic nucleon, the free-particle model implies that

$$\rho(E) = 2^{-1}\pi^{-2}\hbar^{-3}\ pm \quad , \tag{V.2}$$

where m is the mass of the nucleon. The effect of interparticle interactions on the energy spectrum of a star can be represented approximately by writing the energy of each individual nucleon in the form

$$E(p) = c\sqrt{m^2c^2 + p^2} - mc^2 + U(p) \quad , \tag{V.3}$$

where $U(p)$ is the change in the single-particle energy produced by interactions with neighboring nucleons. We define the effective mass $m^*(p)$ by the relation

$$\frac{1}{m^*(p)} = \frac{1}{(m^2 + p^2c^{-2})^{\frac{1}{2}}} + \frac{1}{p}\frac{dU(p)}{dp} \quad , \tag{V.4}$$

which leads to the expression

$$\rho = 2^{-1}\pi^{-2}\hbar^{-3}\ pm^*(p) \tag{V.5}$$

for the density of single-particle states. Note that Eq. (V.4) reduces to the usual[24] non-relativistic definition of an effective mass if p/c

is neglected relative to m in the first term on the right-hand side of Eq. (V.4). The additional relativistic correction ($-\frac{1}{2} p^2 m^{-2} c^{-2}$) is small ($\sim 5\%$) for nuclear matter. We are interested primarily in the density of states near the Fermi momentum P_F, because this is the quantity that enters into neutrino cooling rates. Thus we need calculate only $m_n^*(P_{Fn})$ and $m_p^*(P_{Fp})$, which we can now write more compactly as m_n^* and m_p^*, respectively.

B. Calculation of the Effective Masses

We need the effective masses of both the neutron and the proton for our calculations of cooling rates. There are, however, two important simplifications that result from the fact that the number density of protons is much smaller than the number density of neutrons; one can, with sufficient accuracy, neglect the effect of neutron-proton interactions on the neutron energy as well as the effect of proton-proton interactions on the proton energy.

The nucleons are only slightly relativistic for the densities at which an individual-particle treatment is valid, and the term $p^{-1}\, dU/dp$ in Eq. (V.4) is not large compared to m^{-1}. We thus treat both the relativistic correction ($-\frac{1}{2} p^2 m^{-2} c^{-2}$) and the interaction-correction as small perturbations and do not consider reltivistic corrections to the interaction term in Eq. (V.4). Following the non-relativistic treatment of Gomes *et al.*,[24] we make several simplifying assumptions:

(1) The potential acting in an odd-parity nucleon-nucleon state is negligibly small;

(2) The potential acting in even-parity states is spin-independent and consists of a short-range hard-core potential, $V^{core}(r)$, and a long-range attractive potential, $V^{att}(r)$;

(3) The repulsive core makes a negligible contribution to dU/dp;

(4) The Born approximation provides an accurate estimate of the expectation value of the attractive potential (because of the effect of the exclusion principle on the nucleon wave functions).

Gomes et al.[24] have shown that the above approximations result in small errors at densities near nuclear density.

The four assumptions listed above imply a simple correspondence between nuclear matter and a neutron star with the same number density of neutrons. In computing $U(p)$ for a neutron in a neutron star, we include interactions with only half the neutrons in the star, because assumption (1) and the exclusion principle imply that there is no interaction between neutrons with parallel spin. The corresponding $U(p)$ for nuclear matter (which contains equal numbers of neutrons and protons) includes contributions from half the neutrons and all the protons present. Thus we conclude that

$$U_n^{n.s.}(p;\ \rho_n) \approx \frac{1}{3}\, U_n^{n.m.}(p;\ \rho_n) \qquad (V.6)$$

where superscripts "n.s." and "n.m." denote, respectively, "neutron star" and "nuclear matter", and the subscript "n" represents "neutron". One can use a similar argument to show that

$$U_p^{n.s.}(p;\ \rho_n) \approx \frac{2}{3}\, U_p^{n.m.}(p;\ \rho_n) \quad . \qquad (V.7)$$

The assumptions (1)-(4) can be used to show that the neutron and

proton energies have the form:

$$U_n^{n.s.}(p;\ \rho_n) \approx \tfrac{1}{2}\, U_p^{n.s.}(p;\ \rho_n) \qquad \text{(V.8a)}$$

$$\approx (2\pi\hbar)^{-3} \int_{|\underset{\sim}{q}| < P_{Fn}} d^3q \int d^3r \cos^2(\underset{\sim}{k}\cdot\underset{\sim}{r})\, V^{att}(r)\ , \qquad \text{(V.8b)}$$

where

$$\underset{\sim}{k} = (2\hbar)^{-1}\ (\underset{\sim}{p} - \underset{\sim}{q}) \quad . \qquad \text{(V.8c)}$$

and P_{Fn} is the neutron Fermi momentum.

The effective masses of the neutron and proton have been calculated using Eqs. (V.4) and (V.8). The computations have been carried out for the following potentials: (1) an attractive square well with a repulsive core (the potential used by Gomes et al.); and (2) several combinations of attractive Yukawa potentials and repulsive cores (the potentials suggested by Preston)[34]. There is a significant variation in the values of the effective masses calculated using these potentials, in spite of the fact that all the potentials were chosen to fit the low-energy nucleon-nucleon scattering data. In the next two paragraphs, we describe the general behavior of the effective masses as functions of density, indicating the extent to which the numerical results depend on the particular potential chosen.

1. Neutron Effective Mass

The neutron effective mass takes on its minimum value at a density of the order of ρ_{nucl}. For $0.5 < \rho/\rho_{nucl} < 5$, the neutron effective mass $m_n^{*n.s.}$ is in the range

$$0.90\ m_n < m_n^{*n.s.} < 1.15\ m_n \qquad \text{(V.9)}$$

For $\rho \ll \rho_{nucl}$, the effective mass can be expressed in the form

$$m_n^{*n.s.} \approx m_n \left[1 - \alpha(\rho/\rho_{nucl}) + 0.08\ (\rho/\rho_{nucl})^{2/3}\right] , \qquad (V.10)$$

where $\alpha = 2.5 \pm 0.5$.

2. Proton Effective Mass

The proton effective mass reaches its minimum value m^*_{min} at a density ρ_{min}, where

$$0.5\ m_n < m^*_{min} < 0.75\ m_n \qquad (V.11)$$

and

$$0.9\ \rho_{nucl} < \rho_{min} < 2\ \rho_{nucl} \quad . \qquad (V.12)$$

For $\rho \ll \rho_{nucl}$, the effective mass can be expressed in the form

$$m_p^{*n.s.} \approx m_n \left[1 - \gamma\ (\rho/\rho_{nucl})\right] , \qquad (V.13)$$

where

$$\gamma = 5.0 \pm 1.0. \qquad (V.14)$$

These values of the effective masses will be used in Sections VIII and IX in the calculation of the cooling rates.

VI. NEUTRINO OPACITY

Neutrinos produced by the reactions (I.1)-(I.8) have typical energies of the order of kT, with kT less than or of the order of 100 keV. For neutrinos of such energies, the largest contribution to the neutrino-opacity* comes from neutrino-electron scattering for ν_e and neutrino-muon scattering for ν_μ. This result can easily be established by examining the possible reactions. We consider first electron neutrinos, ν_e.

The following reactions are forbidden for typical neutron-star conditions by conservation of energy and momentum: $\nu_e + n \rightarrow p + e^-$, $\bar{\nu}_e + p \rightarrow n + e^+$, and $\bar{\nu}_e + p + n \rightarrow n + n + e^+$. The reaction $\bar{\nu}_e + n + n \rightarrow p + e^- + n'$ and related reactions involving strange particles, e.g. Λ°'s or Σ^-'s, occur rarely because the cross section is of the order of 10^{-42} cm^2 times several factors of (kT/E_F). Neutrino absorption by heavier elements on the surface of the star is negligible because the cross sections are small and the heavier elements are rare. Thus neutrino-electron scattering is the most important interaction for ν_e.

A similar analysis has been carried out for muon neutrinos; it shows that the only interactions allowed by the selection rules and by energy conservation are $\nu_\mu - \mu^-$ and $\bar{\nu}_\mu - \mu^-$ scattering.

---

*The general problem of the scattering of neutrinos in stellar matter is considered by J. N. Bahcall, Phys. Rev. 36, B1164 (1964).

The mean free path of an electron neutrino passing through a degenerate electron gas can be computed directly using the conserved-vector-current theory[35]. The general result cannot be written exactly in simple form, but, for an electron gas at a temperature T, the mean free path of a neutrino with an energy of the order of kT is given roughly by the relation

$$\lambda_{\nu_e} \approx (1.1 \times 10^7 \text{km})\left(\frac{P_{Fe}c}{100 \text{ MeV}}\right)^{-2} T_9^{-3} \quad , \qquad \text{(VI.1)}$$

where T_9 is the temperature in units of 10^9 °K.

The mean free path of an electron neutrino in a neutron star is, therefore, of the order of 10^6 times the radius of a neutron star; the mean free path of an electron antineutrino is of the same order of magnitude. Muon neutrinos and antineutrinos have somewhat longer mean free paths because muons are less numerous than electrons. We therefore conclude that the opacity of a neutron star to low-energy neutrinos and antineutrinos is completely negligible.

VII. COOLING: GENERAL DISCUSSION AND HEURISTIC CALCULATIONS

In order to compute cooling times, one must consider the excited states of a neutron star. A neutron star is almost completely isothermal, except for an extremely thin atmosphere. For the purposes of calculating the rate of neutrino emission, one can neglect the atmosphere and imagine that the excited states of the star are populated (according to the usual Boltzmann factor) by placing the star in contact with a thermal bath at a finite temperature T. The star then has a definite baryon number and total electric charge but does not have definite energy. The rate of energy loss (cooling) by neutrino emission is given by an expression of the form:

$$L_\nu = (2\pi/\hbar) \sum_\nu \sum_{\beta < \alpha} |\langle S_\beta; \nu | H_w | S_\alpha \rangle|^2 E_\nu \delta(E_\alpha - E_\beta - E_\nu) \exp(-E_\alpha/kT) \quad , \tag{VII.1}$$

where S_α, S_β are states of the entire star, H_w is the weak interaction Hamiltonian, E_ν is the energy of the emitted neutrino ν, and the summation over β is limited to states for which $E_\beta < E_\alpha$.

In practice, cooling rates must be computed with the help of a model; we employ the particle model. We also approximate the thermal average (Eq. VII.1) over the states of the star by assigning a Fermi-Dirac or Bose-Einstein distribution to each kind of particle in the star. As we discussed earlier, it is not possible to decide at present whether or not neutron stars contain a significant number of quasi-free pions; hence our calculations have been carried out for both assumptions, pions present and pions not present.

One can estimate the order of magnitude of the energy loss due to processes (I.1)-(I.8) by a simple heuristic argument that is not entirely fraudulent. The main feature of this argument is that only Fermions on the edge of their degenerate seas can undergo elastic scattering. Thus only a small fraction of the order of (kT/E_F) of the Fermions of a given type can participate in the cooling reactions. Since neutrinos escape from a neutron star (see Section VI), this argument does not apply to them. However, the net amount of energy transferred to a neutrino in any of the cooling reactions must be, by conservation of energy, of the order of kT. It is reasonable to replace the dimensionless neutrino phase space, which is proportional to E_ν^2, by $(kT)^2/[E_{Fn}E_{Fp}]$ for reactions (I.1) and (I.2) and similar factors for reactions (I.3) and (I.4).

The energy loss from reaction (I.1) can now be crudely estimated from the familiar arguments of kinetic theory. One writes for the energy loss from a volume Ω by reaction (I.1):

$$L_\nu^{(1)} \sim \Omega\, n_n^{\,2} \langle \sigma v \rangle\, E_\nu \left[\frac{kT}{E_{Fn}}\right]^{+6} \frac{kT}{E_{Fp}} \quad , \qquad \text{(VII.2)}$$

where n_n is the neutron number density, the weak-interaction cross section $\sigma \sim 10^{-43}\,(E_{Fn}/1\ \text{MeV})^2\ \text{cm}^2$, the relative velocity $v \sim c/3$, the neutrino energy $E_\nu \sim kT/3$, and the various Fermi energies can be estimated from Eqs. (III.4). We have included in Eq. (VII.2) one factor of kT/E_F for each degenerate Fermion that occurs in process (I.1); we have also made use of the fact that E_{Fe} is, according to Sec. III, approximately equal to E_{Fn}. We consider a mass M_s of neutron-star matter at a uniform density ρ and a uniform temperature T. Using

Eq. (III.4) in Eq. (VII.2), one finds that the neutrino luminosity due to reaction (I.1) is given by

$$L_\nu^{(1)} \sim (6 \times 10^{39} \text{ erg-sec}^{-1})(M_s/M_\odot)(\rho_{nucl}/\rho)^3 \, T_9^{\,8} \quad , \qquad \text{(VII.3)}$$

where $M_\odot$ is the mass of the sun and T_9 is the temperature in billions of degrees. Equation (VII.3) yields energy losses that are not enormously different from the energy losses computed from our more complicated analysis of Sec. VIII. Moreover, Eq. (VII.3) gives correctly the crucial dependence of $L_\nu^{(1)}$ on temperature, although the density dependence cannot be obtained correctly without a more careful analysis.

A similar crude argument can be used to obtain an estimate of the energy losses from reaction (I.3). Note that process (I.3) contains two fewer Fermions than processes (I.1) and (I.2); hence the rate of (I.3) is faster than (I.1) by a factor of the order of $(E_{Fn}/kT)^2$. Thus:

$$L_\nu^{(3)} \sim (4 \times 10^{45} \text{ erg-sec}^{-1})(n_\pi/n_n)(M_s/M_\odot)(\rho_{nucl}/\rho)^{8/3} \, T_9^{\,6} \qquad \text{(VII.3a)}$$

The heuristic arguments show clearly what quantities must be calculated in a careful analysis, namely, the phase-space integrals (which we have approximated by factors of kT/E_F) and the nuclear matrix elements (which we have approximated by an average weak-interaction cross section).

VIII. NUCLEON-NUCLEON COOLING

A. General Expressions

We now make explicit use of the particle model to calculate the rate of reaction (I.1). We describe the state of the entire star in terms of the states of its individual particles, introducing corrections to account for the interactions among the various particles. Following the work of Gomes et al.,[24] we label each single-particle state by its momentum $\underline{p}$; the energy assigned to a state of particle species i with momentum $\underline{p}$ is given by

$$E_i(p) = \sqrt{m_i^2 c^4 + p^2 c^2} + U_i(p) - m_i c^2 \quad . \qquad \text{(VIII.1)}$$

The Fermi energy E_{Fi} is defined by

$$E_{Fi} = \sqrt{m_i^2 c^4 + (P_{Fi})^2 c^2} - m_i c^2 \quad , \qquad \text{(VIII.2)}$$

where P_{Fi} is the Fermi momentum for a particle of species i. The zero point of $U_i(p)$ is defined such that $U_i(P_{Fi})$ is equal to the binding energy B_i, which was defined in Sec. III-A. Thus, $E_i(p)$ is the energy required to take a particle of type i from infinity and place it in the neutron star in a state with momentum $\underline{p}$ (gravitational interactions not considered). The quantities $W_i(p)$ and W_{Fi} are defined to be equal, respectively, to $E_i(p) + m_i c^2$ and $E_{Fi} + m_i c^2$.

The neutrino luminosity $L_\nu^{(1)}$ arising from reaction (I.1) $(n + n \rightarrow n + p + e^- + \bar{\nu}_e)$ in a volume Ω is:

$$L_\nu^{(1)} = \pi \hbar^{-1} \sum_{\text{spins}} \int d^3n_1 \, d^3n_2 \, d^3n_1' \, d^3n_p \, d^3n_e \, d^3n_{\bar{\nu}} \, S \times E_{\bar{\nu}} \, \delta(E_i - E_f) \, |\langle n,p,e,\bar{\nu}_e | H_w | n,n \rangle|^2 \, , \qquad \text{(VIII.3a)}$$

where the subscripts 1, 2, 1′, p, e, and $\bar{\nu}$ denote the two initial neutrons, the final neutron, the proton, the electron, and the anti-neutrino, respectively. We have included a factor of one-half which arises from the identity of the two initial neutrons. The density of individual-particle states can be expressed in terms of the particle momenta as follows:

$$d^3n_i = (2\pi\hbar)^{-3}\ \Omega\ p_i^{\,2}\ dp_i\ d\Omega_i \quad . \qquad \text{(VIII.3b)}$$

The quantity S is a product of Fermi-Dirac distribution functions for each particle appearing in reaction (I.1), except the neutrino; S corrects the density-of-state factors for the effect of the exclusion principle in the final state and gives the appropriate occupation numbers in the initial state. More explicitly,

$$S = \prod_{i=1}^{5} S_i \quad , \qquad \text{(VIII.3c)}$$

where for the two initial neutrons,

$$S_n = [1 + \exp\beta(E_n - E_{Fn} - B_n)]^{-1} \quad , \qquad \text{(VIII.3d)}$$

and for the final neutron, proton, and electron,

$$S_i = [1 + \exp\beta(E_{Fi} + B_i - E_i)]^{-1} \quad . \qquad \text{(VIII.3e)}$$

We have set $(kT)^{-1}$ equal to β in Eqs. (VIII.3d) and (VIII.3e). The weak Hamiltonian is:

$$H_w = 2^{-\frac{1}{2}} G \int d^3x\ \bar{\psi}_p(\underset{\sim}{x})\ \gamma_\alpha(C_V - C_A\ \gamma_5)\ \psi_n(\underset{\sim}{x})\quad \bar{\psi}_e\ \gamma_\alpha(1 + \gamma_5)\ \psi_\nu + \text{h.c.}$$

$$\text{(VIII.3f)}$$

One can separate out the center-of-mass motion of the nucleons in the matrix element $\langle n, p, e, \bar{\nu}_e | H_w | n, n \rangle$ by introducing the following center-of-mass and relative coordinates:

$$\underset{\sim}{K} = (\underset{\sim}{k}_1 + \underset{\sim}{k}_2) \quad , \tag{VIII.4a}$$

$$\underset{\sim}{k} = 2^{-1} (\underset{\sim}{k}_1 - \underset{\sim}{k}_2) \quad , \tag{VIII.4b}$$

$$\underset{\sim}{R} = 2^{-1} (\underset{\sim}{r}_1 + \underset{\sim}{r}_2) \quad , \tag{VIII.4c}$$

and

$$\underset{\sim}{r} = (\underset{\sim}{r}_1 - \underset{\sim}{r}_2) \quad , \tag{VIII.4d}$$

where $\underset{\sim}{k}_1$, $\underset{\sim}{k}_2$, $\underset{\sim}{r}_1$, and $\underset{\sim}{r}_2$ are, respectively, the wave numbers and positions of the two nucleons in the initial state. Primed variables will be used for the analogous final-state quantities. The nucleonic wave functions in the initial and final states are of the form:

$$\Psi_{nn} = \Omega^{-1} \exp (i \underset{\sim}{K} \cdot \underset{\sim}{R}) \psi_{nn}^{S} (\underset{\sim}{k}; \underset{\sim}{r}) \chi(S, M_S) \tag{VIII.5a}$$

and

$$\Psi_{np} = \Omega^{-1} \exp (i \underset{\sim}{K}' \cdot \underset{\sim}{R}) \psi_{np}^{S'} (\underset{\sim}{k}'; \underset{\sim}{r}) \chi(S', M_{S'}) \quad . \tag{VIII.5b}$$

In Eqs. (VIII.5) the functions ψ describe the relative motion of the pairs of nucleons; the incoming part of the asymptotic form of $\psi_{np}^{S'} (\underset{\sim}{k}'; \underset{\sim}{r})$ is the same as the incoming part of a plane wave with wave vector $\underset{\sim}{k}'$. The function $\chi(S', M_{S'})$ describes a two-particle spin-state with total spin S' and z-component $M_{S'}$.

The nucleon matrix element that appears in Eq. (VIII.3a) can now be expressed as an integral over the relative wave functions ψ_{nn}^{S} and $\psi_{np}^{S'}$. Before writing down an explicit formula for the matrix element, we make two simplifications: (1) We assume that the nucleon-nucleon potential acts only in even-parity states; and (2) we neglect all terms involving

the lepton momenta. The first assumption has frequently been used in nuclear-matter calculations and does not appear to give rise to any large errors. The second simplification can be shown to introduce errors of the order of 15% if the first approximation is valid.

Making the simplifications described above, we square the matrix element and sum over all spins, obtaining

$$\sum_{\text{spins}} |\langle n,p,e,\bar{\nu}_e \mid H_W \mid n,n\rangle|^2$$

$$= 8\, G^2 \left[C_V^{\,2} \left|M_V\right|^2 + 3\, C_A^{\,2} \left|M_A\right|^2 \right] (2\pi)^3\, \lambda\!\!\!^{-}_{\pi}{}^{6}\, \Omega^{-5}\, \delta^{(3)}(\underset{\sim}{K}' - \underset{\sim}{K}) \quad , \text{(VIII.6a)}$$

where $\lambda\!\!\!^{-}_{\pi}$ is the Compton wavelength of the pion; the dimensionless matrix elements are defined by

$$M_V = \lambda\!\!\!^{-}_{\pi}{}^{-3} \int d^3r\, \psi^{*0}_{np}(\underset{\sim}{k}';\, \underset{\sim}{r})\, \psi^{0}_{nn}(\underset{\sim}{k};\, \underset{\sim}{r}) \qquad \text{(VIII.6b)}$$

and

$$M_A = \lambda\!\!\!^{-}_{\pi}{}^{-3} \int d^3r\, \psi^{*1}_{np}(\underset{\sim}{k}';\, \underset{\sim}{r})\, \psi^{0}_{nn}(\underset{\sim}{k};\, \underset{\sim}{r}) \quad . \qquad \text{(VIII.6c)}$$

Substituting Eq. (VIII.6) in Eq. (VIII.3) we find:

$$L_\nu^{(1)} = 64\, \pi^4\, \Omega\, G^2\, \hbar^{-1}\, \lambda\!\!\!^{-}_{\pi}{}^{-9} \left[C_V^{\,2} \left|M_V\right|^2 + 3\, C_A^{\,2} \left|M_A\right|^2 \right] P, \text{(VIII.7)}$$

where the dimensionless phase-space factor P is given by the following equation:

$$P = \Omega^{-6}\, \lambda\!\!\!^{-}_{\pi}{}^{15} \int \prod_{i=1}^{6} d^3n_i\; S\, E_{\bar{\nu}}\, \delta^{(3)}(\underset{\sim}{K}' - \underset{\sim}{K})\, \delta(E_f - E_i) \quad . \text{(VIII.8)}$$

Since each factor d^3n_i is proportional to the volume Ω, the phase-space integral P is actually independent of Ω. Thus $L_\nu^{(1)}$ is proportional to Ω.

Inserting the appropriate numerical values in the expression for $L_\nu^{(1)}$, one finds:

$$\Omega^{-1} L_\nu^{(1)} = (5.2 \times 10^{48} \text{ erg-cm}^{-3}\text{-sec}^{-1}) P (|M_V|^2 + 4.3|M_A|^2) \quad . \tag{VIII.9}$$

As was apparent from our earlier heuristic discussion, two types of quantities must be calculated, the nuclear matrix elements M_A and M_V and the phase-space factor P. Equation (VIII.9) has been derived only for the case of reaction (I.1); we shall consider in Sec. VIII-D the modifications necessary to account for reactions (I.2), (I.5), and (I.6).

B. The Phase-Space Factor

1. General Discussion

Chemical equilibrium among the different types of particles present in a neutron star is ensured by various weak-interaction processes, particularly reactions (I.1) and (I.5). The concentrations of the various particles can be brought to their equilibrium values in typical weak-interaction times of the order of 10^{-6} to 10^{-8} sec. However, the exclusion principle greatly inhibits all these reactions when the stellar matter is near chemical equilibrium at low temperature. For example, the lifetime of a neutron in a neutron star at equilibrium at 10^9 $^\circ$K is, assuming a normal Fermi fluid, of the order of 10^{12} sec, which is 10^{+18} to 10^{+20} times longer than the time required to establish chemical equilibrium. Superfluidity in the neutron or proton gas can increase the neutron lifetime at equilibrium still further.

This enormous reduction in the reaction rates near equilibrium results from a decrease in the number of available initial and final states. Equation (III.2) states that, in a neutron star at equilibrium at $0^{\circ}K$, two neutrons at the top of their Fermi distribution have just enough energy to produce a neutron, a proton, and an electron at the top of their respective Fermi seas, plus a zero-energy neutrino. At temperatures greater than zero but still small compared to the relevant Fermi energies, neutrons with energies near E_{Fn} have sufficient energy to produce a neutron, proton, and electron in unoccupied states near the tops of their respective Fermi seas, plus a neutrino with an energy of the order of kT. Thus the neutrons destroyed in reaction (I.1) all come from a narrow band of states with energies within a few kT of E_{Fn}, and the neutrons, protons, and electrons produced in reaction (I.1) must have energies within a few kT of their respective Fermi energies. The relatively slow rate of reactions (I.1) and (I.5) at equilibrium is due to the fact that only a small fraction of the total number of particle states can actually be involved in the reactions. The phase-space factor P of Eq. (VIII.8), which we evaluate in the following paragraphs, contains a quantitative description of the inhibition of the reaction rate due to the small number of available states. The phase-space factors for the allowed reactions (I.1) and (I.5) are the principal quantities that determine their absolute rates, just as the ordinary phase-space factor (usually denoted by f)primarily determines the laboratory decay rates of superallowed nuclear beta decays.

2. Initial Approximations

The integrations involved in the phase-space factor P can all be performed analytically for the case of a normal Fermi fluid; the approximations required for carrying out the integrations give rise to errors of only a few percent. One can evaluate the integrals relatively accurately because of the simplifications that result from the fact that kT is, for the problems of interest, much less than the relevant Fermi energies. For example, the energy kT is 0.086 MeV at 10^9 °K, whereas E_{Fn}, E_{Fe}, and E_{Fp} are, respectively, of the order of 70 MeV, 70 MeV, and 3 MeV at nuclear density.

The integrand of P is negligible except in the restricted "important" region of phase space where all the particle energies are within a few kT of their Fermi energies. It is convenient to neglect contributions to the integral from certain regions that are far from the "important" region. In particular, we consider only those parts of the region of integration that satisfy the inequalities

$$p_s + |p_1 - p_2| < p_1' < p_1 + p_2 - p_s \qquad \text{(VIII.10)}$$

and

$$p_1 > p_s \quad , \qquad \text{(VIII.11a)}$$

where

$$p_s = p_p + p_e + p_{\bar{\nu}} \quad . \qquad \text{(VIII.11b)}$$

The largest error made in restricting ourselves to the domain described by relations (VIII.10) and (VIII.11) is of the order of $e^{-E_{Fp}/kT}$, which is less than 10^{-3} for the temperatures and densities of interest.

3. The Angular Integral

We begin the evaluation of the phase-space factor P given in (VIII.8) by performing the integrations over the solid angles. Let the angular integral be defined by the relation

$$A = \int d\Omega_1 \int d\Omega_p \int d\Omega_e \int d\Omega_{\bar{\nu}} \int d\Omega_2 \int d\Omega_1' \; \delta^3(\underset{\sim}{K}' - \underset{\sim}{K}) \quad . \tag{VIII.12}$$

We can rewrite $\delta^3(\underset{\sim}{K}' - \underset{\sim}{K})$ as follows:

$$\delta^3(\underset{\sim}{K}' - \underset{\sim}{K}) = \hbar^3 \; (p_1')^{-2} \; \delta^2(\Omega_1' - \Omega_{\underset{\sim}{q}}) \; \delta(p_1' - q) \tag{VIII.13}$$

where $\underset{\sim}{q} = \underset{\sim}{p}_1 + \underset{\sim}{p}_2 - \underset{\sim}{p}_p - \underset{\sim}{p}_e - \underset{\sim}{p}_{\bar{\nu}}$. The angular delta function $\delta^2(\Omega_1' - \Omega_{\underset{\sim}{q}})$, which requires that the directions of $\underset{\sim}{p}_1'$ and $\underset{\sim}{q}$ be the same, allows one to perform the integration on Ω_1' immediately. We note that

$$\delta(p_1' - q) = \delta\left[p_1' - (s^2 + p_2^2 + 2s\, p_2 \mu)^{\frac{1}{2}}\right] \quad , \tag{VIII.14}$$

where $\underset{\sim}{s} = \underset{\sim}{p}_1 - \underset{\sim}{p}_p - \underset{\sim}{p}_e - \underset{\sim}{p}_{\bar{\nu}}$ and μ is the cosine of the angle between $\underset{\sim}{p}_2$ and $\underset{\sim}{s}$. Inequality (VIII.10) requires that the quantity $p_1' - q$ equal zero for some value of μ between -1 and +1. Hence the integral over Ω_2 can be carried out immediately, with the result that

$$A = 2\pi \hbar^3 \; (p_2 \; p_1')^{-1} \int d\Omega_1 \int d\Omega_p \int d\Omega_e \int d\Omega_{\bar{\nu}} \; s^{-1} \quad . \tag{VIII.15}$$

Repeated use of inequality (VIII.11) allows one to perform the remaining integrations directly. One finds that

$$A = (4\pi)^5 \hbar^3 \; (2 \; p_1 \; p_2 \; p_1')^{-1} \quad . \tag{VIII.16}$$

4. The Radial Integral (Normal Fermi Fluid)

We now perform the integrations on the lengths of the momentum vectors in Eq.(VIII.8). Substituting Eq. (VIII.16) into Eq. (VIII.8) and using Eq. (VIII.3b), we obtain:

$$P = B \int \prod_{i=1}^{6} p_i^2 \, dp_i \; S \, E_{\bar{\nu}} \; \delta(E_f - E_i) \; (p_1 \; p_2 \; p_1')^{-1} \quad , \qquad \text{(VIII.17a)}$$

where

$$B = 2^{-9} \; \pi^{-13} \; (m_\pi c)^{-15} \quad . \qquad \text{(VIII.17b)}$$

The integration over the neutrino momentum $p_{\bar{\nu}}$, which one can perform immediately using the energy delta function, contributes a factor $(E_1 + E_2 - E_1' - W_e - E_p)^3 \; c^{-3}$. We now explicitly assume that the neutrons and protons form a normal Fermi fluid with no gap in its excitation spectrum. Defining the effective masses as in Section V, we find that

$$p_p \, dp_p = m_p^* \, (p_p) \, dE_p \qquad \text{(VIII.18a)}$$

and

$$p_n \, dp_n = m_n^* \, (p_n) \, dE_n \quad . \qquad \text{(VIII.18b)}$$

The electron energy W_e is nearly equal to $p_e c$, since the electrons are highly relativistic.

It is convenient to express P in terms of the following dimensionless variables:

$$x_1 = \beta \left(E_1 - E_{Fn} - B_n \right) \quad , \qquad \text{(VIII.19a)}$$

$$x_2 = - \beta \left(E_1' - E_{Fn} - B_n \right) \quad , \qquad \text{(VIII.19b)}$$

$$x_3 = -\beta \left(W_e - W_{Fe} \right) \quad , \qquad \text{(VIII.19c)}$$

$$x_4 = \beta \left(E_2 - E_{Fn} - B_n \right) \quad , \qquad \text{(VIII.19d)}$$

and

$$x_5 = -\beta\left(E_p - E_{Fp} - B_p - m_p + m_n\right) \quad . \qquad \text{(VIII.19e)}$$

Substituting Eqs. (VIII.18) and (VIII.19) into the expression for P, and using the equilibrium condition, Eq. (III.3), we obtain

$$P = B\, c^{-4}(kT)^8 \int_{-y_n}^{\infty} dx_1 \int_{-\infty}^{y_n} dx_2 \int_{-\infty}^{y_e} dx_3 \int_{-y_n}^{\infty} dx_4 \int_{-(x_1+x_2+x_3+x_4)}^{y_p} dx_5 \quad J \quad , \qquad \text{(VIII.20a)}$$

where

$$y_n = \beta\left[E_{Fn} + B_n - E_n(\underset{\sim}{p} = 0)\right] \quad , \qquad \text{(VIII.20b)}$$

$$y_e = \beta\left[W_{Fe} - m_e c^2\right] \quad , \qquad \text{(VIII.20c)}$$

$$y_p = \beta\left[E_{Fp} + B_p + m_p - m_n - E_p(\underset{\sim}{p} = 0)\right] \quad , \qquad \text{(VIII.20d)}$$

$$J = \left[\sum_{i=1}^{5} x_i\right]^3 \theta\left[\sum_{i=1}^{5} x_i\right] \prod_{i=1}^{5} \left(1 + e^{x_1}\right)^{-1}$$

$$\times \prod_{i=1}^{3} m_n^*(E_i) \times m_p^*(E_p)\, p_p(E_p)\, p_e^2(W_e) \quad . \qquad \text{(VIII.20e)}$$

The function $\theta(y)$ is defined to be equal to unity when y is positive and zero when y is negative.

The factor $\theta(\Sigma_i x_i)\, \Pi_i\, (1 + e^{x_i})^{-1}$ is always less than e^{-x_5}. Hence, replacing the limit y_p by infinity increases the integral in Eq. (VIII.20) by a term proportional to e^{-y_p}. The quantity y_p is approximately equal to βE_{Fp}, which is greater than ten for the temperatures of interest here. Hence, terms proportional to e^{-y_p} can be neglected and the limit y_p can be replaced by infinity. The limits y_n and y_e can also be replaced by infinity since they are at least ten times larger than y_p.

The effective masses and momenta contained in J can be expanded in a power series. For example, one can express $m_n^*(E_1)$ in the form

$$m_n^*(E_1) = m_n^*(E_{Fn} + B_n) + \sum_{i=1}^{\infty} x_1^n (kT/E_{Fn})^n a_n \quad .$$

Thus if we neglect small terms of order e^{-y_p}, the integral P can be expressed as a power series in kT. Since kT/E_{Fp} is less than one-tenth for neutron-star temperatures and densities of interest, we can obtain an adequate approximation for P by considering just the first term in the power series expansion of

$$\prod_{i=1}^{3} m_n^*(E_i) \; m_p^*(E_p) \; p_p(E_p) \; p_e^2(W_e) \quad .$$

We then obtain

$$P = B\,(kT)^8\, c^{-4} (m_n^*)^3\, m_p^*\, P_{Fp}\, P_{Fe}^2\, I \quad , \qquad \text{(VIII.21a)}$$

where

$$I = \int_{-\infty}^{\infty} dx_1 \int_{-\infty}^{\infty} dx_2 \int_{-\infty}^{\infty} dx_3 \int_{-\infty}^{\infty} dx_4 \int_{-(x_1+x_2+x_3+x_4)}^{\infty} dx_5$$

$$\times \left[\sum_{i=1}^{5} x_i\right]^3 \prod_{i=1}^{5} \left[1 + e^{x_1}\right]^{-1} \qquad \text{(VIII.21b)}$$

$$= \frac{11{,}513\,\pi^8}{120{,}960} \qquad \text{(VIII.21c)}$$

$$\approx 903 \qquad \text{(VIII.21d)}$$

and

$$m_n^* = m_n^*(E_{Fn} + B_n) \quad , \qquad \text{(VIII.21e)}$$

$$m_n^* = m_p^*(E_{Fp} + B_p) \quad . \qquad \text{(VIII.21f)}$$

Setting P_{Fp} and P_{Fe} equal to $c^{-1} W_{Fe}$, one can write the phase-space factor in the convenient form

$$P \approx 2.6 \times 10^{-29} \left[\frac{m_n^*}{m_n}\right]^3 \left[\frac{m_p^*}{m_p}\right] \left[\frac{W_{Fe}}{m_\pi c^2}\right]^3 T_9^8 \quad . \qquad \text{(VIII.22)}$$

The phase-space factor is, as expected from the heuristic argument given in Sec. VII, proportional to T^8; it is also proportional to the product of the effective masses of the four nucleons involved, because the number of single-nucleon states per unit energy is proportional to the nucleon effective mass.

Although the integrations involved in P are accurate to within a few percent, the numerical value of P is difficult to estimate to much better than an order of magnitude because of the uncertainties in the effective masses and the electron Fermi energy. Using Eqs. (V.9) - (V.15), we estimate that the product $(m_n^*/m_n)^3 (m_p^*/m_p)$ is equal to 0.6 ± 0.3. The electron Fermi energy depends on $B_n - B_p$, the difference between the binding energies of the neutron and proton. This difference might easily be as large as 50 MeV at nuclear density, but unfortunately no reliable theoretical estimates of $B_n - B_p$ are yet available. We shall assume that $B_n - B_p$ is much smaller than 70 MeV and use the free-particle relation, Eq. (III.4c), for the electron Fermi energy. We then obtain a simple but highly approximate expression for P,

$$P \approx 1.9 \times 10^{-30} (\rho/\rho_{nucl})^2 T_9^8 \quad . \qquad \text{(VIII.23)}$$

5. The Radial Integral (Superfluid)

We first consider the situation where the protons are superconducting but the neutrons are not, a situation that probably obtains for densities between $0.5\,\rho_{nucl}$ and $2.8\,\rho_{nucl}$, according to the results of Sec. IV-C.

In the Bardeen-Cooper-Schrieffer (BCS) theory[28], the ground-state of a superconducting gas involves pairing of particles with opposite spins and momenta. The state vector for the whole system is expressed in the second-quantization formalism as the product of the state vectors for the pairs. The four possible state vectors for the pair $(\underset{\sim}{k}\uparrow, -\underset{\sim}{k}\downarrow)$ are given by

$$\left|S_{\underset{\sim}{k}}(1)\right\rangle = \left[h_{\underset{\sim}{k}}^{\frac{1}{2}} a^{\dagger}_{\underset{\sim}{k}\uparrow}\, a^{\dagger}_{-\underset{\sim}{k}\downarrow} + (1-h_{\underset{\sim}{k}})^{\frac{1}{2}}\right] | 0\rangle \qquad \text{(VIII.24a)}$$

$$\left|S_{\underset{\sim}{k}}(2)\right\rangle = a^{\dagger}_{\underset{\sim}{k}\uparrow}|0\rangle \qquad \text{(VIII.24b)}$$

$$\left|S_{\underset{\sim}{k}}(3)\right\rangle = a^{\dagger}_{-\underset{\sim}{k}\downarrow}|0\rangle \qquad \text{(VIII.24c)}$$

and

$$\left|S_{\underset{\sim}{k}}(4)\right\rangle = \left[(1-h_{\underset{\sim}{k}})^{\frac{1}{2}}\, a^{\dagger}_{\underset{\sim}{k}\uparrow}\, a^{\dagger}_{-\underset{\sim}{k}\downarrow} - h_{\underset{\sim}{k}}^{\frac{1}{2}}\right] | 0\rangle \ , \qquad \text{(VIII.24d)}$$

where $a^{\dagger}_{\underset{\sim}{k}\uparrow}$, for example, is the creation operator for a particle with momentum $\underset{\sim}{k}$ and spin up, and $|0\rangle$ is the vacuum state. The coefficient $h_{\underset{\sim}{k}}$ is defined by

$$h_{\underset{\sim}{k}} = \tfrac{1}{2}\left(1 - \epsilon_{\underset{\sim}{k}}/E_{\underset{\sim}{k}}\right)^{\frac{1}{2}} \ , \qquad \text{(VIII.24e)}$$

where

$$\epsilon_{\underset{\sim}{k}} = (\hbar^2/2m)\,(k^2 - k_F^2) \ , \qquad \text{(VIII.25a)}$$

and

$$E_{\underset{\sim}{k}} = \sqrt{\epsilon_{\underset{\sim}{k}}^2 + \epsilon_0^2} \ . \qquad \text{(VIII.25b)}$$

The quantity ϵ_o is approximately independent of $\underset{\sim}{k}$.

State $|S_{\underset{\sim}{k}}(1)\rangle$ is the ground-state of the $(\underset{\sim}{k}\uparrow\ -\underset{\sim}{k}\downarrow)$ system. The energies of states $|S_{\underset{\sim}{k}}(2)\rangle$ and $|S_{\underset{\sim}{k}}(3)\rangle$ are greater than the energy of $|S_{\underset{\sim}{k}}(1)\rangle$ by an amount $E_{\underset{\sim}{k}}$. The fourth state has an energy of $2E_{\underset{\sim}{k}}$.

We now apply this formalism to the treatment of reaction (I.1). Consider the case where there is a gap ϵ_{op} in the proton spectrum, and let the wave number of the proton emitted in reaction (I.1) be $\underset{\sim}{k}_p$. The matrix elements of the transitions in which the energy in the $(\underset{\sim}{k}_p\uparrow, -\underset{\sim}{k}_p\uparrow)$ system is raised by $E_{\underset{\sim}{k}_p}$ are proportional to $(1 - h_{\underset{\sim}{k}_p})^{\frac{1}{2}}$, and the matrix elements of the transitions in which the energy in the $(\underset{\sim}{k}_p\uparrow, -\underset{\sim}{k}_p\downarrow)$ system is decreased by $E_{\underset{\sim}{k}_p}$ are proportional to $h_{\underset{\sim}{k}_p}^{\frac{1}{2}}$. The statistical factors for these two types of transitions are, respectively, $[(1 + \exp(-\beta E_{\underset{\sim}{k}_p})]^{-1}$ and $[1 + \exp(\beta E_{\underset{\sim}{k}_p})]^{-1}$. We thus find that

$$I = P_{SC}\, C^{-1} \qquad \text{(VIII.26a)}$$

$$\approx \beta^8 \int_{-\infty}^{\infty} d\epsilon_1 \int_{-\infty}^{\infty} d\epsilon_2 \int_{-\infty}^{\infty} d\epsilon' \int_{-\infty}^{\infty} d\epsilon_p \int_{-\infty}^{\infty} d\epsilon_e\ S'$$

$$\times \left[\frac{h_{\underset{\sim}{k}_p}\ (\epsilon_1 + \epsilon_2 + E_{\underset{\sim}{k}_p} - \epsilon' - \epsilon_e)^3}{1 + \exp(\beta E_{\underset{\sim}{k}_p})} + \frac{(1-h_{\underset{\sim}{k}_p})(\epsilon_1 + \epsilon_2 - E_{\underset{\sim}{k}_p} - \epsilon' - \epsilon_e)^3}{1 + \exp(-\beta E_{\underset{\sim}{k}_p})} \right] \qquad \text{(VIII.26b)}$$

where

$$S' = \left[(1 + e^{\beta\epsilon_1})(1 + e^{\beta\epsilon_2})(1 + e^{-\beta\epsilon'})(1 + e^{-\beta\epsilon_e})\right]^{-1} \quad . \qquad \text{(VIII.26c)}$$

The term proportional to $h_{\underset{\sim}{k}_p}$ is defined to be zero when $(\epsilon_1 + \epsilon_2 + E_{\underset{\sim}{k}_p} - \epsilon' - \epsilon_e)$ is negative, and the term proportional to $(1-h_{\underset{\sim}{k}_p})$ is similarly defined to be zero when $(\epsilon_1 + \epsilon_2 - E_{\underset{\sim}{k}_p} - \epsilon' - \epsilon_e)$ is negative.

The expression for I that is given in Eq. (VIII.26) is, in the limit as $\beta\epsilon_{op}$ goes to zero, the same as Eq. (VIII.21b). In that case, we found that I was approximately 903. We therefore define a correction factor $Y(\beta\epsilon_{op})$ such that

$$Y(\beta\epsilon_{op}) = I(\beta\epsilon_{op})/903 \quad ; \qquad \text{(VIII.27a)}$$

$$= P_{SC}(\beta\epsilon_{op})/P(0) \quad . \qquad \text{(VIII.27b)}$$

The correction factor Y is plotted against $\beta\ \epsilon_{op}$ in Figure 1.

It should be noted that ϵ_{op} is a function of temperature[28] and is zero above the critical temperature T_c, where

$$kT_c \approx 0.57\ \epsilon_{op}(0) \quad ,$$

and $\epsilon_{op}(0)$ is the energy gap at zero temperature. But $\epsilon_{op}(T)$ goes rapidly to $\epsilon_{op}(0)$ when T is small compared to T_c. Figure 1 indicates that the superconductivity correction is in any case unimportant for $\beta\ \epsilon_{op}(T)$ less than 5, or, in other words, T greater than about $0.35\ T_c$. Thus the temperature-dependence of the energy gap is unimportant for the present purposes and one might just as well consider ϵ_{op} equal to $\epsilon_{op}(0)$.

ii) Superconducting Neutrons

The energy-gap speculations in Sec. IV-C indicate that the neutrons should form a superfluid at densities less than about $0.5\ \rho_{nucl}$ and that the energy gap should be greater than 1 MeV over most of the superfluid range. We therefore assume that the neutron energy gap is large compared to both the proton energy gap and kT.

In the low-temperature limit, the phase-space integral can be

written, for the case of a neutron superfluid, in the form

$$P_{SC} = CI \quad , \tag{VIII.28a}$$

where

$$C = 2^{-9}\ \pi^{-13}\ m_\pi^{-15}\ m_n^{*3}\ m_p^{*}\ P_{Fp}\ P_{Fe}^{2}\ (kT)^8\ c^{-19} \quad , \tag{VIII.28b}$$

and

$$I \approx \frac{\beta^8}{8} \int_{-\infty}^{\infty} d\epsilon_1 \int_{-\infty}^{\infty} d\epsilon_2 \int_{-\infty}^{\infty} d\epsilon' \int_{-\infty}^{\infty} d\epsilon_p \int_{-\infty}^{\eta} d\epsilon_e\ S'(\eta - \epsilon_e)^3 \quad . \tag{VIII.28c}$$

The quantities η and S are given by

$$\eta = E_1 + E_2 + E' - \epsilon_p \quad . \tag{VIII.28d}$$

and

$$S = \left[(1+e^{\beta E_1})(1+e^{\beta E_2})(1+e^{-\beta E'})(1+e^{-\beta\epsilon_p})(1+e^{-\beta\epsilon_e})\right]^{-1} \quad . \tag{VIII.28e}$$

The integral I can be evaluated easily in the low-temperature limit, with the following result:

$$I \approx 0.123\ (\beta\epsilon_{on})^7\ e^{-2\beta\epsilon_{on}} \quad , \tag{VIII.29}$$

where ϵ_{on} is the neutron energy gap. Using Eqs. (VIII.28a), (VIII.28b), (VIII.29), and (III.4f), we find that

$$P_{SC}(\beta\epsilon_{on}) \approx 7 \times 10^{-27}\ \epsilon_{on}^{7}\ e^{-2\beta\epsilon_{on}} (\rho/\rho_{nucl})^2\ T_9 \, , \tag{VIII.30}$$

where ϵ_{on} is expressed in MeV. Comparison of Eqs. (VIII.23) and (VIII.30) indicates that $P_{SC}(\beta\epsilon_{on})$ is much smaller than P for temperatures less than 10^9 °K if ϵ_{on} is greater than 1 MeV.

C. Estimates of the Matrix Elements

1. Definitions

The dimensionless matrix elements of Eq. (VIII.6) can be written as follows:

$$M_V = \lambda_\pi^{-3} \int d^3\underset{\sim}{r}\, [\cos \underset{\sim}{k}' \cdot \underset{\sim}{r} + \Delta^0_{np}(\underset{\sim}{r})]^* [\cos \underset{\sim}{k} \cdot \underset{\sim}{r} + \Delta^0_{nn}(\underset{\sim}{r})]; \tag{VIII.31}$$

$$M_A = \lambda_\pi^{-3} \int d^3\underset{\sim}{r}\, [\cos \underset{\sim}{k}' \cdot \underset{\sim}{r} + \Delta^1_{np}(\underset{\sim}{r})]^* [\cos \underset{\sim}{k} \cdot \underset{\sim}{r} + \Delta^0_{nn}(\underset{\sim}{r})] \quad . \tag{VIII.32}$$

The initial-state wave function $[\cos \underset{\sim}{k} \cdot \underset{\sim}{r} + \Delta^0_{nn}(\underset{\sim}{r})]$ describes the relative motion of two neutrons with total spin zero. The functions $[\cos \underset{\sim}{k}' \cdot \underset{\sim}{r} + \Delta^0_{np}(\underset{\sim}{r})]$ and $[\cos \underset{\sim}{k}' \cdot \underset{\sim}{r} + \Delta^1_{np}(\underset{\sim}{r})]$ correspond to neutron-proton pairs in states with spin zero and spin one, respectively. We consider only states that are even under exchange of positions of the two nucleons, because we have neglected nucleon-nucleon scattering in odd-parity states.

Our lack of detailed knowledge of the effects of strong interactions makes accurate calculation of M_A and M_V difficult. In the following subsection, we use a dimensional argument to guess the order of magnitude and density dependence of the matrix elements. We then use two specific models for the nucleon-nucleon collisions to obtain more detailed estimates of M_A and M_V.

2. Dimensional Estimate

The integrals over $\underset{\sim}{r}$ in Eqs. (VIII.31) and (VIII.32) must yield a quantity proportional to the cube of a length. Thus we can estimate M_V and M_A by considering the physical lengths involved in the problem.

There are two lengths associated with the nucleon-nucleon potential: the attractive potential has a range of about $\lambda\!\!\!^{-}_{\pi}$ and the core radius is about $0.4\ \lambda\!\!\!^{-}_{\pi}$. The relevant wave numbers K, k, and k′ are all large fractions of $P_{Fn}\hbar^{-1}$ and $\hbar\ P_{Fn}^{-1} \approx 0.4\ \lambda\!\!\!^{-}_{\pi}(\rho/\rho_{nucl})^{-1/3}$.

Since all the lengths involved are nearly equal at nuclear density, we expect $|M_A|^2$ and $|M_V|^2$ to be of the order of unity at nuclear density. Furthermore, the effective range of Δ is probably determined primarily by k, k′, or $P_{Fn}\hbar^{-1}$. Thus we might expect M_A and M_V to be proportional to P_{Fn}^{-3}, i.e., to decrease as ρ^{-1}. In any event, we expect M_A and M_V to decrease slowly with increasing density, for moderate densities.

3. Scattering Model

In this model, we assume that the function Δ in Eqs. (VIII.31) and (VIII.32) is an outgoing scattered wave; that is, we assume that

$$\Delta \sim \sum_L e^{i\delta_L} \sin\delta_L\ P_L(\Omega)\ e^{ikr}/kr \qquad \text{(VIII.33)}$$

for $kr \gg 1$. Equation (VIII.33) does not describe the wave function for the region $kr < 1$, a region which contributes a large part of the integrals M_V and M_A. In order to estimate the wave function for small radii, we must assume a specific form for the interaction potential. We adopt the separable potential suggested by Yamaguchi[36]. The corresponding s-wave scattering wave function is given by

$$\cos \underline{k}\cdot\underline{r} + e^{i\delta}\sin\delta\ (e^{ikr} - e^{-\beta r})(kr)^{-1} \quad , \qquad \text{(VIII.34)}$$

where

$$e^{i\delta}\sin\delta = \left\{-i + \frac{\beta}{k}\left[-\frac{1}{2} + \frac{1}{2}\left(\frac{k}{\beta}\right)^2 + (2\pi^2\lambda\beta)^{-1}(\beta^2+k^2)^2\right]\right\}^{-1} \quad . \qquad \text{(VIII.35)}$$

The parameters λ and β, which represent, respectively, the coupling strength and range of the separable potential, can be determined from the singlet and triplet scattering data. The effective Hamiltonians acting on the space parts of the singlet and triplet wave functions are different. But the two singlet wave functions contained in M_V are eigenfunctions of the same Hamiltonian; since the two eigenfunctions correspond to different nucleon energies, they are orthogonal. Thus the free-scattering model implies that M_V equals zero.

We have computed M_A using values of β and λ that reproduce the experimental phase shifts between 25 and 100 MeV. The resulting expression for M_A is complicated, but, for $\rho \lesssim \rho_{nucl}$ it can be accurately approximated as follows:

$$|M_A|^2 \approx 0.3 \, (\rho_{nucl}/\rho)^{7/3} \quad . \qquad \text{(VIII.36)}$$

Note that the model described above neglects all correlations between the colliding nucleons and the other nucleons that are present.

4. Nuclear Matter Calculation

In using the scattering model discussed above, we have neglected the fact that the exclusion principle prohibits scattering into occupied states. Nearly all the states that are energetically accessible to two colliding nucleons are, in fact, occupied in a neutron star; hence there is almost no free scattering. The wave function describing the relative motion of two nucleons in a neutron star or in nuclear matter is a symmetrized plane wave, except for some distortion for small internucleon separations. This distortion is described by the

functions Δ in Eqs. (VIII.31) and (VIII.32). One can describe the collision between two particles most simply by using a two-particle Schrödinger equation. The effect of the interactions between the two colliding particles and the other nucleons can be represented approximately by replacing the free-particle masses by the effective masses. However, the Schrödinger equation must also be modified to take account of the fact that the states below the relevant Fermi levels are largely occupied; the appropriate modified form of the Schrödinger equation is the Bethe-Goldstone equation, which is often used in nuclear-matter calculations[24]. In the Bethe-Goldstone equation, the usual potential-energy term $V(r)\ \psi(\underset{\sim}{r})$ is replaced by $qV(\underset{\sim}{r})\ \psi(\underset{\sim}{r})$, where q is a projection operator that eliminates those Fourier components of $V(r)\ \psi(\underset{\sim}{r})$ that correspond to occupied states. Since the operator $qV(\underset{\sim}{r})$ is not hermitian, the solutions to the Bethe-Goldstone equation for different energies are not necessarily orthogonal. Thus M_V need not be zero as it was in the scattering model of subsection 3.

We follow Gomes *et al.*[24] in assuming spin-independent forces, which implies that M_A and M_V are equal. However, Δ_{nn} and Δ_{np} are not equal, since the exclusion principle differentiates between neutrons and protons. Using the fact that $|\underset{\sim}{k}|$ is different from $|\underset{\sim}{k}'|$ to show that

$$\int d^3r \cos \underset{\sim}{k}' \cdot \underset{\sim}{r} \cos \underset{\sim}{k} \cdot \underset{\sim}{r} = 0 \quad ,$$

we can rewrite Eqs. (VIII.31) and (VIII.32) in the form

$$M_A = M_V \qquad \text{(VIII.37)}$$
$$= \lambda_\pi^{-3} \int d^3r \left[\cos \underset{\sim}{k}' \cdot \underset{\sim}{r}\, \Delta_{nn}(\underset{\sim}{r}) + \cos \underset{\sim}{k} \cdot \underset{\sim}{r}\, \Delta_{np}(\underset{\sim}{r}) + \Delta_{np}(\underset{\sim}{r})\, \Delta_{nn}(\underset{\sim}{r})\right] .$$

The function $\Delta_{nn}(\underset{\sim}{r})$ has no Fourier components corresponding to the scattering of either neutron into an occupied state, i.e., $\Delta_{nn}(\underset{\sim}{r})$ has no components with wave number $\underset{\sim}{p}$ for which $\left|\frac{1}{2}\underset{\sim}{K} + \underset{\sim}{p}\right| < P_{Fn}\hbar^{-1}$. Since $\underset{\sim}{k}'$ is approximately one-half $\underset{\sim}{K}$, $\Delta_{nn}(\underset{\sim}{r})$ has no Fourier component with wave number $\pm\,\underset{\sim}{k}'$, and

$$\int d^3r \cos \underset{\sim}{k}' \cdot \underset{\sim}{r}\, \Delta_{nn}(\underset{\sim}{r}) = 0 \quad .$$

We follow Gomes et al. in assuming that the nucleon-nucleon potential consists of an attractive square well and a hard core. The long-range attractive well has little effect on the wave function for densities comparable to ρ_{nucl}; the distortion functions Δ are due almost entirely to the hard core. We consider the case where the core radius, a, is much less than $\hbar[P_{Fn}]^{-1}$. The resulting low-density approximation should be reasonably accurate up to densities about equal to nuclear density. In the low-density limit, one can make the following simplifications: first, we need only consider s-waves; second, we can neglect the last term in Eq. (VIII.37) because the product $\Delta_{np}(\underset{\sim}{r})\,\Delta_{nn}(\underset{\sim}{r})$ is of second order in $P_{Fn}a/\hbar$; third, in computing $\Delta_{np}(\underset{\sim}{r})$ we can neglect the leakage of the wave function inside the core as well as the changes in the wave function's normalization caused by the distortion terms Δ. One can then use the Bethe-Goldstone equation to find the Fourier component of $\Delta_{np}(\underset{\sim}{r})$ that corresponds to the momentum $\underset{\sim}{k}$. In this way, one finds that

$$\begin{aligned} |M_A|^2 &= |M_V|^2 \\ &= \left[(4\pi a)\,(k'^2 - k^2)^{-1}\,\lambda_\pi^{-3}\right]^2 \quad . \end{aligned} \tag{VIII.38}$$

The values of k and k′ are determined by kinematics and the exclusion principle. We found in Sec. VIII-B that the particles involved in reactions (I.1) and (I.5) must be in a narrow band of states at the top of their respective Fermi seas. Thus the momentum of each particle involved in a reaction must be nearly equal to the Fermi momentum for that particle. The neutron Fermi momentum is large compared to the proton and electron Fermi momenta; the neutrino momentum, which is of the order of kT/c, is completely negligible. Hence the momentum $\underset{\sim}{p}_1'$ of the final neutron must be approximately equal to the momentum in the initial state, $\underset{\sim}{p}_1 + \underset{\sim}{p}_2$. If we neglect the momenta of all particles except the neutrons, we find that the three neutron momenta form an equilateral triangle with sides of length P_{Fn}. It follows that k is equal to $3^{\frac{1}{2}}(2\hbar)^{-1} P_{Fn}$ and k′ is equal to $(2\hbar)^{-1} P_{Fn}$. Substituting these values of k and k′ in Eq. (VIII.38) using Eq. (III.4e), and choosing the core radius a to be 4×10^{-14} cm, we find that

$$|M_A|^2 = |M_V|^2$$

$$= 1.0 \, (\rho_{nucl}/\rho)^{4/3} \quad . \qquad \text{(VIII.39)}$$

5. Summary

The scattering model and the model based on the usual picture of nuclear matter both predict that $|M_A|^2$ is of the order of unity near nuclear density and that $|M_A|^2$ decreases with increasing density. The relatively small difference between Eqs. (VIII.36) and (VIII.39), and the agreement of both equations with a dimensional analysis, indicates that the value of the total matrix element is not critically sensitive

to the uncertainty in our knowledge of the strong internucleon force.

D. Related Reactions

1. The Inverse Reaction

We have calculated so far only the rate of neutrino energy loss via reaction (I.1). At the temperatures and densities for which reactions (I.1) and (I.5) are the dominant means of ensuring chemical equilibrium in the n-e-p system, the rates of reactions (I.1) and (I.5) must be equal in order to preserve the equilibrium. We shall now show that the rates of neutrino energy loss by the two reactions are in fact equal within the approximations we have used in calculating the rate of reaction (I.1).

For reaction (I.1), Eq. (VIII.6) provides an evaluation of $\Sigma_{\text{spins}} |\langle f | H | i \rangle|^2$; this equation is accurate if the lepton momenta are small compared to the neutron momenta. The expression for $\Sigma_{\text{spins}} |\langle f | H | i \rangle|^2$ for reaction (I.5) is identical to Eq. (VIII.6) if the lepton momenta are again neglected. The nucleon matrix elements M_A and M_V for reaction (I.5) are the complex conjugates of M_A and M_V for reaction (I.1). Furthermore, one can easily show that Eq. (VIII.20) for the phase-space factor P holds equally well for reactions (I.1) and (I.5). Thus, Eq. (VIII.7), which gives the neutrino luminosity in terms of M_V, M_A, and P, predicts the same rates of energy loss for the direct and inverse reactions.

2. Muon Production

Muons are present in a neutron star if the electron Fermi energy is greater than the muon rest energy $m_\mu c^2$; muon neutrinos are then produced by reactions (I.2) and (I.6). The rate of reactions (I.2) and (I.6) can be computed by the method used for reactions (I.1) and (I.5). The only difference in the rates of production of muon and electron neutrinos results from the fact that the density of muon states at the top of the muon Fermi sea differs from the density of electron states at the top of the electron Fermi sea by a factor F, where, for W_{Fe} greater than $m_\mu c^2$,

$$F = P_{F\mu}/P_{Fe} \quad . \tag{VIII.40}$$

Using the equilibrium relations (Eq. (III.5)), we obtain

$$F = [1-(m_\mu c^2/W_{Fe})^2]^{\frac{1}{2}} \quad . \tag{VIII.41}$$

The ratio F is, of course, zero when W_{Fe} is less than $m_\mu c^2$. Using Eq. (III.40) to estimate W_{Fe}, we find that

$$F = \left[1 - 2.25\ (\rho_{nucl}/\rho)^{4/3}\right]^{\frac{1}{2}} \quad \text{for} \quad \rho > 1.8\ \rho_{nucl} \tag{VIII.42a}$$

and

$$F = 0 \quad \text{for} \quad \rho < 1.8\ \rho_{nucl} \quad . \tag{VIII.42b}$$

E. Numerical Expressions

We now combine the results of the last few subsections to obtain a numerical expression for energy loss by neutrino emission by reactions (I.1), (I.2), (I.5), and (I.6). We consider densities high enough to ensure that the neutrons do not form a superfluid and that the nucleon

gas is stable to the formation of "nuclei".

We substitute Eqs. (VIII.23) and (VIII.39) into Eq. (VIII.9), multiply by $2(1 + F)$ to take account of reactions (I.2), (I.5), and (I.6), and multiply by Y to correct for proton superconductivity. We then obtain

$$L_\nu^{nn} \approx (10^{20} \text{ erg cm}^{-3} \text{ sec}^{-1})(\rho/\rho_{nucl})^{2/3} T_9^8 \, Y(1 + F), \quad \text{(VIII.43)}$$

where F is given in Eq. (VIII.42) and Y is plotted in Figure 1.

The luminosity of a mass M_s of neutron-star matter with a uniform density ρ is given by the expression

$$L_\nu^{nn} \approx (6 \times 10^{38} \text{ erg sec}^{-1}) \, (M_s/M_\odot) \, (\rho_{nucl}/\rho)^{1/3} \, T_9^8 \, Y(1 + F) \, , \quad \text{(VIII.44)}$$

where $M_\odot$ is the mass of the sun.

F. Comparison with Previous Work

Several authors have previously calculated the rates of nucleon-nucleon reactions using the model of a normal Fermi gas. Chiu and Salpeter[15] first suggested that reactions (I.1) and (I.5) might contribute importantly to the cooling of neutron stars. They used a dimensional analysis to obtain the expression

$$L_\nu^{CS} = (2 \times 10^{36} \text{ erg/sec}) \, T_9^8 \, (E_{Fn}/50 \text{ MeV})^{-2.25} (M_s/M_\odot)$$

for the rate of energy loss by neutrinos produced in reactions (I.1) and (I.5). The result given by Chiu and Salpeter has the correct temperature dependence, but it is typically two or three orders of magnitude smaller than our best estimate (as given in Eq. (VIII.44), if proton superconductivity is neglected.

Finzi[21] has performed a detailed calculation of the rate of reaction (I.1) at a density of 1.6 ρ_{nucl}. His treatment of the matrix element differs from ours in several ways. First, he neglected the effects of the exclusion principle on the relative motion of two colliding nucleons. Second, he treated the strong nucleon-nucleon interaction as a first-order perturbation; the nucleon scattering matrix element was assumed to be equal to a constant, which was determined by the requirement that the same first-order perturbation treatment yield a value of 3×10^{-26} cm^2 for the scattering cross section for free nucleons. Third, he treated the nucleons and leptons as scalar particles (instead of Fermions) in calculating the amplitude associated with the weak vertex. Finzi's treatment of the phase-space factor P differs from ours in two ways: First, a minor error in his integrations results in an extra factor that is approximately equal to 2/3; second, he uses the free masses m_n and m_p instead of effective masses m_n^* and m_p^* to describe the density of single-particle states. Finzi gave the following expression for the luminosity of 0.6 $M_\odot$ of neutron star matter at 1.6 ρ_{nucl}:

$$L_\nu^F = (8.83 \times 10^{37} \text{ erg/sec})\, T_9^8 \quad .$$

This result differs from the luminosity predicted by Eq. (VIII.44) for the same mass and density by about a factor of one-fifth (if we set F equal to zero and neglect superconductivity). The disagreement between the two answers is small compared to the obvious uncertainties in either approach. The closeness of the two results for the rate of energy loss arises partly from the fact that the matrix element is, as we mentioned in Sec. VIII-C, relatively insensitive to the details of the model used

to calculate it.

Ellis[22] has recently reported a similar calculation of the rate of energy loss by reactions (I.1) and (I.5). Following Finzi, he employed second-order perturbation theory to estimate the transition amplitude, using the known nucleon-nucleon scattering data to determine the coupling at the strong vertex; he also neglected the effects of the surrounding neutrons on the relative motion of the colliding nucleons. Unlike Finzi, Ellis treated the nucleons and leptons as Fermions, and he performed the calculation for a range of densities. Although he did treat the nucleons relativistically, he did not consider the protons to be degenerate, despite the fact that E_{Fp}/kT is of the order of 50 for most temperatures and densities expected in neutron stars. Ellis performed part of the integration over phase space by a Monte Carlo technique; he gave the following formula, which accurately represents his numerical results:

$$L_\nu^E = (6 \times 10^{38} \text{ erg/sec}) \, (E_{Fn}/50 \text{ MeV})^{-1.9} \, (M_s/M_\odot) \, T_9^{8.7} \quad .$$

The peculiar temperature dependence is due primarily to the fact that he assumed that the protons were non-degenerate. The above relation does not differ from that obtained by Finzi or by us by more than a factor of ten in the most interesting domains of temperature and density.

IX. PION COOLING

A. General Discussion

In this section we calculate the rates of several neutrino-producing reactions that will occur if quasi-free pions are present neutron-star matter. Quasi-free pions, if they are present at all in a neutron star, must be highly degenerate; that is, nearly all the pions must be in the lowest-energy single-particle state. The momentum $\underset{\sim}{p}_{\pi}$ and energy ω_{π} of this lowest single-particle state are not known. The reaction rate fortunately does not depend sensitively on $\underset{\sim}{p}_{\pi}$, and we can assume $\underset{\sim}{p}_{\pi}$ is zero without making a serious error. The energy ω_{π} can be written

$$\omega_{\pi} = B_{\pi^-} + m_{\pi} c^2 \quad , \tag{IX.1}$$

where B_{π^-}, the pion binding energy, was defined in Sec. III.

Reactions (I.3), (I.4), (I.7), and (I.8) should be the most important reactions involving quasi-free pions. We shall first derive an expression for the rate of energy loss by reaction (I.3), and then modify the formula to take account of the other reactions.

The rate of energy loss per pion by reaction (I.3) is given by

$$L_{\nu}^{(3)} = 2\pi \hbar^{-1} \sum_{\text{spins}} \int d^3n_1 \, d^3n_1' \, d^3n_e \, d^3n_{\bar{\nu}} \, S \, \delta(E_f - E_i) \, E_{\bar{\nu}} \, |\langle (n, e^-, \bar{\nu}) | H_W | (n, \pi^-) + \rangle|^2 \tag{IX.2}$$

The notation used in Eq. (IX.2) is similar to that used in Eq. (VIII.3): the differentials d^3n_1, d^3n_1', d^3n_e, and $d^3n_{\bar{\nu}}$ refer to the initial neutron, the final neutron, the electron, and the antineutrino,

respectively. The statistical factor S is identical to that defined in Eq. (VIII.3c), except that it only includes factors for the two neutrons and the electron (all pions are assumed to be in the lowest energy state). The initial state vector $|(n,\pi^-)+\rangle$ is an eigenstate of the strong Hamiltonian; the incoming part of $|(n,\pi^-)+\rangle$ corresponds to a neutron with momentum $\underset{\sim}{p}_1$ and a pion with momentum $\underset{\sim}{p}_\pi$. The final state vector $(n,e^-,\bar{\nu})\rangle$ is a product of momentum eigenstates representing a neutron (with momentum $\underset{\sim}{p}_1'$), an electron (with momentum $\underset{\sim}{p}_e$), and a neutrino (with momentum $\underset{\sim}{p}_{\bar{\nu}}$).

We again find it convenient to separate the neutrino luminosity into a dimensionless phase-space factor, a dimensionless matrix element, and a constant factor. The matrix element is nearly constant over those regions of phase space where the statistical factor S is non-negligible. Thus we can remove the matrix element from the integral and write the neutrino luminosity in the form

$$L_\nu^{(3)} = P\, M^2\, G^3\, (2\pi)^4\, \hbar^{-1}\, \lambda_\pi^{-6} \quad , \qquad \text{(IX.3a)}$$

where

$$P = (2\pi)^{-12}(m_\pi c)^{-9} \int d^3p_1\, d^3p_1'\, d^3p_e\, d^3p_{\bar{\nu}}\; \delta(E_f - E_i)\; \delta^3(\underset{\sim}{P}_f - \underset{\sim}{P}_i)\; S\, E_{\bar{\nu}} \quad , \qquad \text{(IX.3b)}$$

$$M^2\, \delta^3(\underset{\sim}{P}_f - \underset{\sim}{P}_i) = G^{-2}\, \Omega^4\, \lambda_\pi^{-3} (2\pi\hbar)^{-3} \times \sum_{\text{spins}} |\langle (n,e^-,\bar{\nu}) \,|\, H_w \,|\, (n,\pi^-)+\rangle|^2 \quad , \qquad \text{(IX.3c)}$$

and $\underset{\sim}{P}_i$ and $\underset{\sim}{P}_f$ are the initial and final momenta, respectively.

In the following sections, we estimate the values of P and M^2, employing arguments that are analagous to those we have previously used to calculate the nucleon-nucleon cooling rate. We shall see, however, that our knowledge of the relevant matrix elements is much less accurate for pionic cooling than it is for nucleon-nucleon cooling.

B. The Phase-Space Factor

As in the case of the nucleon-nucleon cooling, we describe the density of available initial and final states by the phase-space factor P, which, for reaction (I.3), is defined in Eq. (IX.3b). It is unlikely that quasi-free pions could occur at densities less than nuclear density and it seems likely that the neutrons in a neutron star do not have a gap in their spectrum for densities greater than nuclear density. Hence we do not consider neutron superfluidity in the calculation of the rate of cooling by pion reactions. We exclude the formation of "nuclei" for the same reason: We saw in Sec. IV-B that such "nuclei" should not be stable at densities greater than nuclear density.

The integrand in Eq. (IX.3b) is concentrated in the small "important region" of phase space where the energy of each particle is within a few kT of its Fermi energy. Just as in Sec. VIII-B, we neglect the contribution to the integral P from certain regions far from the "important region"; in particular, we consider only the parts of phase space satisfying the following inequalities:

$$p_1 + p_{\bar{\nu}} + p_\pi - p_e < p_1' < p_1 - p_{\bar{\nu}} - p_\pi + p_e \quad ; \qquad \text{(IX.4a)}$$

$$p_1 > p_{\bar{\nu}} + p_\pi \quad . \qquad \text{(IX.4b)}$$

The phase-space factor for reaction (I.3) can be evaluated by the methods used to calculate P for reaction (I.1). We use inequalities (IX.4) to evaluate the angular integral A, where

$$A = \int d\Omega_1 \int d\Omega_{\bar{\nu}} \int d\Omega_e \int d\Omega_1' \; \delta^3(\underset{\sim}{p}_1 + \underset{\sim}{p}_\pi - \underset{\sim}{p}_1' - \underset{\sim}{p}_e - \underset{\sim}{p}_{\bar{\nu}}). \qquad \text{(IX.5)}$$

The result is

$$A = 32\pi^3 \, (p_1' \, p_e \, p_1)^{-1} \quad . \qquad \text{(IX.6)}$$

Substituting Eq. (IX.6) into Eq. (IX.3b) and using the energy delta function to integrate over the neutrino momentum yields

$$P = D \int_0^\infty p_1 \, dp_1 \int_0^\infty p_1' \, dp_1' \int_0^{p_m} p_e \, dp_e \, (E_o)^3 \, S \quad , \qquad \text{(IX.7a)}$$

where

$$D = 2^{-7} \, \pi^{-9} \, m_\pi^{-9} \, c^{-12} \quad , \qquad \text{(IX.7b)}$$

$$E_o = E_1 + \omega_\pi - E_1' - W_e \quad , \qquad \text{(IX.7c)}$$

and p_m is defined such that E_o is equal to zero when p_e equals p_m.

As in Sec. VIII-B, it is convenient to change variables: We define $m_n^*(E_n)$, x_1, x_2, and x_3 by Eqs. (VIII.18b) and (VIII.19a-c), respectively. We then use the conditions of chemical equilibrium (Eqs. (III.10)) to obtain

$$P = D \, (kT)^6 c^{-2} \int_{-y_n}^{\infty} m_n^*(E_1) \, dx_1 \int_{-\infty}^{y_n} m_n^*(E_1') \, dx_2 \int_{-(x_1 + x_2)}^{y_e} dx_3$$

$$\times \, (\omega_\pi - kT \, x_3) \; (x_1 + x_2 + x_3)^3 \; S \quad , \qquad \text{(IX.8)}$$

ere y_n and y_e were defined in Eqs. (VIII.20b) and (VIII.20c). To lowest order in kT/E_{Fn} we can set the effective masses equal to their value at the neutron Fermi energy and neglect x_3 kT relative to ω_π. Replacing the limits y_n and y_e by infinity causes errors of the order of $e^{-\beta E_{Fn}}$ and $e^{-\beta E_{Fe}}$, respectively; these errors can be neglected since βE_{Fn} and βE_{Fe} are both much greater than 100. We then obtain the following expression for the phase-space factor:

$$P = 2^{-7}\,\pi^{-9}(\omega_\pi/m_\pi c^2)\;\;(m_n^*/m_\pi)^2\,I\,(kT/m_\pi c^2)^6 \quad , \qquad \text{(IX.9a)}$$

where

$$I = \int_{-\infty}^{\infty} dx_1 \int_{-\infty}^{\infty} dx_2 \int_{-(x_1+x_2)}^{\infty} dx_3\;(x_1+x_2+x_3)^3 \prod_{i=1}^{3}\left[1+e^{x_i}\right]^{-1} \quad , \qquad \text{(IX.9b)}$$

$$= (457/5040)\,\pi^6 \quad . \qquad \text{(IX.9c)}$$

The phase-space factor is proportional to T^6, as expected from the heuristic argument in Sec. VII. The factor P for reaction (I.3) depends on the density only through the effective mass m_n^* and the pion ground-state energy ω_π. Referring to the results of Sec. V-B, we assume that the neutron effective mass is 1.0 m_n. We also assume that the pion binding energy B_{π^-} is small compared to $m_\pi c^2$. Then the pion phase-space factor can be conveniently expressed in the form

$$P = 5.6 \times 10^{-23}\,T_9^6 \quad . \qquad \text{(IX.10)}$$

C. Matrix Element

It is much more difficult to estimate the matrix element for reaction (I.3) than it was to determine the matrix element for reaction (I.1), because the pions must be treated relativistically and it is thus

difficult to describe the pion-nucleon scattering by means of a potential. We use a dimensional argument to estimate the pion matrix elements, using specific crude models for the interaction to indicate which of the relevant lengths are in fact important in the matrix element.

The most obvious physical lengths involved in the matrix element M are the following: $\hbar c\omega_\pi^{-1}$, $\hbar(m_e c)^{-1}$, $\hbar(m_n c)^{-1}$, $\hbar(P_{Fe})^{-1}$, $\hbar c(E_{\bar{\nu}})^{-1}$, $\hbar(P_{Fn})^{-1}$, and the range of the pion-nucleon potential. The range of the pion-nucleon potential is of the order of the scale length λ_π. The pion binding energy B_{π^-} is probably not large compared to $m_\pi c^2$; $\hbar c\omega_\pi^{-1}$ and $\hbar(P_{Fe})^{-1}$ are thus also of the order of λ_π. If these physical lengths were the only ones important in M, one would conclude that the dimensionless matrix element is of the order of unity.

However, there remain four relevant lengths that are not approximately equal to λ_π: $\hbar c\, E_{\bar{\nu}}^{-1}$, $\hbar(m_e c)^{-1}$, $\hbar(P_{Fn})^{-1}$, and $\hbar(m_n c)^{-1}$. To obtain some idea of the importance of each of these lengths in the matrix element M^2, we calculated the matrix element using the models indicated by the Feynman diagrams of Figure 2. In the first diagram, the reaction is assumed to occur through decay of a pion, while the pion is colliding with a neutron. This assumption provides some insight because it enables one to separate the contributions from the strong and weak vertices. In evaluating the contributions from diagrams (2b) and (2c) we used the simple pion-nucleon Hamiltonian[37]

$$H_s = i\, g\, \bar{\psi}_N\, \underset{\sim}{\tau} \gamma_5\, \psi_N \cdot \underset{\sim}{\varphi} \quad , \qquad \text{(IX.11a)}$$

where

$$g \approx 14 \quad . \qquad \text{(IX.11b)}$$

Diagrams of higher order in g than (2b) and (2c) would, of course, make significant contributions, because of the large value of g. We still use diagrams (2b) and (2c), however, to indicate what lengths are important

We find that the energy $E_{\bar{\nu}}$ enters the problem only through $E_e \pm E_{\bar{\nu}}$. Since E_e is much larger than $E_{\bar{\nu}}$, the length $\hbar c\, E_{\bar{\nu}}^{-1}$ does not affect the reaction rate appreciably.

The momentum and energy transferred to the leptons do not depend strongly on P_{Fn}, and, at least for the simple models we considered, the amplitudes at the strong vertices do not depend strongly on P_{Fn} either. Thus the matrix element is not critically dependent on $\hbar(P_{Fn})^{-1}$.

The momentum and energy transferred to the leptons do not depend on m_e; the strong-vertex contribution and the energy denominators are thus largely independent of $\hbar(m_e c)^{-1}$. For diagrams that involve pion decay, as (2a) and (2b) do, the amplitude at the weak vertex is proportional to m_e. The same factor occurs in the rate of the electron-decay of the free pion. The contributions to M^2 from diagrams like those in Figs. (2a) and (2b) are therefore reduced by the small factor $(m_e/m_\pi)^2$. The neutron-decay diagram (2c) is not inhibited by such a factor, and the contribution from diagram (2c) is consequently much larger than the contributions from the diagrams of Figs. (2a) and (2b). The contributions from the dominant diagrams that do not involve pion decay are essentially independent of m_e, and the total reaction rate thus does not vary significantly with $(\hbar/m_e c)$.

All of the lengths that are important in determining M^2 are thus of the order of $\lambda\!\!\!^{-}_\pi$, except for one length, $\hbar/m_n c$, which differs from

$\lambda\!\!\!^{-}_{\pi}$ by a factor of m_π/m_n. The effect of the nucleon mass on the matrix element is subtle; the masses of the hadrons and the coupling constants characterizing their interactions are connected in a complicated way. The ratio $(\lambda\!\!\!^{-}_{\pi}/\lambda\!\!\!^{-}_{n})$, or m_n/m_π, is typical of the dimensionless quantities arising in strong-interaction calculations. Our dimensional reasoning can only suggest that M should be of the order of unity, within perhaps a couple of factors of m_n/m_π.

Explicit calculation of the dimensionless matrix element using the diagram of Fig. 2c implies that M^2 is of the order of ten, and we shall use that value in numerical expressions, realizing that our guess for M^2 could easily be wrong by at least an order of magnitude.

D. Related Reactions

Muons are expected to be present in neutron stars that contain pions if ω_π is greater than $m_\mu c^2$ (cf. Eqs. (III.6), (III.10), and (IV.1)). When muons are present, reaction (I.4) contributes to the rate of neutrino production. The phase space factor for reaction (I.4) is the same as for reaction (I.3) if, as expected, $\omega_\pi - m_\mu c^2$ is much larger than kT. The matrix element M is, on the other hand, not the same for decays producing muons and electrons. In Sec. IX-C we found that diagrams such as Fig. 2c that involve the decay of a neutron into a proton, electron, and antineutrino were much more important than diagrams such as Figs. 2a and 2b that involve the decay of a virtual π^- into an e^- and a $\bar{\nu}_e$. However, the pion-decay processes that are inhibited by a factor of $(m_e/m_\pi)^2$ in the case of decay into a e and $\bar{\nu}_e$ are only inhibited by a factor of $(m_\mu/m_\pi)^2$ in the case of decay into a μ and $\bar{\nu}_\mu$. Thus diagrams such as Figs. 2a and 2b may contribute importantly to the rate of production

of muon neutrinos. The rates of production of electron and muon neutrinos may nevertheless be of the same order of magnitude, and, lacking an accurate estimate of either rate, we shall assume that the rates of energy loss by muon and electron neutrinos are equal.

As in the case of the nucleon-nucleon reactions, the rate of energy loss by the inverse processes (reactions (I.7) and (I.8) can be proved equal to the rate of energy loss by the forward processes (reactions (I.3) and (I.4)).

E. Numerical Expressions

The rate of energy loss by neutrinos produced in pion reactions can be obtained by substituting values of M^2 and P in Eq. (IX.3a). In particular, we use Eq. (IX.10) for the phase space factor and set M^2 equal to ten. Multiplying by four to account for the muonic decay (reaction (I.4)) and the inverse processes (reaction (I.7) and (I.8), we find the expression

$$L_\nu^{\pi n} \approx 10^{-11} \text{ erg/sec} \qquad \text{(IX.12)}$$

for the rate of energy loss per pion. The neutrino luminosity of a mass M_s of stellar matter is then given by

$$L_\nu^{\pi n} \approx (10^{46} \text{ erg/sec})\, T_9^{\,6}\, (n_\pi/n_b)(M_s/M_\odot) \quad , \qquad \text{(IX.13)}$$

where n_π/n_b is the ratio of the number density of quasi-free pions to the number density of baryons. Equations (IX.12) and (IX.13) are probably accurate to within a factor of something like one-hundred. The result given in Eq. (IX.13) is about twice the rate indicated by the

heuristic discussion in Sec. VII. We note that the energy loss by the pionic processes is of the order of $10^7\ T_9^{-2}$ times the energy loss by the nucleon-nucleon processes if a significant number of quasi-free pions are present.

X. COOLING TIMES AND OBSERVABILITY

A. Specific Heat of a Neutron Star

Consider a system consisting of a mass M_s of neutron-star matter with uniform density ρ and uniform temperature T. The contribution of the neutron gas to the specific heat of the system is given approximately by

$$C_{neut} \approx (10^{48}\ \text{erg}/10^{9}\ ^{o}\text{K})\ T_9\ (\rho/\rho_{nucl})^{-2/3} \times (M_s/M_0)\ Q_{neut} \quad , \qquad (X.1a)$$

where T_9 is the temperature in units of $10^9\ ^{o}$K, and Q_{neut} represents the change that superfluidity causes in the specific heat of the neutron gas. The factor Q_{neut} is equal to unity above the critical temperature for superfluidity. A large superfluid gap in the spectrum of the gas greatly reduces the specific heat, and Q_{neut} goes exponentially to zero as the temperature decreases below T_c, the critical temperature for superfluidity. Bardeen et al.[28] have shown that the modification in the specific heat caused by superconductivity is represented reasonably accurately for most $T < T_c$ by

$$Q_{neut} \approx 8.5\ (T_c/T)\ e^{-1.44\ T_c/T} \quad , \qquad (X.1b)$$

where

$$kT_c = 0.57\ \epsilon_{on}(T=0) \quad . \qquad (X.1c)$$

If "nuclei" are not present in the neutron-star matter, the proton specific heat is given approximately by

$$C_{prot} \approx C_{neut} \, (m_p^*/m_n^*) \, (P_{Fp}/P_{Fn}) \, (Q_{prot}/Q_{neut}), \quad (X.2)$$

where Q_{prot} is the correction caused by proton superconductivity. Assuming that m_p^*/m_n^* is about 0.6 and using Eqs. (III.4) to estimate (P_{Fp}/P_{Fn}), we find that

$$C_{prot} \approx 0.1 \, C_{neut} \, (Q_{prot}/Q_{neut}) \quad (X.3)$$

near nuclear density.

Similarly, the electron specific heat is given approximately by

$$C_{elect} \approx C_{neut} \, (P_{Fe}/m_n^* c) \, (P_{Fe}/P_{Fn}) \, (1/Q_{neut}) \quad (X.4)$$

$$\approx 0.01 \, C_{neut} \, (1/Q_{neut}) \quad (X.5)$$

near nuclear density. The electrons in a neutron star should not be superconducting; consequently the electron specific heat would be dominant if both the neutron and proton energy gaps were large compared to kT.

The muon specific heat is always small compared to the electron specific heat; it is given by

$$C_{muon} = (P_{F\mu}/P_{Fe}) \, (m_\mu c/P_{Fe}) \, C_{elect}. \quad (X.6)$$

Pions would not contribute significantly to the specific heat of a star even if a large number of π^-'s were present. Since the degeneracy temperature for a pion gas is given roughly by

$$T_{deg} \approx (4 \times 10^{12} \, ^\circ K) \, (n_\pi/n_n)^{2/3} \, (\rho/\rho_{nucl})^{2/3}, \quad (X.7)$$

pions are highly degenerate in a neutron star if they are present in significant numbers. If there is no gap in the pion excitation spectrum, the pion specific heat is proportional to $(T/T_{deg})^{3/2}$ and is small compared to the electron specific heat for temperatures less than 10^9 °K. Any gap in the pion spectrum would reduce the pion specific heat still further.

Thermal excitations such as sound waves, plasma waves, spin waves, and isospin waves contribute negligibly to the specific heat because the density of such thermal excitations goes rapidly to zero as the temperature goes to zero.

B. Sample Cooling Rates

We consider neutron-star matter cooling by the following processes: radiation of photons from the surface, the plasma-neutrino process ($\gamma \rightarrow \nu + \bar{\nu}$), the nucleon-nucleon processes (reactions (I.1), (I.2), (I.5), and (I.6)), the neutrino-bremsstrahlung process ($e^- + Z \rightarrow e^- + Z + \nu + \bar{\nu}$), and the pion-nucleon reactions (reactions (I.3), (I.4), (I.7), and (I.8)).

We assume that the star radiates photons from its surface like a black body; the detailed atmospheric calculations of Orszag[38] indicate that the black-body assumption is a reasonable overall approximation. The photon luminosity is then given by

$$L_\gamma = (7 \times 10^{36} \text{ erg sec}^{-1}) \, T_{e7}^{\,4} \, R_{10}^{\,2} , \qquad (X.8)$$

where T_{e7} is the effective surface temperature in units of 10^7 °K, and R_{10} is the radius of the star in units of 10 km.

Emission of neutrinos by the plasma process takes place primarily

close to the surface of the star. Chiu and Salpeter[15] have used the results of neutron-star model calculations to arrive at the following approximate expression for the neutrino luminosity by the plasma process:

$$L_\nu^{pl} \approx (2 \times 10^{36} \text{ erg/sec})(M_s/M_\odot)^{-1} R_{10}^{\ 4} T_9^{\ 10} . \qquad (X.9)$$

We consider the nucleon-nucleon reaction at densities high enough that the neutrons do not form a superfluid. The rate is then

$$L_\nu^{nn} \approx (6 \times 10^{38} \text{ erg sec}^{-1}) (M_s/M_\odot) \times (\rho_{nucl}/\rho)^{1/3} T_9^{\ 8} Y (1 + F) , \qquad (VIII.44)$$

where Y represents the correction for proton superconductivity and $(1 + F)$ is the factor allowing for the presence of muons.

Ruderman[25] has calculated the rate of the neutrino bremsstrahlung reaction,

$$e^- + Z \longrightarrow e^- + Z + \nu + \bar{\nu} , \qquad (X.10)$$

where Z represents a "nucleus" of charge Z. Reaction (X.10) occurs only at densities low enough that the "nuclei" are stable. Ruderman's expression for the rate of reaction (X.10) implies that a mass M_s of uniform neutron-star matter would have a neutrino luminosity given by

$$L_\nu^{Ze} = (2 \times 10^{39} \text{ erg sec}^{-1}) (M_s/M_\odot) \times Z^2 (n_Z/n_b) T_9^{\ 6} , \qquad (X.11)$$

where n_Z is the number density of nuclei and n_b is the number

density of baryons.

Finally, the neutrino luminosity caused by the pion-nucleon reactions is written

$$L_\nu^{\pi n} \approx (10^{46} \text{ erg sec}^{-1}) (M_s/M_\odot) (n_\pi/n_b) T_9^6 . \qquad (X.12)$$

The rate of change of the interior temperature can easily be computed (if the ratio of the interior to surface temperature is known) using the relation

$$C_{neut} \frac{dT}{dt} \approx - L_\gamma - L_\nu^{pl} - L_\nu^{nn} - L_\nu^{Ze} - L_\nu^{\pi n} , \qquad (X.13)$$

where we have assumed that the neutrons make the dominant contribution to the specific heat.

We now reproduce the equations of cooling for a few simple cases. Neglecting neutron superfluidity, the effects of "nuclei" and pions, and the plasma-neutrino process, we find that the time required for a star's interior to cool from T(i) to T(f) is given by

$$\Delta t \approx a \alpha^6 \left\{ \left[\alpha T_9(f)\right]^{-2} - \left[\alpha T_9(i)\right]^{-2} + b \left[\tan^{-1} x_f - \tan^{-1} x_i \right] \right\} , \qquad (X.14a)$$

where

$$a \approx (1900 \text{ yr}) (M_s/M_\odot)^{1/3} , \qquad (X.14b)$$

$$b \approx 8.5 (\rho / \rho_{nucl})^{1/6} (M_s/M_\odot)^{1/6} , \qquad (X.14c)$$

$$x_i = b \left[\alpha T_9(i)\right]^2 , \qquad (X.14d)$$

and

$$x_f = b \left[\alpha\, T_9(f)\right]^2 \qquad \text{(X.14e)}$$

We have assumed that the temperature parameter $\alpha(T)$, defined by

$$\alpha(T) = 10^{-2}\, T/T_e \qquad \text{(X.15a)}$$

or

$$\alpha(T) = T_9/T_{e7} \quad , \qquad \text{(X.15b)}$$

is approximately constant for T between T(i) and T(f).

It is clear from Eq. (X.14) that the cooling rate depends strongly on the parameter $\alpha(T)$, which must be determined from theoretical models of neutrons stars. We wish to stress that α is, in fact, the only quantity derived from neutron-star models that enters sensitively into the theoretical predictions of the cooling rates. It is primarily through α that the models affect the question of the observability of the surface radiation from neutron stars, and future model calculations should therefore attempt to establish the uncertainty in α due, for example, to uncertainties in the equation of state.

If the neutrino-bremsstrahlung process is dominant, the time required for the interior to cool from $T_9(i)$ to $T_9(f)$ is

$$\Delta t(Z) = (4\ \text{yr})\, Z^{-2}\, (n_b/n_Z)\, (\rho/\rho_{\text{nucl}})^{-2/3} \times \left[T_9(f)^{-4} - T_9(i)^{-4}\right] \quad . \qquad \text{(X.16)}$$

A similar expression

$$\Delta t(\text{pions}) = (8 \times 10^{-7}\ \text{yr})\, (n_b/n_\pi)\, (\rho/\rho_{\text{nucl}})^{-2/3} \times \left[T_9(f)^{-4} - T_9(i)^{-4}\right] \qquad \text{(X.17)}$$

gives the cooling rate when the pion-nucleon processes are dominant.

Figure 3 shows the results of cooling-time calculations performed for a typical neutron star with average density ρ_{nucl} and mass $M_{\odot}$. The "nn + γ", "Ze", and "π n" curves are based on Eqs. (X.14), (X.16), and (X.17), respectively. The values of α used are listed in Table I. We set Z equal to ten in Eq. (X.16) and adopted the value 0.001 for n_Z/n_b, in agreement with Eq. (III.4). The cooling times with the plasma-neutrino and photon processes operating together were taken from the results plotted by Tsuruta.*

C. Minimum Cooling Rate

In this subsection we establish a lower limit on the cooling rate of a neutron star, a limit that is valid despite the obvious theoretical uncertainties and despite the variation of the cooling rate with stellar mass. With the present uncertainty about emission of neutrinos from the dense matter deep in the interior of a neutron star, one can best establish a minimum cooling rate by considering primarily processes that involve the relatively low-density material near the star's surface. Two such processes are the plasma-neutrino reaction ($\gamma \longrightarrow \nu + \bar{\nu}$) and surface emission of thermal photons. The rates of these two

---

* In her thesis, Miss Tsuruta (Ref. 6) used the general expressions for the rate of the plasma-neutrino process that are given by J. B. Adams, M. A. Ruderman, and C H. Woo, Phys. Rev. 129, 1383(1965). Minor errors in these general expressions have recently been pointed out by M. H. Zaidi, Nuovo Cimento (to be published). The corresponding corrections have been made in the "plasma + γ" curve in Fig. 3.

processes have been considered in Tsuruta's detailed neutron-star models, and the cooling rate she obtained for one model is plotted in Fig. 3.

The "plasma + γ" curve in Fig. 3 is a reasonable lower limit for the cooling rate of a neutron star. The reasons for choosing the plotted "plasma + γ" rate as a lower limit are summarized in the following three paragraphs:

(1) Most neutrinos emitted by the plasma-neutrino process[15] originate far out in a neutron star, where the density is of the order of 10^{10} or 10^{11} gm/cc. The photons originate from matter of even lower density. The rate of emission of photons and plasma-produced neutrinos thus depends on the properties of very high-density matter only through their dependence on the mass-radius relation of the star. The rate of energy loss by the plasma and photon processes is thus independent of the details of the excitation spectrum of matter at densities near ρ_{nucl} and is not strongly dependent on the equation of state assumed at high densities.

(2) Superfluidity and the existence of "nuclei" in the interior of a neutron star tend to reduce the specific heat of the star. The cooling rates plotted in Fig. 3 were calculated under the assumption that the nucleons form a normal Fermi fluid. Hence the cooling rates due to the plasma and photon processes would be increased, rather than decreased, by gaps in the energy spectrum of dense neutron-star matter.

(3) The cooling rates do depend somewhat on the mass (or, alternatively, the central density) chosen for the stellar model; the cooling rates for the plasma and photon processes vary inversely with the central density. The model corresponding to the curve plotted in Fig. 3 had a central density of about 1.9 ρ_{nucl}. The plasma and photon processes would proceed more rapidly in a star with lower central density. In a star with central density greater than 1.9 ρ_{nucl}, the pion-nucleon and/or nucleon-nucleon processes should proceed rapidly because "nuclei" should not exist at such high densities, and the neutron energy spectrum should not have a gap in it. The nucleon-nucleon processes would be faster than the plasma-neutrino process if the proton gap is less than about 1 Mev, and the energy-gap calculations described in Sec. IV-C indicate that the proton gap is, in fact, considerably less than 1 Mev. We thus conclude that the cooling rates of stars with central densities greater than 1.9 ρ_{nucl} should be greater than the rate indicated by the "plasma + γ" curve in Fig. 3, despite the fact that the rate of cooling by the plasma and photon processes alone would, for such dense stars, be slightly lower than the plotted rate.

We conclude that the "plasma + γ" curve in Fig. 3 is a lower limit for the cooling rate of a neutron star.

D. Cooling Times and Observability

The probability of ever observing a neutron star by detecting radiation from its surface depends strongly on the rates at which

such stars cool. A star that contains quasi-free pions, or one in which ordinary neutron-decay can take place (see Appendix), would emit detectable -rays for no more than a few days, and the probability of observing it would be small. A star that cools only by the nucleon-nucleon and photon processes would be detectable for a longer time.

We now consider the flux of photons that would be produced at a distance r by a neutron star with effective temperature T_e. The flux Φ of photons with wavelengths less than λ_m is given approximately by

$$\Phi \approx \frac{1}{2.5 \text{ cm}^2 \text{ sec}} \left[\frac{R_{10}}{r_{kpc}}\right]^2 \left[\frac{T_e}{3 \times 10^6 \text{ }^\circ\text{K}}\right]^3 (\tfrac{1}{2} x^2 + x + 1)\, e^{-x} , \quad \text{(X.13a)}$$

where R_{10} is the stellar radius in units of 10 km, r_{kpc} is the distance to the star in kiloparsecs (1 kpc $\approx 3.08 \times 10^{21}$ cm), and x is defined as follows:

$$x = 4.8 \, (10 \text{ Å}/\lambda_m) \, (3 \times 10^6 \text{ }^\circ\text{K}/T_e) \quad . \quad \text{(X.13b)}$$

Approximately ten X-ray sources have been identified by Giacconi et al.,[9] Bowyer et al.,[10],[11] and Clark et al.[12]. These sources are concentrated near the galactic plane, and about half of them are located in the direction of the galactic center. The weakest source detected by Bowyer et al.[11] produced a measured flux of 0.7 $\text{cm}^{-2}\text{sec}^{-1}$, and, because of absorption in the earth's atmosphere and in the counter itself, the observed X-rays must have been concentrated in the wavelength range from 1.5 Å to 8 Å; since the sun is approximately 8 kiloparsecs from the center of the galaxy, we conclude from Eq. (X.13) that the effective temperature of an observed source located at the galactic center must be greater than 2×10^7 °K, if the source is no larger than

a neutron star. Comparison with the "plasma + γ" curve in Fig. 3 indicates that a neutron star with a temperature of 2×10^7 °K would have to be less than a week old. The X-ray sources in the direction of the galactic center have been observed several times in the last few years,[9],[11],[19] and the flux from these sources has not changed, within the observational uncertainties (about a factor of two or three). Hence we conclude that the sources in the direction of the galactic center are not neutron stars.

APPENDIX

We consider here a number of obvious reactions and classes of reactions, indicating the densities at which some of them may be important, and showing that the rest of them are always slower than reactions (I.1)-(I.8) in neutron-star matter.

1. Ordinary Neutron Decay

At chemical equilibrium, momentum and energy conservation imply that

$$n \rightarrow p + e^- + \bar{\nu} \qquad \text{(A.1a)}$$

proceeds at an extremely slow rate unless

$$P_{Fn} < P_{Fp} + P_{Fe} \qquad \text{(A.1b)}$$

Equations (III.4) make it clear that inequality (A.1b) cannot be satisfied at reasonable densities in the free-particle approximation. But strong interactions can raise P_{Fp} and P_{Fe} significantly above their free-particle values, because the quantity $B_n - B_p$ in Eq. (III.3) is positive and can be comparable to E_{Fn}. One cannot, with much confidence, calculate binding energies at densities much greater than ρ_{nucl}, but rough estimates of B_n and B_p indicate that inequality (A.1b) may be satisfied for densities greater than about $3\,\rho_{nucl}$. If inequality (A.1b) is satisfied, the neutrino luminosity due to reaction (A.1a) and its inverse is

$$L_\nu^n \approx (1 \times 10^{45}\ \text{erg-sec}^{-1})(M_s/M_\odot)(\rho_{nucl}/\rho)\, T_9^6 \quad . \qquad \text{(A.1c)}$$

Thus neutron-star matter satisfying inequality (A.1b) would cool very rapidly--at about the rate indicated by the "πn" curve in Fig. 3.

2. Extra Particles

Reactions that involve large numbers of Fermions are slow because only a small fraction (of the order of kT/E_{Fi}) of the particles of a given species i are near enough to their Fermi level to scatter into unoccupied states. For example, the reaction

$$n + n + n \rightarrow n + n + p + e^- + \bar{\nu} \qquad (A.2)$$

is slower than reaction (I.1) by a factor of the order of $(kT/E_{Fn})^2$.

3. Positron Reactions

A reaction that, like

$$e^+ + n + n \rightarrow n + p + \bar{\nu} \ , \qquad (A.3a)$$

involves an incident positron, produces few neutrinos because the concentration of positrons is proportional to $\exp(-E_{Fe}/kT)$. Positron-producing reactions like

$$n + p \rightarrow n + n + e^+ + \bar{\nu} \qquad (A.3b)$$

are slowed by the same factor of $\exp(-E_{Fe}/kT)$, because the number of neutron-proton pairs with enough energy to produce two neutrons in unoccupied states is proportional to $\exp(-E_{Fe}/kT)$.

4. Reactions Involving Sound Waves

Several types of sound waves may exist in nuclear matter or low-temperature neutron-star matter: density waves, spin waves, and isospin waves[39],[40],[41]. The number density of charge-carrying isospin waves is extremely small because excitation of such a wave requires an energy of the order of E_{Fn}. The other types of sound mentioned above

have dispersion relations of the form

$$\omega = kv^{-1} \tag{A.4a}$$

for wave numbers k small compared to $\hbar^{-1} P_{Fn}$. The velocity v is usually comparable to the velocity of a neutron at the Fermi level.

Let ξ represent a sound wave with dispersion relation (A.4a).

The reaction

$$\xi \longrightarrow \nu + \bar{\nu} \tag{A.4b}$$

could not proceed because of conservation of momentum and energy, because v must be less than the speed of light.

A reaction of the form

$$n + \xi \longrightarrow n + \nu + \bar{\nu} \tag{A.4c}$$

is allowed by conservation of energy and momentum, but it would proceed at a very slow rate because (1) the number density of thermal sound waves, which is proportional to $(kT)^3$, is small at low temperatures, (2) the phase space available to the neutrinos is small ($\propto (kT)^6$), (3) a small fraction ($\propto kT$) of the neutron-states are near enough to the top of the Fermi sea to be involved in the reaction, and (4) the coupling would be indirect and would necessarily involve a factor of α because an electron-positron pair would have to be formed. Reaction (A.4c) would be at least six or eight orders of magnitude slower than reaction (I.1).

A reaction of the form

$$\xi + n \longrightarrow p + e^- + \bar{\nu} \tag{A.4d}$$

could only conserve momentum and energy if the sound wave had an energy comparable to the neutron Fermi energy; thus the rate would be proportional to an extremely small quantity $e^{-\zeta E_{Fn}/kT}$, where ζ is of the order of unity.

We conclude that reactions involving thermal sound waves are not important.

5. Plasma Vibrations

Photons propagating through neutron-star matter interact with the charged particles in the medium. Creation of one of these quasi-free photons (usually called "plasmons") requires an energy greater than $\hbar\omega_o$ where ω_o is the plasma frequency in the medium[41]. Consequently, the rate of a reaction such as

$$\gamma \longrightarrow \nu + \bar{\nu} \quad , \tag{A.5}$$

which involves one external plasmon, is proportional to $e^{-\hbar\omega_o/kT}$. The plasma frequency is of the order of 5 MeV at nuclear density, and the rate of reaction (A.5) is small in the interior of a neutron star. Very near the surface of the star, reaction (A.5) does contribute significantly[15]. The cooling rate of a star emitting neutrinos only by reaction (A.5) is shown in Fig. 3.

6. Conversion of Muons to Electrons

Reactions involving more than one neutrino are generally slow because of the small amount of phase space available to such processes. The amount of phase space available to a neutrino with energy less than kT is proportional to $(kT)^3$. Consequently, the rate of the reaction

$$p + \mu^- \longrightarrow p + e^- + \bar{\nu}_e + \nu_\mu \quad , \tag{A.6}$$

is smaller than the rate of reaction (I.1) by a factor of the order of $(kT/E_{Fn})^2$.

7. Neutrino Bremsstrahlung

The rate of the reaction

$$e^- + p \rightarrow e^- + p + \nu + \bar{\nu} \qquad \text{(A.7a)}$$

is, like the rate of reaction (I.1), proportional to T^8. The rate of reaction (A.7a) also contains a factor of α^2, however, which causes it to be smaller than the rate of reaction (I.1) by about a factor of 10^4.

At densities low enough that a lattice of "nuclei" can form, the "nuclei" can transfer momentum to the electrons in the process

$$e^- + Z \rightarrow e^- + Z + \nu + \bar{\nu} \quad . \qquad \text{(A.7b)}$$

Ruderman's expression for the rate of reaction (A.7b) is given in Eq. (X.11). The rate is proportional to $(kT)^6$ because the "nucleus" in reaction (A.7b), being bound in a lattice, does not contribute any factors of (kT) to the reaction rate. Consequently, the reaction (A.7b) is important when "nuclei" are stable.

8. Pionic Reactions

Turning to reactions involving quasi-free pions, we can use some of the arguments presented in the last few paragraphs to show that the following types of pion reactions are slower than reactions (I.3), (I.4), (I.7), and (I.8): the free decay of the pion ($\pi^- \rightarrow \mu^- + \bar{\nu}_\mu$), reactions involving large numbers of Fermions, positron processes, and pionic reactions involving more than one neutrino.

The reaction

$$\pi^- + \pi^- \rightarrow \pi^- + \mu^- + \bar{\nu}_\mu \quad , \qquad \text{(A.8a)}$$

however, might be faster than reactions (I.3), (I.4), (I.7), and (I.8)

if the lowest quasi-free pion state has a momentum greater than about $\frac{1}{3} P_{F\mu}$; the momentum of the lowest pion-state is completely unknown.

Similarly, the reactions

$$\pi^- + Z \rightarrow \mu^- + Z + \bar{\nu}_\mu \qquad \text{(A.8b)}$$

and/or

$$\pi^- + Z \rightarrow e^- + Z + \bar{\nu}_e \qquad \text{(A.8c)}$$

would be extremely fast in the unlikely event that quasi-free pions and "nuclei" were both present simultaneously in the same neutron-star matter.

The question of whether reactions (A.8) could proceed faster than reactions (I.3), (I.4), (I.7), and (I.8) is not particularly important, because reactions (I.3), (I.4), (I.7), and (I.8) alone would be sufficient to cause a neutron star to cool fast enough to make the star nearly impossible to observe by surface radiation.

FIGURE CAPTIONS

RATES OF NUCLEAR REACTIONS IN WHITE-DWARF STARS

Fig. 1. Central temperatures and densities of various types of stars. The solid-state approach to nuclear reactions applies to Region I on the figure. In Region II, most nuclear motion is vibrational, but the nuclei most likely to react have enough energy to break through the lattice. In Regions III and IV, the nuclei move like atoms in a gas. In Region III, the electrons are degenerate, while in Region IV they are nondegenerate.

Fig. 2. Predictions of proton lifetimes at 10^5 gm/cc. The lifetimes predicted by the method of Salpeter are compared to those computed by the solid-state method using oscillator frequencies obtained by analyzing the dynamics of the lattice. The dotted line indicates a reasonable interpolation between the two formulae.

Fig. 3. Predictions of the lifetimes of protons and C^{12} nuclei. The lifetimes computed using oscillator frequencies based on an analysis of lattice dynamics are compared with the lifetimes computed assuming a rigid lattice. Proton lifetimes calculated by Wildhack and carbon lifetimes calculated by the method of Cameron are also shown.

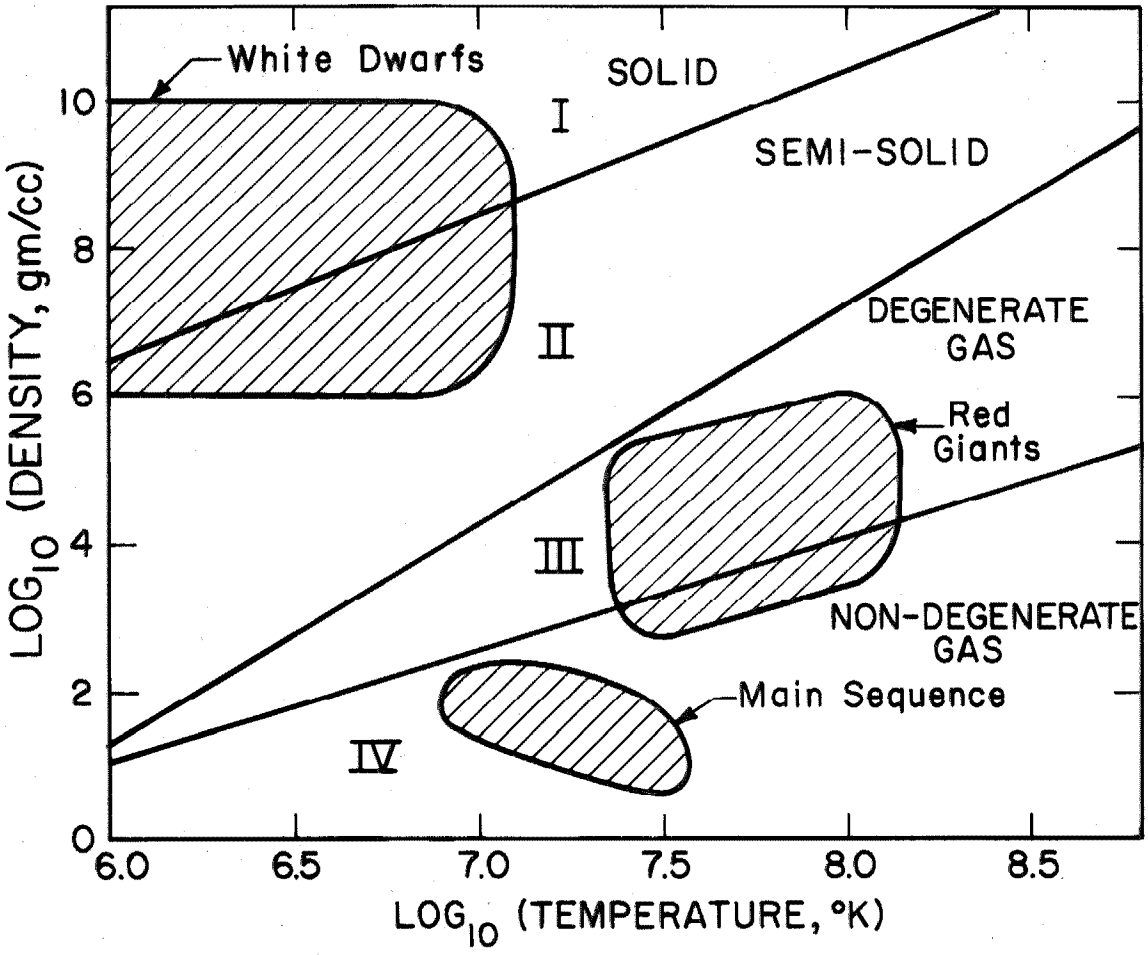
White Dwarfs
SOLID
I
SEMI-SOLID
II
DEGENERATE GAS
Red Giants
III
NON-DEGENERATE GAS
Main Sequence
IV
10
8
6
4
2
0
LOG10 (DENSITY, gm/cc)
6.0
6.5
7.0
7.5
8.0
8.5
LOG10 (TEMPERATURE, °K)

Figure 1

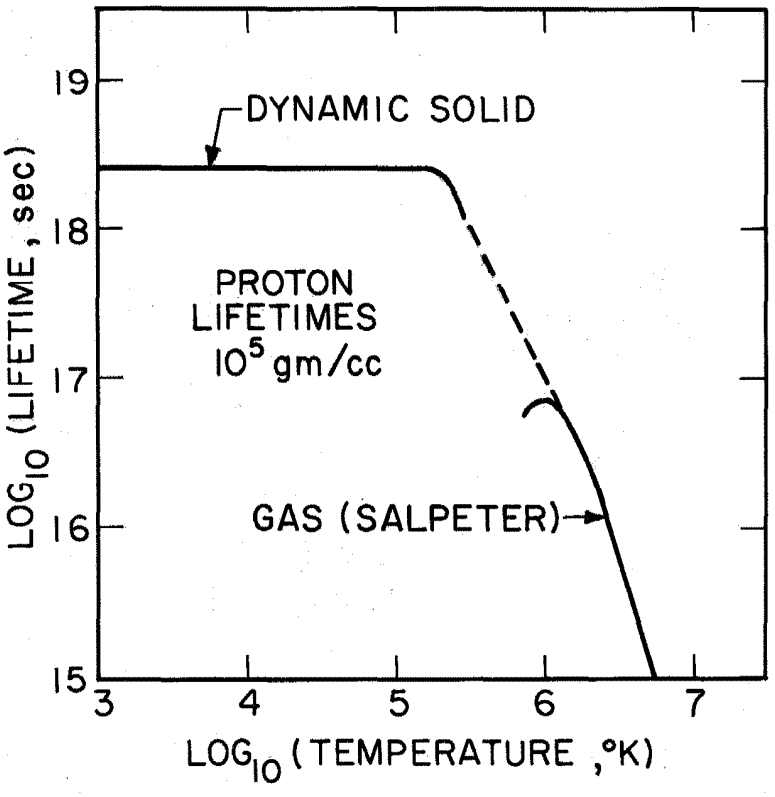
DYNAMIC SOLID
PROTON
LIFETIMES
10^5 gm/cc
GAS (SALPETER)
19
18
17
16
15
3
4
5
6
7
LOG_{10} (LIFETIME, sec)
LOG_{10} (TEMPERATURE, °K)

Figure 2

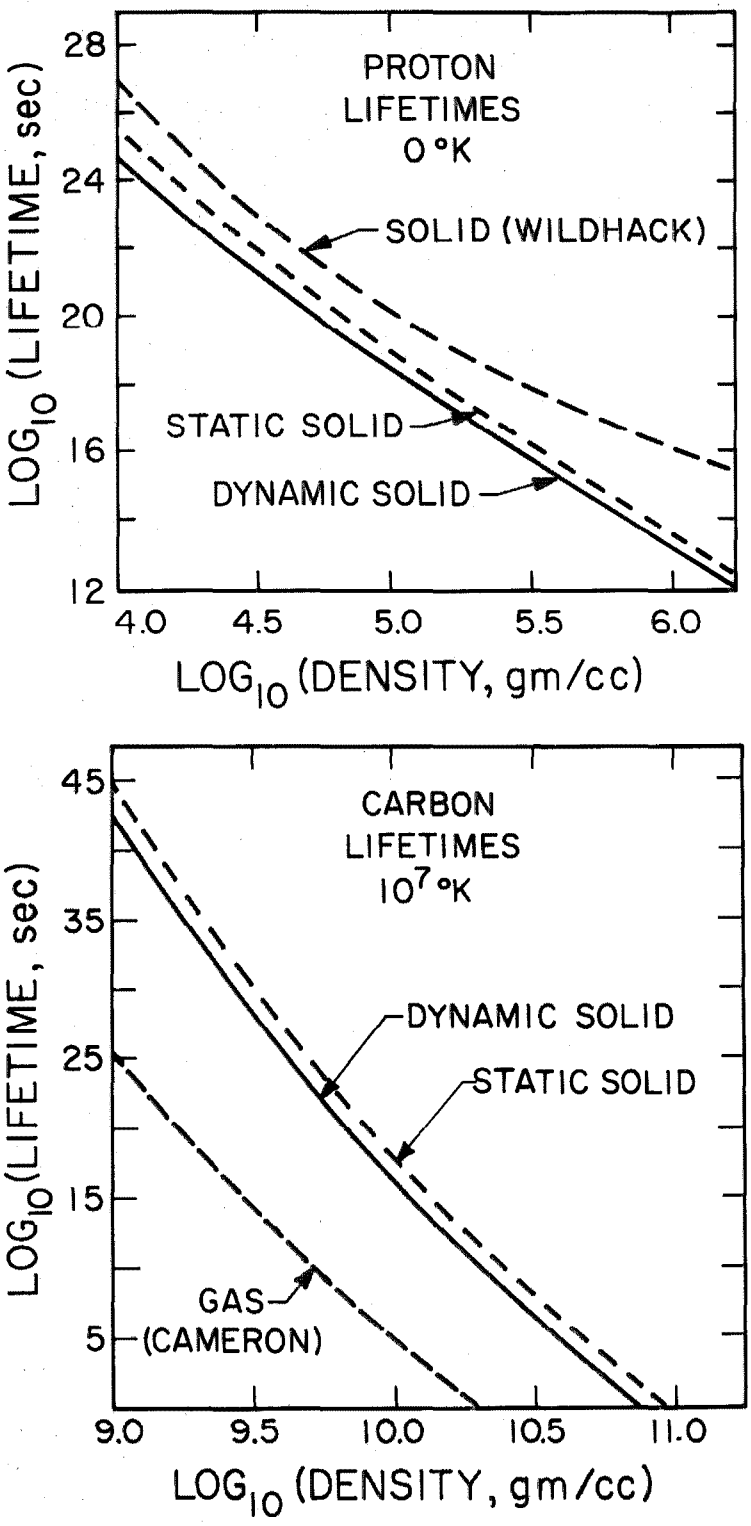
PROTON
LIFETIMES
0 °K
SOLID (WILDHACK)
STATIC SOLID
DYNAMIC SOLID
LOG10 (LIFETIME, sec)
28
24
20
16
12
4.0
4.5
5.0
5.5
6.0
LOG10 (DENSITY, gm/cc)
CARBON
LIFETIMES
10^7 °K
DYNAMIC SOLID
STATIC SOLID
GAS
(CAMERON)
LOG10(LIFETIME, sec)
45
35
25
15
5
9.0
9.5
10.0
10.5
11.0
LOG10 (DENSITY, gm/cc)

Figure 3

FIGURE CAPTIONS

THE COOLING OF NEUTRON STARS

Fig. 1. The proton-superconductivity correction factor for the rate of the nucleon-nucleon reactions. The logarithm of the correction factor is plotted against the ratio ϵ_{op}/kT.

Fig. 2. Several Feynman diagrams for the reaction $n + \pi^- \rightarrow n' + e^- + \bar{\nu}_e$.

Fig. 3. Cooling times calculated for a typical neutron star. The curves marked "πn" and "Ze" give the cooling times for a neutron star emitting neutrinos by the pion-nucleon and neutrino-bremsstrahlung processes, respectively. The "γ"-curve represents a star cooling just by surface photon emission, while the "nn + γ" and "plasma + γ" curves represent stars emitting neutrinos by the nucleon-nucleon processes and the plasma neutrino process, respectively, as well as surface photons. All curves refer to a star of about one solar mass with average density ρ_{nucl}.

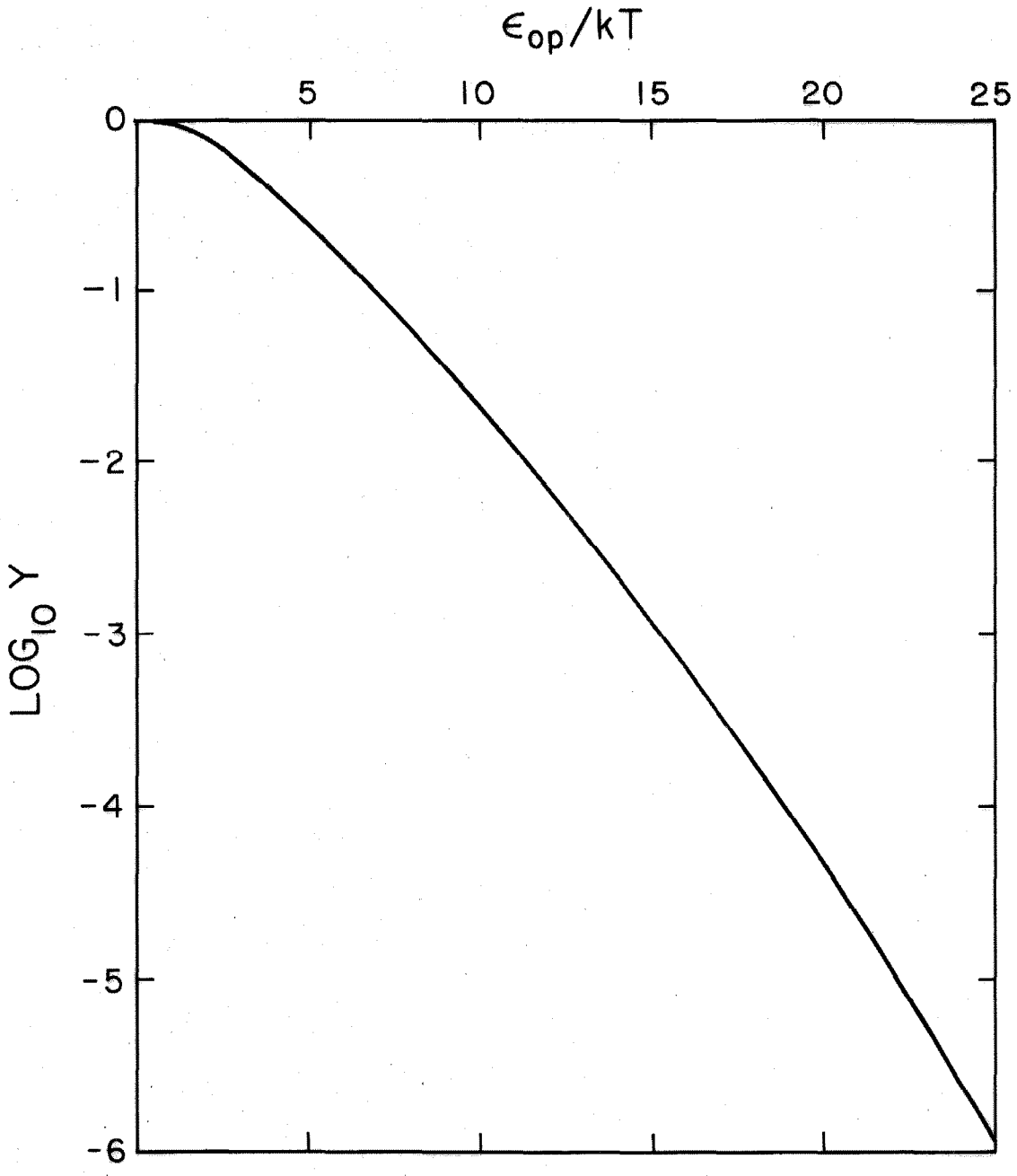

Figure 1

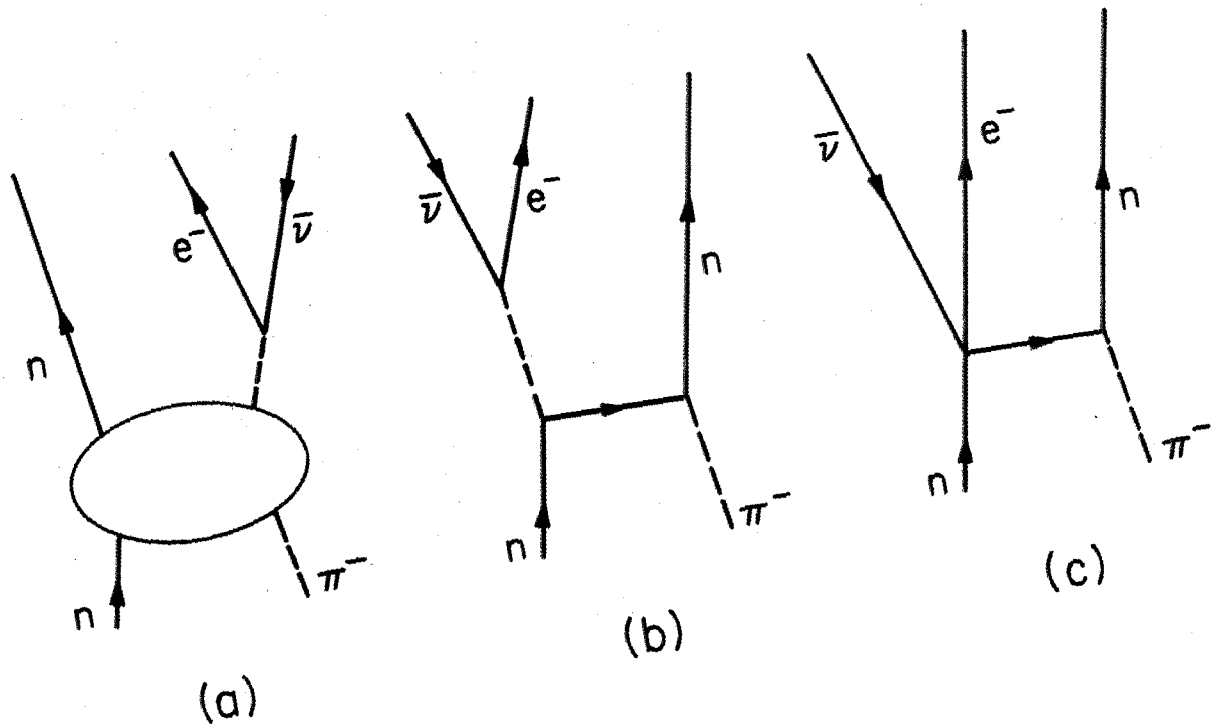

Figure 2

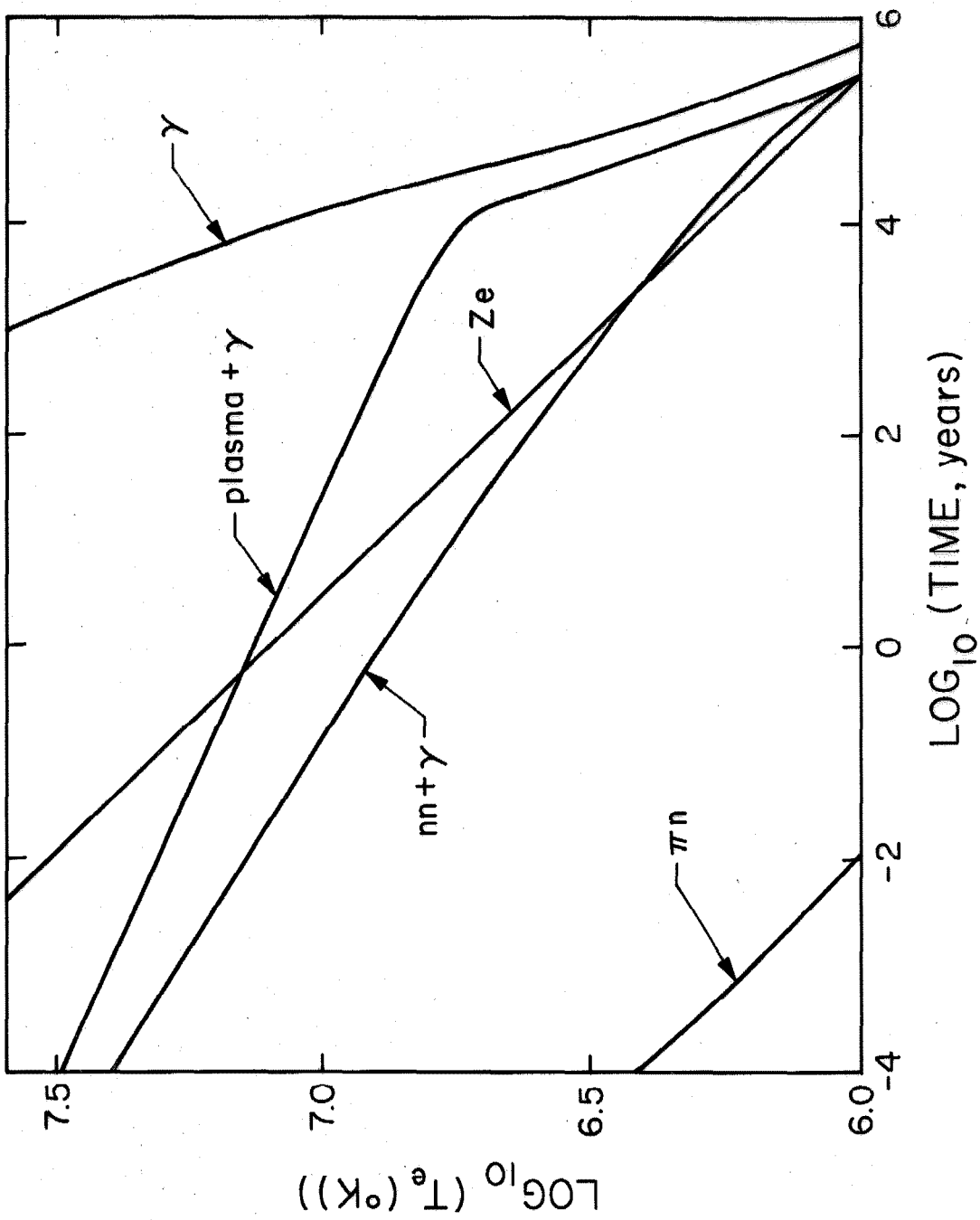
γ
plasma + γ
Ze
nn + γ
πn
7.5
7.0
6.5
6.0
6
4
2
0
-2
-4
LOG10 (Te (°K))
LOG10 (TIME, years)

Figure 3

TABLE I.

Temperature parameter $\alpha(= 10^{-2}\ T/T_e)$. The values of α were obtained by interpolation of a table given by Tsuruta.[a]

T_{e7}	α
2.0	1.92
1.0	1.65
0.8	1.61
0.6	1.59
0.4	1.53
0.3	1.48
0.2	1.39
0.1	1.10

a) S. Tsuruta, Ph.D. thesis, Columbia University (1964) (unpublished), p. 322.

REFERENCES

on

RATES OF NUCLEAR REACTIONS IN WHITE-DWARF STARS

1. W. A. Wildhack, Phys. Rev. 57, 81 (1940).

2. E. E. Salpeter, Astrophys. J. 134, 916 (1959).

3. D. A. Kirzhnits, Soviet Physics JETP 11, 365 (1960).

4. A. G. W. Cameron, Astrophys. J. 130, 916 (1959).

5. T. Hamada and E. E. Salpeter, Astrophys. J. 134, 683 (1961).

6. H. Van Horn, Ph.D. thesis, Cornell University (1965), unpublished.

7. V. P. Kopyshev, Soviet Astronomy AJ 8, 691 (1961).

8. E. E. Salpeter, Australian J. Phys. 7, 373 (1954).

9. W. J. Carr, Jr., Phys. Rev. 122, 1437 (1961).

10. F. L. Yost, J. A. Wheeler, and G. Breit, Phys. Rev. 49, 174 (1936).

11. P. D. Parker, J. N. Bahcall, and W. A. Fowler, Astrophys. J. 139, 602 (1964).

12. F. W. de Wette, Phys. Rev. 135, A287 (1964).

13. P. Nozieres and D. Pines, Phys. Rev. 111, 442 (1958).

14. N. F. Mott, Phil. Mag. 6, 287 (1961).

15. H. Reeves, Astrophys. J. 135, 779 (1962).

REFERENCES

on

THE COOLING OF NEUTRON STARS

1. L. Landau, Nature 141, 333 (1938).
2. W. Baade and F. Zwicky, Astrophys. J. 88, 411 (1938).
3. J. R. Oppenheimer and G. M. Volkoff, Phys. Rev. 55, 374 (1939).
4. A. G. W. Cameron, Astrophys. J. 130, 884 (1959).
5. T. Hamada and E. E. Salpeter, Astrophys. J. 134, 683 (1961).
6. S. Tsuruta, Ph.D. thesis, Columbia University (1964), unpublished; S. Tsuruta and A. G. W. Cameron, Nature 207, 364 (1965).
7. A. G. W. Cameron, Nature 206, 787 (1965).
8. A. Finzi, Phys. Rev. Letters 15, 599 (1965).
9. R. Giacconi, H. Gursky, F. R. Paolini, and B. B. Rossi, Phys. Rev. Letters 9, 439 (1962) and 11, 530 (1963).
10. S. Bowyer, E. T. Byram, T. A. Chubb, and H. Friedman, Nature 201, 1307 (1964).
11. S. Bowyer, E. T. Byram, T. A. Chubb, and H. Friedman, Science 147, 394 (1965).
12. G. Clark, C. Garmire, M. Oda, M. Wada, R. Giacconi, H. Gursky, and J. R. Waters, Nature 207, 584 (1965).
13. D. C. Morton, Nature 201, 1308 (1964).
14. A. Finzi, Astrophys. J. 139, 1398 (1964).
15. H-Y. Chiu and E. E. Salpeter, Phys. Rev. Letters 12, 413 (1964).
16. G. R. Burbidge, R. J. Gould, and W. H. Tucker, Phys. Rev. Letters 14, 289 (1965).

17. P. Morrison and L. Sartori, Phys. Rev. Letters 14, 771 (1965).

18. S. Bowyer, E. T. Byram, T. A. Chubb, and H. Friedman, Science 146, 912 (1964).

19. R. Giacconi, H. Gursky, and J. R. Waters, Nature (to be published).

20. G. Chodil, R. C. Jopson, Hans Mark, F. D. Seward, and C. D. Swift, Phys. Rev. Letters 15, 605 (1965).

21. A. Finzi, Phys. Rev. 137, B472 (1965).

22. D. G. Ellis, Phys. Rev. 139, B754 (1965).

23. V. A. Ambartsumyan and G. S. Saakyan, Soviet Astronomy AJ 4, 187 (1960) and 5, 601 (1962).

24. L. C. Gomes, J. D. Walecka, and V. F. Weisskopf, Ann. Phys. (N. Y.) 3, 241 (1958).

25. M. A. Ruderman, (private communication).

26. E. E. Salpeter, Astrophys. J. 134, 669 (1961).

27. V. L. Ginzburg and D. A. Kirzhnits, Soviet Physics JETP 20, 1346 (1965).

28. J. Bardeen, L. N. Cooper, and J. R. Schrieffer, Phys. Rev. 108, 1175 (1957).

29. A. Bohr, B. R. Mottleson, and D. Pines, Phys. Rev. 110, 936 (1958).

30. T. Ericson, Advances in Physics 9, 425 (1960).

31. D. W. Lang, Nucl. Phys. 42, 353 (1960).

32. K. A. Brueckner, T. Soda, P. W. Anderson, and P. Morel, Phys. Rev. 118, 1442 (1960).

33. V. J. Emery and A. M. Sessler, Phys. Rev. 119, 248 (1960).

34. M. A. Preston, Physics of the Nucleus (Addison-Wesley Publishing Co., Inc., Reading, Mass., 1962), Chap. 2, pp. 27-29.

35. R. P. Feynman and M. Gell-Mann, Phys. Rev. 109, 193 (1958).

36. Y. Yamaguchi, Phys. Rev. 95, 1628 (1954).

37. G. Källen, Elementary Particle Theory (Addison-Wesley Publishing Co., Inc., Reading, Mass., 1964), pp. 141 and 119.

38. S. A. Orszag, Astrophys. J. 142, 473 (1965).

39. A. E. Glassgold, W. Heckrotte, and K. M. Watson, Ann. Phys. (N.Y.) 6, 1 (1950).

40. S. Fujii, Nucl. Phys. 52, 144 (1964).

41. A. G. Sitenko and I. V. Simenog, Nucl. Phys. 53, 409 (1964).

42. J. B. Adams, M. A. Ruderman, and C-H. Woo, Phys. Rev. 129, 1383 (1963).